www.sciencemag.org/cgi/content/full/science.aat4100/DC1

Supplementary Materials for

Missing enzymes in the biosynthesis of the anticancer drug vinblastine in Madagascar periwinkle

Lorenzo Caputi, Jakob Franke, Scott C. Farrow, Khoa Chung, Richard M. E. Payne, Trinh-Don Nguyen, Thu-Thuy T. Dang, Inês Soares Teto Carqueijeiro, Konstantinos Koudounas, Thomas Dugé de Bernonville, Belinda Ameyaw, D. Marc Jones, Ivo Jose Curcino Vieira, Vincent Courdavault,* Sarah E. O'Connor*

*Corresponding author. Email: sarah.oconnor@jic.ac.uk (S.E.O.); vincent.courdavault@univ-tours.fr (V.C.)

Published 3 May 2018 on *Science* First Release
DOI: 10.1126/science.aat4100

This PDF file includes:

Other Supplementary Material for this manuscript includes the following:
(available at www.sciencemag.org/cgi/content/full/science.aat4100/DC1)

Materials and Methods

Chemicals and molecular biology kits

All solvents used for extractions, chemical synthesis and preparative HPLC were of HPLC grade, whilst solvents for UPLC/MS analysis were of MS grade. All were purchased from Fisher Scientific. Catharanthine **3** was purchased from Sigma Aldrich, whilst tabersonine **2** was obtained from Ava Chem Scientific. Stemmadenine was purified by Prof. Ivo J. Curcino Vieira as previously described (*30*). Kanamycin sulfate, carbenicillin and gentamycin were from Formedium, whilst rifampicin was from Sigma Aldrich. All gene and fragment amplifications were performed using Platinum Superfi polymerase (Thermo Fisher) whilst colony PCRs were performed using Phire II master mix (Thermo Fisher). PCR product purifications were performed using the Macherey-Nagel PCR clean-up kit. Plasmids purifications were performed using Promega Wizard minipreps. cDNA was prepared using Superscript IV VILO master mix and Turbo DNAse (Thermo Fisher). qPCR was performed using Sensi-FAST Sybr No-ROX kit (Bioline). All restriction enzymes and ligase were from NEB.

RNA-seq data and analysis for biosynthetic gene candidates

Analysis of the *C. roseus* gene expression profile data was performed on the transcriptome dataset available from the Medicinal Plant Genomics Resource website (http://medicinalplantgenomics.msu.edu/final_version_release_info.shtml) (*31*). Co-expression analysis by hierarchical clustering was performed on the FPKM matrix using the algorithms embedded in the Multi Experiment Viewer (MeV v.4.8), whilst self-organizing maps analysis was performed as described in Payne et al. (*32*). A cluster of ca. 3600 co-regulated contigs was identified. This cluster contained all the known genes involved in the *C. roseus* MIA biosynthetic pathway. After further analysis based on functional annotation and gene onthology, a list of ca. 300 genes of interest was compiled, from which we selected candidates for VIGS analysis based on putative function. We also used an RNA-seq dataset composed of control leaves, Maduca sexta fed leaves (ERP016279) (*33*), leaves treated with coronatine (ERP107957) and adventitious roots (ERP104058) (*34*) to generate an additional expression matrix. Reads were pseudo-mapped on the CDF97 reference transcriptome (*35*) and quantified with Salmon v0.7.2 (*36*). Transcript annotation was performed in (*35*). Pairwise correlations (Pearson) between each possible gene pair were calculated in parallel and subsquently ranked to determine highest reciprocal ranks (HRR, similar approach to mutual ranking) for each gene pair as described by (*37*). For each known gene from the MIA pathway, best co-expressed genes from the whole transcriptome were retained if their HRR<250. A network was next constructed to visualize the resulting associations in R v3.4.4 (*38*) with the 'igraph' package v1.0.1 (*39*). Communities of closely co-expressed genes were identified with a fast greedy algorithm (*40*). Among those communities, one contained 468 transcripts, including many MIA-related genes such as GS and GO and 2-hydroxyisoflavanone dehydratases such as TS (see Data S1).

Virus induced gene silencing, metabolite analysis and qPCR

Fragments for CS and TS silencing were selected on the 3'-UTR regions, due to the high sequence similarity between the two genes, whilst fragments for PAS and DPAS silencing were designed using sequence from the ORF regions. Primers are shown in Table S1. A BLAST search against the transcriptome for each of the regions suggested that the VIGS fragments selected did not contain regions of homology that have significant overlap to other genes in the plant that could cause potential cross-silencing. The silencing fragments for CS, TS and DPAS

were amplified from cDNA using the primers listed in Table S1, treated with restriction enzymes *Bam*HI and *Xho*I and ligated into pTRV2 vector using T4 ligase. The fragment for PAS silencing was amplified from cDNA using the set of primers in Table S1 and cloned into the USER compatible VIGS plasmid pTRV2u as previously described (*41*).

VIGS experiments were performed using the *C. roseus* Little Bright Eye variety grown in a growth chamber at 25 °C with a 12 h dark/12 h light regime as described previously (*42*). Briefly, each construct was infiltrated into 10 to 12 *C. roseus* seedlings (8 weeks old). Additionally, eight seedlings were infiltrated with pTRV2 lacking an insert (empty vector negative control) and four plants were infiltrated with a vector containing a fragment of the protoporphyrin IX magnesium chelatase gene (ChlH), which provided a visual marker (bleaching) to act as a positive control. After 21 days, seedlings infiltrated with the pTRV-ChlH vector displayed substantial yellowing of leaves; the last leaf pair to emerge above the inoculation site was harvested, frozen in liquid nitrogen and homogenized using a cryo bead mill. A portion of each sample (10-20 mg) was used for metabolite analysis, whilst the remaining of the samples were used for RNA extraction.

Samples for metabolite analysis were extracted with 1 mL of MeOH containing 1 µg/mL ajmaline as internal standard, filtered and diluted 1:4 with MeOH before LC/MS analysis using the method described in the UPLC/MS section.

Relative transcript abundance was determined by qRT-PCR on a BioRad CFX96 Q-PCR instrument using cDNA synthesized from isolated total RNA and the primers listed in Table S1. Eight biological replicates and three technical replicates were analyzed for each gene using two reference genes: Expressed protein, EXP, and N2227-like family protein, N2227 (*43*). Efficiencies for all primer sets were approximately equal and always >90%. The entire VIGS experiment was performed in triplicate with essentially identical results.

Expression and purification of proteins

CS, TS and DPAS expression in E. coli

The full-length sequences of CS, TS and DPAS were amplified from *C. roseus* cDNA using the primers listed in Table S1. The PCR products were purified from agarose gel, ligated into the *Bam*HI and *Kpn*I restriction sites of the pOPINF vector (*44*) using the In-Fusion kit (Clontech Takara) and transformed into chemically competent *E. coli* Stellar cells. Recombinant colonies were selected on LB agar plates supplemented with carbenicillin (100 µg/mL). Positive clones were identified by colony PCR using T7_Fwd and pOPIN_Rev primers (see Table S1). Plasmids were isolated from positive colonies grown overnight. Identities of the inserted sequences were confirmed by Sanger sequencing.

Chemically competent SoluBL21 *E. coli* cells (Amsbio) were transformed by heat shock at 42 ℃. Transformed cells were selected on LB agar plates supplemented with carbenicillin (100 µg/mL). Single colonies were used to inoculate starter cultures in 50 mL of 2 x YT medium supplemented with carbenicillin (100 µg/mL) that were grown overnight at 37 ℃. Starter culture (10 mL) was used to inoculate 1 L of 2 x YT medium containing the antibiotic. The cultures were incubated at 37 ℃ until OD600 reached 0.6 and then transferred to 16 ℃ for 30 min before induction of protein expression by addition of IPTG (0.2 mM). Protein expression was carried

out for 16 h. Cells were harvested by centrifugation and re-suspended in 50 mL of Buffer A (50 mM Tris-HCl pH 8, 50 mM glycine, 500 mM NaCl, 5% glycerol, 20 mM imidazole,) with EDTA-free protease inhibitors (Roche Diagnostics Ltd.). Cells were lysed by sonication for 4 minutes on ice. Cell debris was pelleted by centrifugation at 35,000 *g* for 20 min.

His_6-tagged enzymes were purified on an AKTA Pure system (GE Healthcare) using a HisTrap HP 5 mL column (GE Healthcare) equilibrated with Buffer A. Samples were loaded at a flow rate of 2 mL/minute and step-eluted using Buffer B (50 mM Tris-HCl pH 8, 50 mM glycine, 500 mM NaCl, 5% glycerol, 500 mM imidazole). Eluted proteins were subjected to further purification on a Superdex Hiload 16/60 S200 gel filtration column (GE Healthcare) at a flow rate of 1 mL/minute using Buffer C (20 mM HEPES pH 7.5, 150 mM NaCl) and collected in 1.5 mL fractions.

Transient expression of proteins in N. benthamiana

CS, TS and DPAS full-length sequences were cloned into a modified TRBO vector (*45*) in which the cloning cassette of the pOPINF vector was inserted in the *Not*I restriction site. This allowed the vector to be compatible with the PCR products generated for cloning into pOPINF vector and to obtain N-terminal His_6-tagged recombinant proteins. Cloning was performed using the In-Fusion kit. PAS full-length, instead, was cloned into pDONR207 (Thermo Fisher) using primers with attB1 and attB2 overhangs (see Table S1) via BP Clonase reaction, then recombined into pEAQ-HT-DEST3 vector (*46*) for transient expression with a C-terminal His_6-tag using LR Clonase reaction.

The constructs were used for *E. coli* Stellar cells transformation by heat shock and recombinant colonies were selected on LB + Kanamycin (100 µg/mL). Positive colonies were also screened by colony PCR using the primers listed in Table S1 and sequenced. The constructs were then used to transform electrocompetent *A. tumefaciens* strain GV3101 by electroporation. Recombinant colonies were selected on LB agar containing rifampicin (100 µg/mL), gentamycin (50 µg/mL) and kanamycin (100 µg/mL). Single colonies were grown in 10 mL of LB with antibiotics for 48 h at 28 °C, then the cells were collected by centrifugation and re-suspended in 10 mL infiltration buffer (10 mM NaCl, 1.75 mM $CaCl_2$ and 100 µM acetosyringone). After incubation at room temperature for 2 h, the cell cultures were diluted to OD600 0.1 and used to infiltrate *N. benthamiana* leaves. When multiple constructs were infiltrated simultaneously, the corresponding *A. tumefaciens* cell cultures were mixed so that the final OD600 of each would be 0.1. Infiltration was performed using a syringe without needle on leaves of 3-4 weeks old plants. Leaves were harvested 5 days post-infiltration.

Protein purification for proteomics analysis was performed by extraction of 2 g of pulverized frozen tissue in 10 mL of cold Tris-HCl buffer (50 mM, pH 8.0) containing EDTA-free protease inhibitors. After incubation on ice for 1 h and vortexing, the samples were centrifuged for 20 min at 35,000 *g*. The supernatants were collected and incubated with 300 µL of Ni-NTA slurry for 1 h. The slurry was then collected by centrifugation at 1,000 *g* for 1 min and washed 3 times with 10 mL of Tris-HCl buffer. Proteins were eluted by washing the slurry with 600 µL of Tris-HCl buffer containing 500 mM imidazole.

To purify PAS for *in vitro* enzyme activity assays, 300 g of fresh *N. benthamiana* leaves that had been infiltrated with the PAS expression construct were homogenized in 600 mL of Tris-HCl buffer (50 mM, pH 8.0) containing EDTA-free protease inhibitors and 1% insoluble polyvinylpolypyrrolidone (PVPP) using a blender. The homogenate was filtered through two layers of miracloth and then centrifuged at 3,500 *g* for 10 min to remove the insoluble PVPP and tissue debris. The supernatant was further clarified by centrifugation at 35,000 *g* for 20 min. PAS was then bound to a 5 mL Ni-NTA column and eluted with 20 mL of Tris-HCl buffer containing 500 mM imidazole. The eluted protein was dialyzed in ConA binding buffer (20 mM Tris-HCl buffer pH 7.4, 500 mM NaCl, 1 mM $MnCl_2$ and 1 mM $CaCl_2$) and manually applied to a ConA HiTrap 1 mL column (GE Healthcare) at a low flow rate using a syringe. After loading of the protein, the column was washed with 10 mL of binding buffer and then eluted with 10 mL of ConA elution buffer (20 mM Tris-HCl buffer pH 7.4, 500 mM NaCl and 300 mM methyl-D-glucoside). The protein was then dialyzed into Tris-HCl buffer (50 mM, pH 8.0), concentrated and stored at -20 ℃.

Expression of PAS in Pichia pastoris

A truncated version of PAS, lacking the initial 23 amino acids, was generated by PCR (Table S1) and cloned into the pPINK-HC vector (Thermo Fisher) according to the manufacturer's instructions. In this way, the native plant N-terminal signal peptide was replaced with the yeast α-mating sequence for extracellular secretion. The pPINK-HC::*PAS* construct was transformed into *P. pastoris* by electroporation in accordance with the PichiaPink™ Expression System protocol.

A single colony of a *P. pastoris* transformant was inoculated in 10 mL BMGY medium in a 250-mL Erlenmeyer flask and grown for 24 hours at 250 rpm and 30 ℃. The inoculation was then transferred to 100 mL BMGY medium in a 500-mL baffled flask and cultured in the same conditions. After another 24 hours, this culture was transferred to 2 L BMGY medium, split equally into three 2-L baffled flasks, and grown at 220 rpm, 30 ℃ for approximately two days until OD_{600} reached 2 to 3. The cells were then collected by centrifugation at 5,000 *g* for 5 minutes, re-suspended in 700 mL BMMY medium (containing 0.5 % methanol) for protein expression, split equally into two 2-L non-baffled flasks. The culture was allowed to grow at 28 ℃ and 250 rpm. After 120 hours, the culture was centrifuged at 10,000 *g* for 10 minutes.

The medium containing secreted proteins (supernatant) was concentrated using 30,000 MWCO concentrators (Merck Millipore) to approximately 20 mL, dialyzed into 50 mM HEPES buffer pH 7.0 using PD-10 desalting columns (GE Healthcare), and further concentrated to 3 mL. The sample was subjected to IEX chromatography on a HiTrap Q HP 1 mL column (GE Healthcare) to enrich the PAS protein. After loading of the sample, the column was washed with 10 mL of 50 mM HEPES buffer pH 7.0 before elution of the protein with 50 mM HEPES buffer pH 7.0 containing 500 mM NaCl. The sample was dialyzed in 50 mM Tris-HCl pH 8.5 and concentrated to a final volume of 1 mL. BMGY and BMMY media were prepared in accordance with the PichiaPink™ Expression System protocol.

Concentrated *P. pastoris* culture medium containing secreted proteins was analyzed on SDS-PAGE with Coomassie staining. A band corresponding to the size of PAS (ca. 57 kDa) was

visible. To confirm the identity of the protein, the band was excised, de-stained and subjected to trypsin digestion and LC/MS/MS analysis on a nanoLC-orbitrap (see Data S3).

Expression of PAS in Sf9 insect cells

Cloning, expression and purification of PAS in Sf21 insect cells was carried out by MRCPPU Reagents and Services (mrcppureagents.dundee.ac.uk). Briefly, PAS was cloned into the *Bam*H1/*Eco*R1 sites of pFastBac vector (Invitrogen). The resulting construct encoding PAS with an N-terminal His_6-tag was then used to generate recombinant baculovirus using the Bac-to-Bac system (Invitrogen) following the manufacturer's protocol. These baculovirus were used to infect *Spodoptera frugiperda* 21 cells, the infected cells were grown at 27 °C, harvested 48 hours post-infection and the His-tagged PAS protein was purified on Cobalt Agarose (Expedeon) and dialysed into 50 mM Tris-HCl pH 7.5, 0.1 mM EGTA, 150 mM NaCl, 0.1 % 2-mercaptoethanol, 270 mM Sucroe, 0.03 % Brij-35 and stored at -80 °C.

Pathway reconstitution in *N. benthamiana*

Leaves of 3-4 weeks old *N. benthamiana* plants were infiltrated with *A. tumefaciens* GV3101 cultures harbouring the transient protein expression constructs, as described above. After 4 days, each leaf was infiltrated with 1 mL of 50 μM stemmadenine acetate dissolved in infiltration buffer. After 24 h, the infiltrated leaves were harvested and flash-frozen in liquid nitrogen. After grinding in liquid nitrogen, 200-300 mg of pulverised tissue were extracted with 1 volume (w/v) of MeOH containing ajmaline as internal standard. After incubation at room temperature for 1 h and vortexing, the samples were centrifuged at 17,000 *g* for 10 min, filtered and analyzed by UPLC/MS using the same method described in the UPLC/MS section. To confirm the presence of all the proteins, samples were subjected to trypsin digestion and LC/MS/MS analysis on a nanoLC-orbitrap (see Data S2).

In vitro enzyme assays

In vitro assays of PAS alone were performed in 50 mM Tris-HCl buffer pH 9.0, whilst those in which PAS was coupled with the other enzymes were performed in 50 mM Tris-HCl pH 8.5. In all cases 20 μM FAD was added as co-factor. Each assay contained 50 μM stemmadenine acetate (substrate) delivered in methanol (not exceeding 5% of the reaction volume). Due to the very low amounts of PAS purified, the amount of protein in the assays was not accurately determined. However, the amount of enzyme added to each reaction was consistent throughout each set of experiments.

Reactions involving DPAS, CS and TS were performed in 50 mM HEPES buffer pH 7.5. DPAS requires NADPH for activity, therefore 100 μM NADPH was added to each assay. Precondylocarpine acetate (DPAS substrate) (50 μM) delivered in MeOH (not exceeding 5 % of the reaction volume) was added to each reaction. 10-20 μg of enzymes were used in the assays. All reactions were performed at 37 °C for 1 h. For controls, protein sample was replaced with boiled protein sample or sample from culture of non-transformed yeast. After incubation, the reactions were quenched by addition of 1 volume of methanol, filtered through 0.22-μm nylon Spin-X centrifuge filters (Corning) and analyzed by LC/MS as described in the UPLC/MS and UPLC/QqQ-MS sections.

Purification of CS/TS substrate from plant material

Alkaloids from fully expanded leaves of *Tabernaemontana divaricata* "Flore pleno" (50 g) were extracted with acetonitrile (300 mL x 3). The extract was concentrated *in vacuo* and reconstituted in acetonitrile:water (70:30). The hydrophobic components were removed by passing through a C_{18} SPE cartridge (10 g). The flow-through was collected, dried and dissolved in 20 mL of 50 mM phosphate buffer pH 7.0. 5 mL of solution was sequentially applied to 500 mg WCX OASIS cartridges (Waters) equilibrated with phosphate buffer. Each cartridge was washed with buffer (6 mL), acetonitrile (6 mL), acetonitrile:water (50:50) solutions before elution with 100 mM $CaCl_2$ in acetonitrile:water (6 mL, 50:50). Fractions were lyophilized and reconstituted in acetonitrile:water (2 mL, 50:50) before subjection to reverse-phase preparative HPLC.

Preparative HPLC was performed on a Thermo Dionex Ultimate 3000 chromatography apparatus using a Phenomenex Luna C18 (5 µm, 30 x 250 mm) column. The solvents used were 0.01% acetic acid, solvent A, and acetonitrile, solvent B. A linear gradient from 5% B to 50% B over 25 min was used to separate the alkaloids. Chromatography was performed at a flow rate of 30 mL/min and monitored with a UV detector at 254 nm. Fractions (30 mL) were collected and assayed for CS and TS activity as follows. A 200 µL aliquot of each fraction was dried *in vacuo* and re-dissolved in 50 µL of 50 mM HEPES buffer pH 7.5. CS or TS enzyme (1 µg) was added to each sample and the reactions were incubated at 37 °C for 1 h. Control reactions without enzyme were also prepared. After incubation, the reactions were quenched by addition of 50 µL of MeOH, filtered and analyzed by UPLC/QqQ-MS as described above.

Purification of stemmadenine acetate from *C. roseus* leaves.

Leaves of plants in which PAS was silenced by VIGS were harvested 21 days post infection and frozen in liquid nitrogen. 20-50 g of frozen leaves were ground and extracted 3 times with acetonitrile (300 mL x 3). The extract was concentrated *in vacuo* and reconstituted in 100 mL acetonitrile:water (70:30). The hydrophobic components were removed by passing the sample through a C_{18} SPE cartridge (10 g). The flow-through was collected, dried and dissolved in 10 mL of acetonitrile:water (50:50).

Stemmadenine acetate **7** was purified by semi preparative HPLC on a Thermo Dionex Ultimate 3000 chromatography apparatus using a Waters Xbridge BEH C18 (5 µm, 10 x 250 mm) column. Mobile phase A was water containing 0.1% formic acid; mobile phase B was acetonitrile. The flow rate was 5 mL/min, and the gradient profile was 0 min, 10% B; from 0 to 30 min, linear gradient to 35% B; from 30 to 35 min, isocratic 35% B; from 35.1 to 37 min, wash at 95% B then back to the initial conditions of 10% B for 3 min. The injection volume was 500 µL. Elutions of the compounds was monitored at 268 nm. 5 mL fractions were collected throughout the purification and tested for the presence of the compounds by direct injection on an Advion express-ion Compact Mass Spectrometer in ESI^+ mode. Fractions containing the compound of interest were lyophilized.

Liquid-chromatography mass spectrometry analysis

UPLC/MS

This method was applied to the analysis of VIGS leaf extract, *in vitro* enzyme assays and synthetic products, unless otherwise indicated in the description of the experiments. UPLC/MS analysis was performed on a Shimadzu LCMS-IT-TOF Mass Spectrometer coupled to a Nexera

2 chromatographic system. Chromatographic separation was carried out on a Phenomenex Kinetex column 2.6 µm XB-C18 (100 × 2.10 mm), and the binary solvent system consisted of solvent A, H_2O + 0.1% formic acid, and solvent B, acetonitrile. Flow rate was 600 µL/min. A linear gradient from 10% to 30% solvent B in 5 min, allowed the separation of the alkaloids of interest. The column was then washed at 100% B for 1.5 min and re-equilibrated to 10% B. Injection volume was 1 µL.

Mass spectrometry was performed in positive ion mode with scanning over the *m/z* range from 150–1,200. The source settings were the following: heat block temperature 300 °C, nebulizing gas flow 1.4 L/min, CDL temperature 250 °C, detector voltage 1.6 kV. Data analysis was performed using the Shimadzu Profiling Solution software.

UPLC/QqQ-MS

This method was used to analyse samples from the *in vitro* pathway reconstitution using PAS expressed in *P. pastoris* and CS/TS reactions of alkaloid fractions purified from *Tabernaemontana divaricata* "Flore Pleno" leaves. UPLC/QqQ-MS analysis was carried out on a UPLC (Waters) equipped with an Acquity BEH C18 1.7 µm (2.1 x 50 mm) column connected to Xevo TQS (Waters). Chromatographic separation was performed using 0.1% NH_4OH as mobile phase A and acetonitrile as mobile phase B. A linear gradient from 0 to 65% B in 17.5 min was applied for separation of the compounds followed by an increase to 100% B at 18 min, a 2-min wash step and a re-equilibration at 0% B for 3 min before the next injection. The column was kept at 60 °C throughout the analysis and the flow rate was 0.6 mL/min.

MS detection was performed in positive ESI. Capillary voltage was 3.0 kV; the source was kept at 150 °C; desolvation temperature was 500 °C; cone gas flow, 50 L/h; and desolvation gas flow, 800 L/h. Unit resolution was applied to each quadrupole. The MRM transitions used to monitor the elution of the alkaloids of interest are reported in Table S3.

HR-MS

For high resolution MS analysis, compounds were infused at 5-10 µL/min using a Harvard Apparatus syringe pump onto a Synapt G2 HDMS mass spectrometer (Waters) calibrated using a sodium formate solution. Samples were analyzed for 1 minute with a scan time 1 sec in the mass range of 50-1200 m/z. Capillary voltage was 3.5 V, cone voltage 40 V, source temperature 120 ℃, desolvation temperature 350 ℃, desolvation gas flow 800 L/h. Leu-enkephaline peptide (1 ng/µL) was used to generate a dual lock-mass calibration with $[M+H]^+$ = 556.2766 and *m/z* = 278.1135 measured every 10 sec. Spectra were generated in MassLynx 4.1 by combining a number of scans, and peaks were centred using automatic peak detection with lock mass correction.

Proteomic analysis

PAS, DPAS, CS and TS transiently expressed in *N. benthamiana* leaves and pre-purified on NiNTA resin were precipitated with chloroform/methanol (*47*) and dissolved in 0.2 M TEAB/1% sodium deoxycholate (SDC), whilst PAS expressed in *P. pastoris* was extracted from SDS-PAGE. Protein concentration was determined using the Direct Detect™ Assay (Merck). 10 µg of protein was treated with DTT and iodoacetamide to reduce and alkylate cysteine residues and digested with 1 µg of trypsin (Promega) at 50 °C for 8 h. Approx. 0.5 µg of the digested protein

was used for data dependent LC-MS/MS analysis on an Orbitrap-Fusion™ mass spectrometer (Thermo Fisher) equipped with an UltiMate™ 3000 RSLCnano System (Thermo Fisher) using a nanoEase M/Z HSS C18 T3 1.8 µm, 150 µm x 100 mm, (Waters). The samples were loaded and trapped using a pre-column which was then switched in-line to the analytical column for separation. Peptides were eluted with a gradient of acetonitrile in water/0.1% formic acid (main step from 11-30.5% at a rate of 0.19% min^{-1}). The column was connected to a 10 µm SilicaTip™ nanospray emitter (New Objective) for infusion into the mass spectrometer. Data dependent analysis was performed using an HCD fragmentation method with the following parameters: positive ion mode, orbitrap MS resolution = 60k, mass range (quadrupole) = 300-1800 m/z, MS2 in ion trap, threshold $2e^4$, isolation window 1.6 Da, charge states 2-5, MS2 top20, AGC target $1.9e^4$, max inject time 35 ms, dynamic exclusion 1 count, 15 s exclusion, exclusion mass window ± 5 ppm. MS scans were saved in profile mode while MS2 scans were saved in centroid mode.

Raw files were processed with MaxQuant (version 1.6.1.0) (http://maxquant.org) (*48*). The searches were performed using the Andromeda search engine in MaxQuant on a custom database of the *N. benthamiana* sequences available from Uniprot to which the protein sequences of interest were added using trypsin/P with 2 missed cleavages, carbamidomethylation (C) as fixed and oxidation (M), acetylation (protein N-terminus), and deamidation (N,Q) as variable modifications. Mass tolerances were 4.5 ppm for precursor ions and 0.5 Da for fragment ions.

Synthesis procedures

General and NMR analysis

Progress of the reactions was monitored by direct injection on an Advion express-ion Compact Mass Spectrometer in ESI^+ mode. The mobile phase was 0.1% formic acid in water:methanol (10:90). LC/MS analysis was performed using the method described in the UPLC/MS section, unless otherwise stated. High-resolution mass spectrometry was performed as described in the HR-MS section. NMR spectra (1D and 2D NMR) were acquired using a Bruker Avance III 400 NMR spectrometer equipped with a BBFO plus 5 mm probe, unless stated otherwise. The residual ^1H and ^{13}C NMR signals of CD_3OD (δ 3.31 and 49.0, respectively), CD_3CN (δ 1.94 and 1.32, respectively) and $CDCl_3$ (δ 7.26 and 77.16, respectively) were used for calibration. The number of scans depended on sample concentration and are indicated in SI Figures and Tables accordingly.

*Synthesis of stemmadenine acetate (**7**)*

To a 1.5-mL HPLC vial containing stemmadenine **1** (10.2 mg, 0.0289 mmol), pyridine (400 µL) was added. The mixture was sonicated and stirred at r.t until complete dissolution was achieved. Acetic anhydride (50 µL, 0.529 mmol) was subsequently added to the reaction vessel and the reaction was allowed to stir at r.t for 4 h. Reaction progress was monitored by MS direct-injection of 1 µL of the reaction mixture in 100 µL of methanol. The reaction was quenched with methanol (1 mL) once peak for SM at *m/z* 355 was no longer observed. The reaction was then concentrated *in vacuo* at 30 °C. Toluene (350 µL) and methanol (150 µL) was added to reaction vial, sonicated to homogeneity and concentrated *in vacuo* at 30 °C (repeated x4) to afford **33** (ca. 11.4 mg, 0.0287 mmol, 99%) as a dark brown solid.

*Synthesis of precondylocarpine acetate (**10**)*

Synthesis of precondylocarpine acetate was performed as reported by Scott and co-workers (*8*) with some modifications. Briefly, Adam's catalyst (≥ 75 m^2/g, 25.2 mg, 0.112 mmol, 7.5 equivalents) was reduced with H_2 in ethyl acetate (1 mL) for 2 h. The apparatus was flushed with nitrogen for 5 min. The freshly prepared platinum in ethyl acetate was transferred to a 25-mL pear-shaped flask containing stemmadenine acetate **7** (6 mg, 0.0152 mmol) dissolved in ethyl acetate (1 mL) via glass pipette. An oxygen atmosphere was introduced by a balloon to the reaction vessel via Agani 1.5-inch needle. The reaction mixture was allowed to stir vigorously at r.t. Reaction progress was monitored by dissolving 1 µL of the reaction mixture in 100 µl of methanol, filtered through a 0.2 µm PTFE syringe filter before injection on the Advion MS. Fresh batch of Pt catalyst was prepared and added as above when product:SM ratio appeared to stagnate. The reaction was stopped when amount of SM was <5% product (estimated via Advion MS) to prevent formation of by-product(s). After flushing the reaction vessel with N_2, gravity filtration with ethyl acetate (10 mL) gave a pale-yellow solution. The filtrate was concentrated *in vacuo* at 25 °C to afford a dark yellow solid (crude yield: 2.6 mg, ~60% pure based on ^{1}H NMR).

*Synthesis of dihydroprecondylocarpine acetate (**11**)*
Synthesis of dihydroprecondylocarpine acetate was performed as reported by Scott and co-workers (*8*) with some modifications. Briefly, Adam's catalyst (≥ 75 m^2/g, 0.8 mg, 3.524 µmol) was reduced with H_2 in ethanol (400 µL) for 2 h. The apparatus was flushed with nitrogen for 5 min. The freshly prepared platinum in ethanol was transferred to a 1.5-mL HPLC vial containing crude precondylocarpine acetate **10** (ca. 200 µg, 0.508 µmol) dissolved in ethanol (100 µL) via glass pipette. A hydrogen atmosphere was introduced by a balloon to the reaction vessel. The reaction mixture was allowed to stir vigorously at r.t. overnight. The reaction vessel was flushed with N_2, followed by filtration of the reaction mixture using 0.2 µm PTFE syringe filter, and washing of the filter with EtOH (200 µL × 2), and concentrating the filtrate *in vacuo* yielded a compound (yield undetermined due to small scale) which showed activity in enzymatic assays with CS, and TS, forming catharanthine **3**, and tabersonine **2**, respectively. Due to the small scale and instability, the compound could not be further characterized though.

*Synthesis of condylocarpine (**13**)*
Synthesis of condylocarpine was performed analogously to that for precondylocaprine acetate **10**. Adam's catalyst (≥ 75 m2/g,, 2.30 mg, 10.1 µmol, 7.5 equivalents) was reduced with H_2 in ethyl acetate (1 mL) until solution turned black. The apparatus was flushed with nitrogen for 5 min. The freshly prepared platinum in ethyl acetate was transferred to a 1.5-mL HPLC vial containing stemmadenine **1** (0.48 mg, 1.36 µmol). An oxygen atmosphere was introduced by a balloon to the reaction vessel via Agani 1.5-inch needle. Reaction progress was monitored by dissolving 1 µL of the reaction mixture in 100 µl of methanol, filtered through a 0.2 µm PTFE syringe filter before injection on the Advion MS in ESI^+ mode. After 2h, conversion reached ca. 26%, which did not improve by 4 h. The reaction was stopped to prevent formation of by-product(s). After flushing the reaction vessel with N2, the reaction mixture was filtered as above and the catalyst was washed with ethyl acetate (6 mL), and concentrating in vacuo yielded a yellow residue. The product was the isolated by preparative HPLC on a Waters Xbridge BEH C18 (5 µm, 10 x 250 mm) column. Mobile phase A was water containing 0.1% formic acid; mobile phase B was acetonitrile. The flow rate was 5 mL/min, and the gradient profile was 0 min, 10% B; from 0 to 30 min, linear gradient to 40% B; from 30 to 35 min, linear gradient to 95% B; from 35 to 39 min, wash at 95% B then back to the initial conditions of 10% B in 1 min

for 5 min. The injection volume was 500 µL. Elution of the compounds was monitored at 290 nm. 2.5 mL fractions were collected throughout the purification and tested for the presence of the compounds by direct injection on the Advion MS in ESI^+ mode.

Localization and Interaction studies

Subcellular localizations of DPAS, CS and TS were studied by creating fluorescent fusion proteins transiently expressed in *C. roseus* cells using the pSCA-cassette YFPi plasmid (*49*). This plasmid allows the expression of the YFP-fusion protein under the control of the strong constitutive 35S promoter. Full-length open reading frames encoding each enzyme were amplified using specific primer couples (Table S1), which were designed to introduce the *Spe*I restriction site at both cDNA extremities. PCR products were sequenced and cloned at the 5'end of the yellow fluorescent protein (YFP) coding sequence, to generate the DPAS-, TS-, CS-YFP fusion proteins or at the 3'end to express the YFP-DPAS, YFP-TS and YFP-CS fusions. The coding sequences of the first forty or sixty amino acids of PAS encompassing the ER-to-vacuole targeting sequence (as predicted by TargetP1.1 http://www.cbs.dtu.dk/services/TargetP/) were amplified by mixing PAS-YFPfor with PAS40-YFPrev or PAS60-YFPrev (Table S1) before cloning into the *Spe*I restriction site of pSCA-cassette YFPi to express sp40-YFP and sp60-YFP. All final constructs were sequenced before plant cell transformations.

Interactions of DPAS with CS and TS were characterized by bimolecular fluorescence complementation (BiFC) assays using the previously amplified CS and TS PCR products cloned via *Spe*I into the pSCA-SPYNE173 (*50*) to express CS-YFP^N and TS –YFP^N; and using DPAS amplicon cloned into pSCA-SPYCE (MR) (*51*) to express YFP^C-DPAS. Plasmids encoding LAMT-YFP^N and LAMT-YFP^C were used as controls and were constructed previously (*52*). Again, all these plasmids allow expression driven by the constitutive 35S promoter and were sequenced before transient transformations.

Transient transformation of *C. roseus* cells by particle bombardment and fluorescence imaging were performed following the procedures previously described (*49,53*). The *C. roseus* cells used for localization and interaction studies correspond to the C20A strain that has been established previously (*53*). C20A cells were grown in the dark in Gamborg B5 medium at 24°C under continuous shaking (100 rpm) and were sub-cultured every 7 days. For transient transformation, 3 day-old cells were plated onto solid Gamborg B5 medium (8 g/l agar) supplemented with 10 µM naphthalene acetic acid. Plated cells were then cultivated during 48h in the dark at 24°C before bombardment. For each bombardment, 400 ng of pSCA plasmid or 100 ng of BiFC plasmids were coated onto gold particles as described (*54*). *C. roseus* plated cells were then bombarded with these DNA-coated gold particles (1 µm) and 1100 psi rupture disc at a stopping-screen-to-target distance of 6 cm, using the Bio-Rad PDS1000/He system. Cells were cultivated in the dark for either 16 h to 38 h (DPAS, CS and TS) or up to 96 h (PAS) and for 16 hours for interaction studies before being harvested and observed. Before observation, cells were collected from the bombarded Petri dishes and re-suspended in liquid Gamborg B5 medium without hormones and mounted on microscope slides. The subcellular localization was determined using an Olympus BX-51 epifluorescence microscope equipped with an Olympus DP-71 digital camera and a combination of YFP and CFP filters. The pattern of localization presented in this work is representative of *circa* 100 observed cells and each experiment was repeated three times independently. Localizations of the different fusion proteins were confirmed by co-

transformation experiments using a nuclear-CFP marker, an ER-CFP marker, vacuole-CFP marker or a nucleocytosolic-CFP marker (*50,52*). For interaction studies, BiFC plasmids were co-transformed with a plasmid expressing the nucleus CFP marker allowing identification and collect of the transformed cells. Protein interactions were then evaluated in this cell fraction by observing BiFC complex reconstitution through YFP fluorescence. Additional evaluations of interactions were also conducted before cell collection by observing several areas of the transformed plated cells on petri dishes at low magnification.

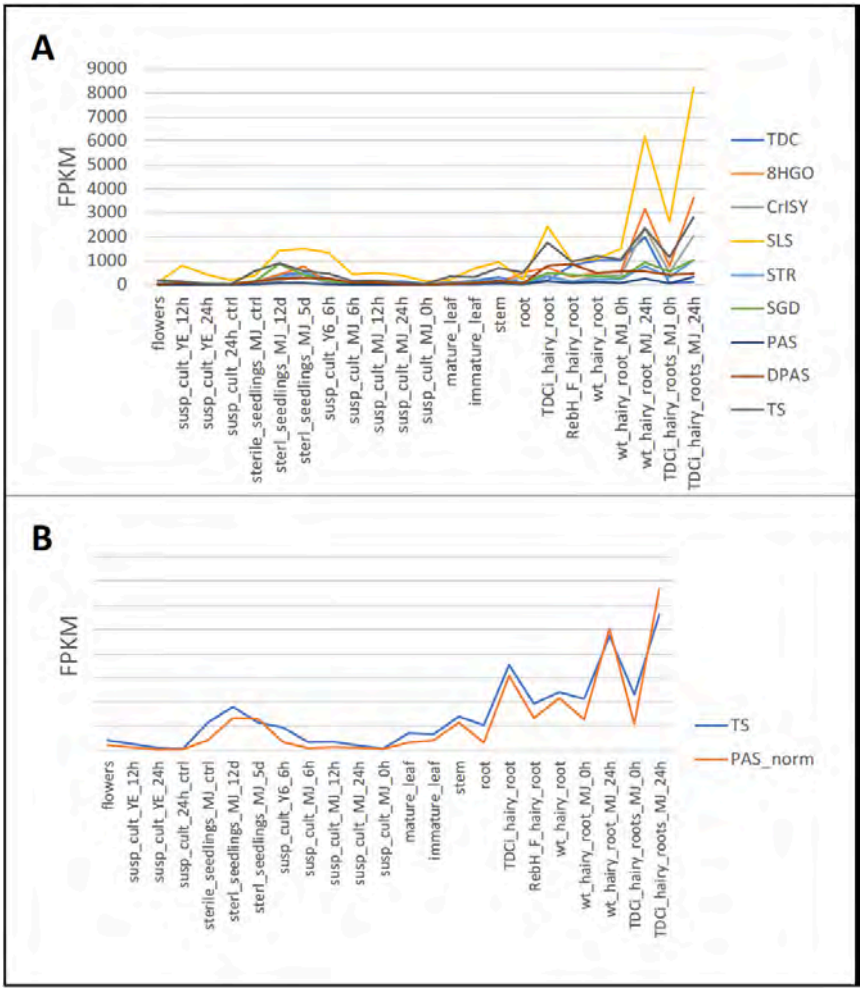

Fig. S1.

Co-expression analysis for biosynthetic gene candidates. **A.** Expression profile of some of the genes involved in *C. roseus* MIA pathway and those investigated in this study. Data were extracted from the http://medicinalplantgenomics.msu.edu/index.shtml database. **B.** Co-expression profile of TS and PAS. The FPKM values for PAS were multiplied by a factor 10 in order to be comparable to those of TS. TDC=Tryptophan decarboxylase; 8HGO=Geraniol 8-hydroxylase; CrISY=Iridoid synthase; SLS=Secologanin synthase; STR=Strictosidine synthase; SGD=Strictosidine-O-beta-D-glucosidase; PAS=Precondylocarpine acetate synthase; DPAS=Dehydroprecondylocarpine acetate synthase; TS=Tabersonine synthase. TS was initially annotated in the transciptome dataset as 2-hydroxyisoflavanone dehydratase.

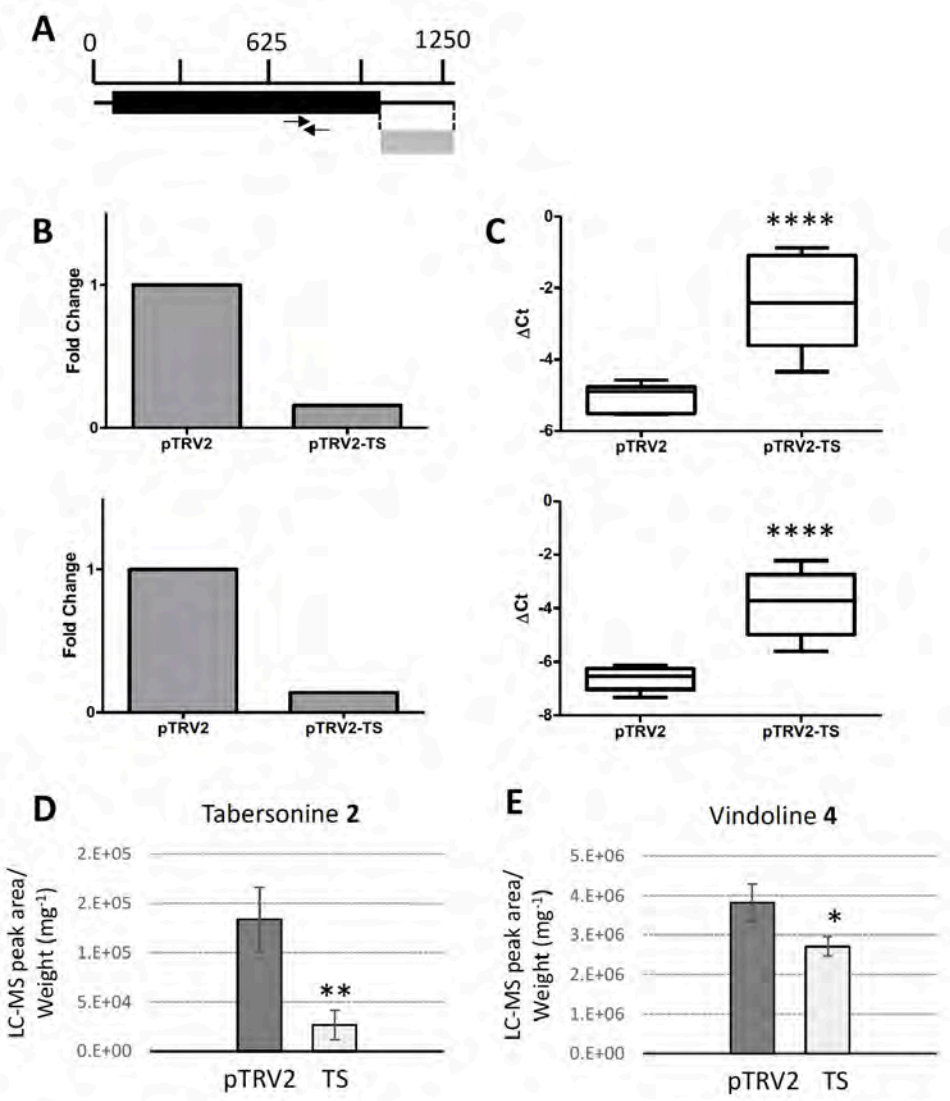

Fig. S2.

Virus-induced gene silencing of TS in *C. roseus* using a unique region of the gene. A. Fragment (grey box) of TS cDNA used to assemble the pTRV2 construct. The black box represents the coding region, whereas the black lines are the flanking untranslated regions. Arrows show the annealing sites of the primers used for qRT-PCR analysis (Table S1). B. Fold transcript change in TS silenced (pTRV2-TS) plants compared to TS control (pTRV2) plants. Values were calculated using $2^{-\Delta\Delta Ct}$. Upper panel calculated using the EXP reference gene. Lower panel calculated using the N2227 reference gene. C. Box plots of ΔCt values of 8 biological replicates for control (pTRV2) and CrTS silenced (pTRV2-TS) plants with median, min and max values indicated. Asterisks represent significant differences determined using an unpaired, two-tailed t test (**** = $p<0.0001$). Upper panel calculated using the EXP reference gene. Lower panel calculated using the N2227 reference gene. D. UPLC-MS analysis of TS silenced leaves showed a significant decrease of tabersonine and vindoline E. Data shown corresponds to average measurements of 12 plants. Error bars indicate standard error of the mean. Statistical significance calculated with Student's t test (pTRV2 in comparison to pTRV2-TS) is indicated as followed: * = $p<0.05$ and ** = $p<0.005$.

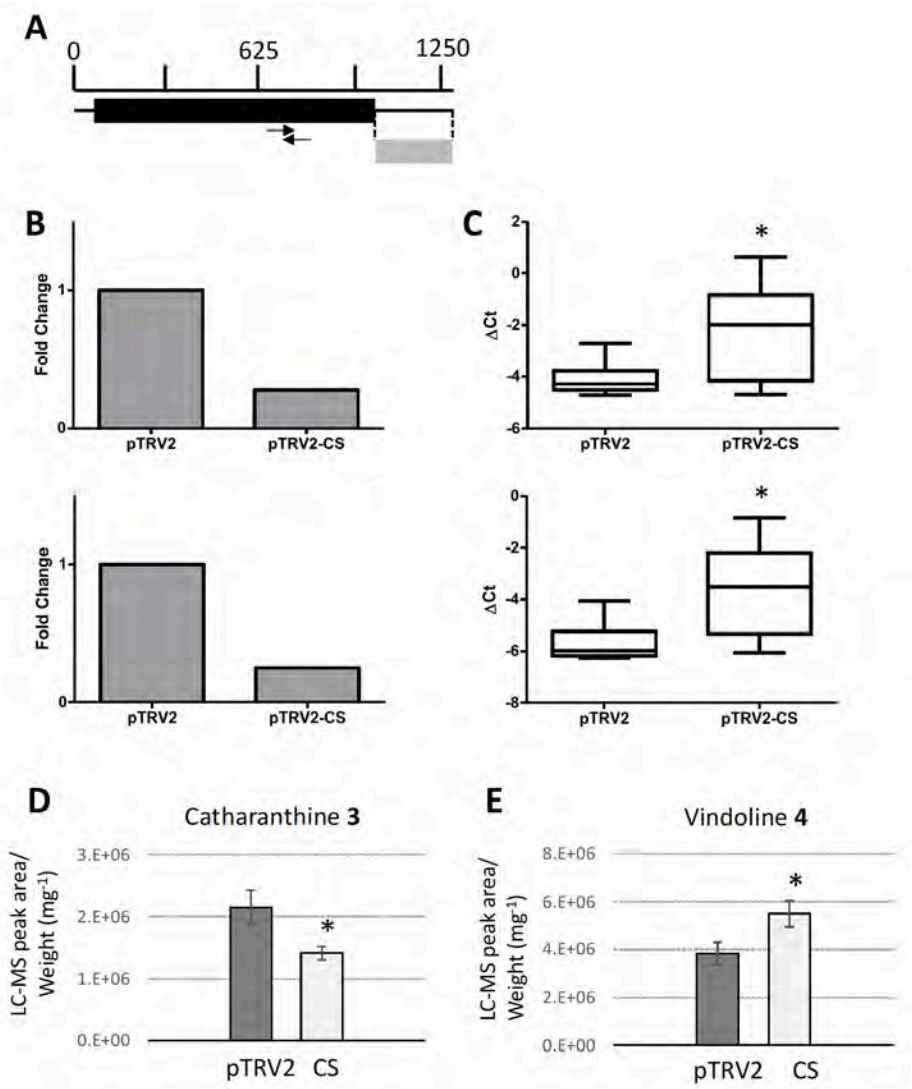

Fig. S3.
Virus-induced gene silencing of CS in *C. roseus* using a unique region of the gene. **A.** Fragment (grey box) of CS cDNA used to assemble the pTRV2 construct. The black box represents the coding region, whereas the black lines are the flanking untranslated regions. Arrows show the annealing sites of the primers used for qRT-PCR analysis (Table S1). **B.** Fold transcript change in CS silenced (pTRV2-CS) plants compared to CS control (pTRV2) plants. Values were calculated using $2^{-\Delta\Delta Ct}$. Upper panel calculated using the EXP reference gene. Lower panel calculated using the N2227 reference gene. **C.** Box plots of ΔCt values of 8 biological replicates for control (pTRV2) and CS silenced (pTRV2-CS) plants with median, min and max values indicated. Asterisks represent significant differences determined using an unpaired, two-tailed t-test (* = $p<0.05$). Upper panel calculated using the EXP reference gene. Lower panel calculated using the N2227 reference gene. **D.** UPLC-MS analysis of CS silenced leaves showed a significant decrease of catharanthine and increase of vindoline (**E**). Data shown corresponds to average measurements of 12 plants. Error bars indicate standard error of the mean. Statistical significance calculated with Student's t test (pTRV2 in comparison to pTRV2-CS) is indicated as followed: * = $p<0.05$.

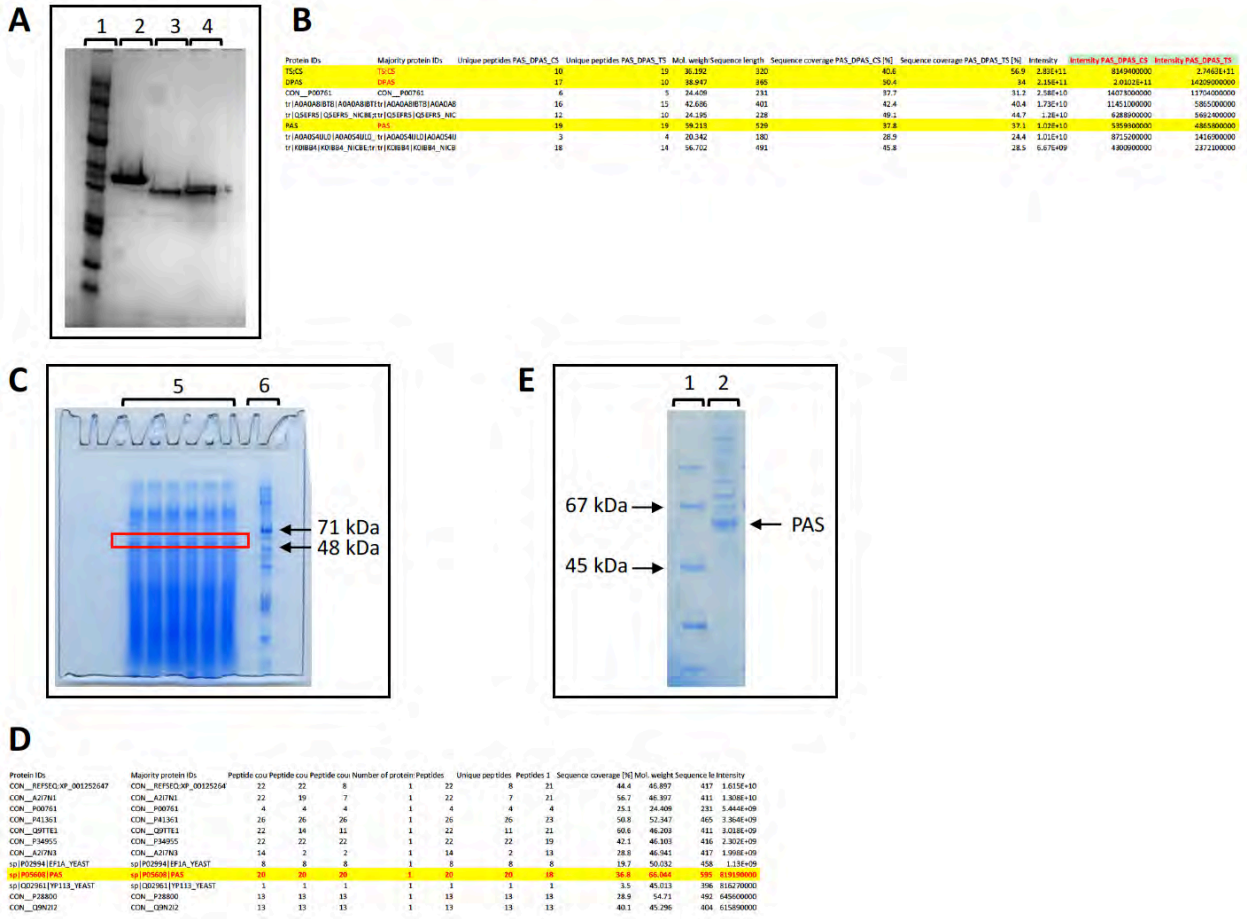

Protein IDs	Majority protein IDs	Unique peptides PAS_DPAS_CS	Unique peptides PAS_DPAS_TS	Mol. weigh/Sequence length	Sequence coverage PAS_DPAS_CS [%]	Sequence coverage PAS_DPAS_TS [%]	Intensity	Intensity PAS_DPAS_CS	Intensity PAS_DPAS_TS
TS;CS	TS;CS	10	19	36.192	320	40.6	56.9	2.83E+11	8149400000	2.74631E+11
DPAS	DPAS	17	10	38.947	345	50.4	34	2.15E+11	2.01213+11	14029000000
CON__P00761	CON__P00761	6	5	24.409	231	37.7	31.2	2.58E+10	14073000000	11704000000
tr|A0A0A8IBT8|A0A0A8IBT8;tr|A0A0A8IBT8|A0A0A8		16	15	42.686	401	42.4	40.4	1.73E+10	11451000000	5865000000
tr|Q5EFR5|Q5EFR5_NICBE;tr|Q5EFR5|Q5EFR5_NIC		12	10	24.195	228	49.1	44.7	1.28E+10	6288900000	5692400000
PAS	PAS	19	19	59.213	539	37.8	37.1	1.03E+10	5359900000	4865800000
tr|A0A0S4IUZ1|A0A0S4IUZ1_	tr|A0A0S4IUZ1|A0A0S4IU	3	4	20.342	180	28.9	24.4	1.01E+10	871200000	1416000000
tr|K0IBB4|K0IBB4_NICBE;tr|K0IBB4|K0IBB4_NICB		18	14	56.702	491	45.8	28.5	6.67E+09	4800900000	2372100000

Protein IDs	Majority protein IDs	Peptide cou	Peptide cou	Peptide cou	Number of protein	Peptides	Unique peptides	Peptides 1	Sequence coverage [%]	Mol. weight	Sequence le	Intensity
CON__REFSEQ:XP_001252647	CON__REFSEQ:XP_00125264	22	22	8	1	22	8	21	44.4	46.897	417	1.61E+10
CON__A2I7N1	CON__A2I7N1	22	19	7	1	22	7	21	56.7	46.397	411	1.30E+10
CON__P00761	CON__P00761	4	4	4	1	4	4	4	25.1	24.409	231	5.44E+09
CON__P41361	CON__P41361	26	26	26	1	26	26	23	50.8	52.347	465	3.36E+09
CON__Q9TTE1	CON__Q9TTE1	22	14	11	1	22	11	21	60.6	46.203	411	3.01E+09
CON__P34955	CON__P34955	22	22	22	1	22	22	19	42.1	46.103	416	2.30E+09
CON__A2I7N3	CON__A2I7N3	14	2	2	1	14	2	13	28.8	46.941	417	1.99E+09
sp|P02994|EF1A_YEAST	sp|P02994|EF1A_YEAST	8	8	8	1	8	8	8	19.7	50.032	458	1.13E+09
sp|P05608|PAS	sp|P05608|PAS	20	20	20	1	20	20	18	36.8	66.044	595	819190000
sp|Q02961|YP113_YEAST	sp|Q02961|YP113_YEAST	1	1	1	1	1	1	1	3.5	45.013	396	816270000
CON__P28800	CON__P28800	13	13	13	1	13	13	13	28.9	54.71	492	645600000
CON__Q9N2I2	CON__Q9N2I2	13	13	13	1	13	13	13	40.1	45.296	404	615890000

Fig. S4.
SDS-PAGE and proteomics were used to analyze the proteins purified for *in vitro* activity assays. **A.** SDS-PAGE of DPAS, CS and TS expressed in *E. coli* and purified by His-trap and gel-filtration. Lane 1: protein molecular markers; lane 2: DPAS; lane 3: CS; lane 4: TS. **B.** Snapshot of the proteomics results (complete analysis can be found in Supplementary dataset 3) of NiNTA-purified PAS, DPAS and CS or PAS, DPAS and TS (pathway reconstitution in *N. benthamiana*) expressed in *N. benthamiana* leaves. **C.** SDS-PAGE of PAS expressed in *P. pastoris*. Lanes indicated with 5 were loaded with PAS enriched medium; lane 6: protein molecular markers. The red box indicates the section of the gel that was excised and used for proteomics analysis. **D.** Snapshot of the proteomics results (complete analysis can be found in Supplementary dataset 2) showing that PAS was indeed present in the sample and it was amongst the most abundant proteins. **E.** SDS-PAGE of PAS expressed in insect cells and purified by His-trap. Lane 1: protein molecular markers; lane 2: PAS

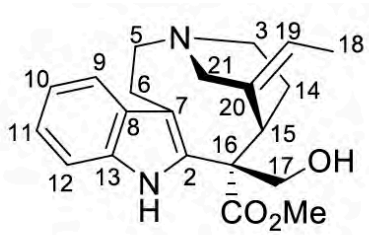

^{1}H NMR

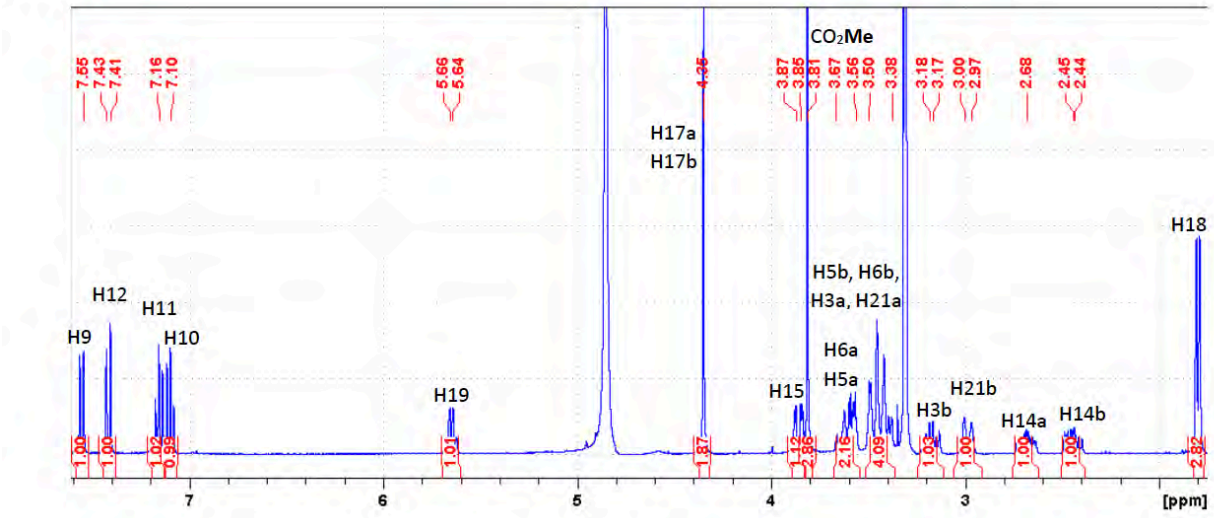

COSY

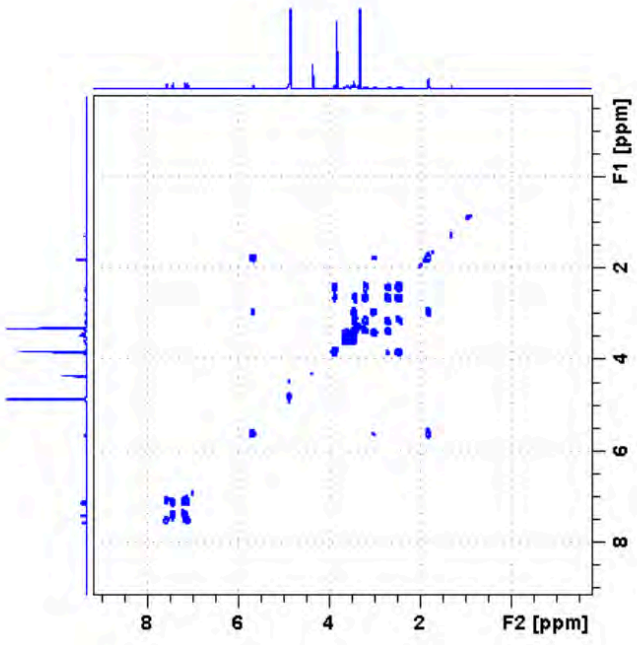

Fig. S5.

NOESY

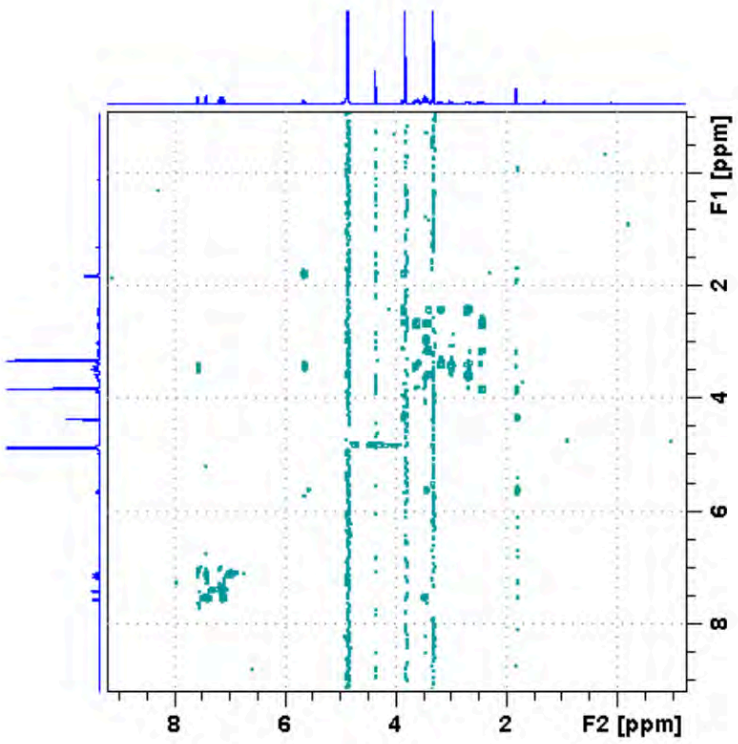

^{13}C NMR

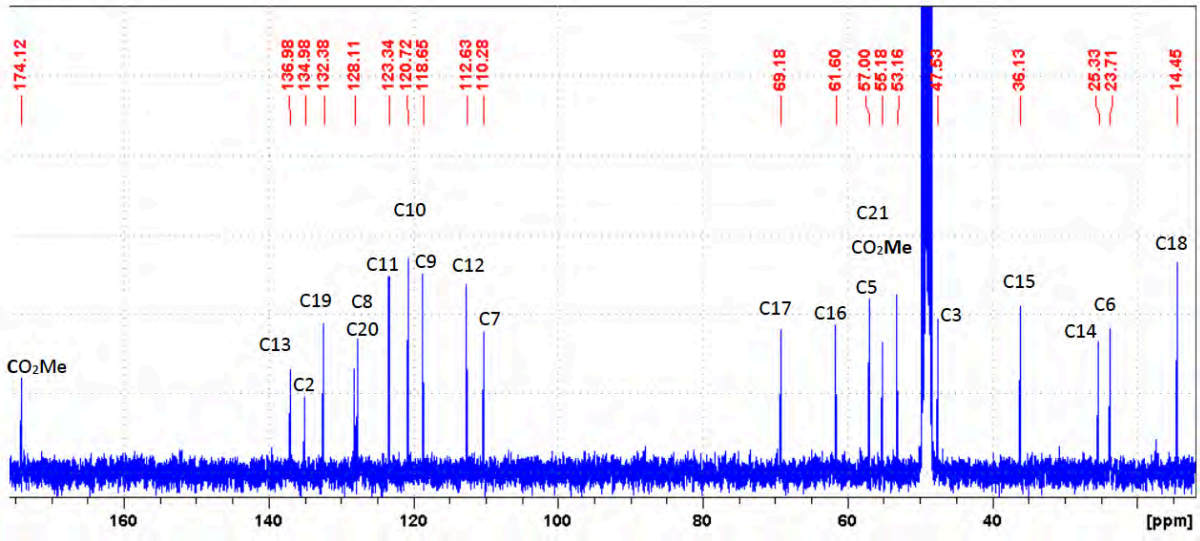

Fig. S5. (Continued)

HSQC

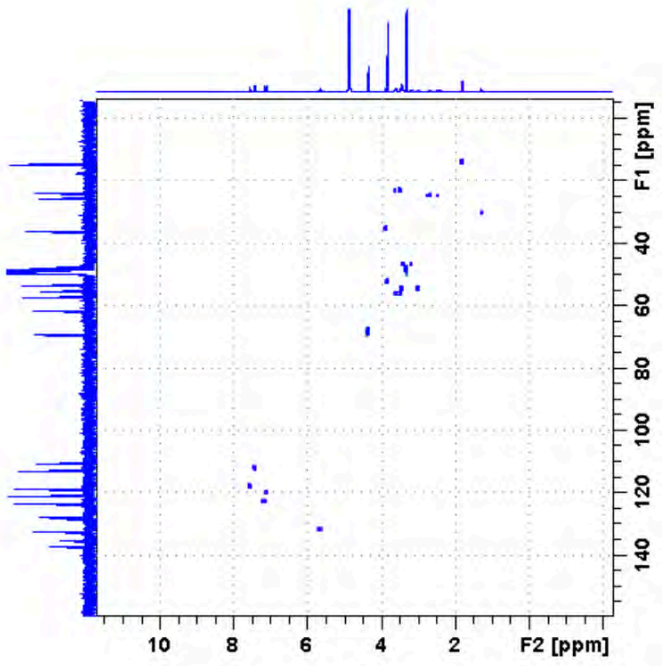

HMBC

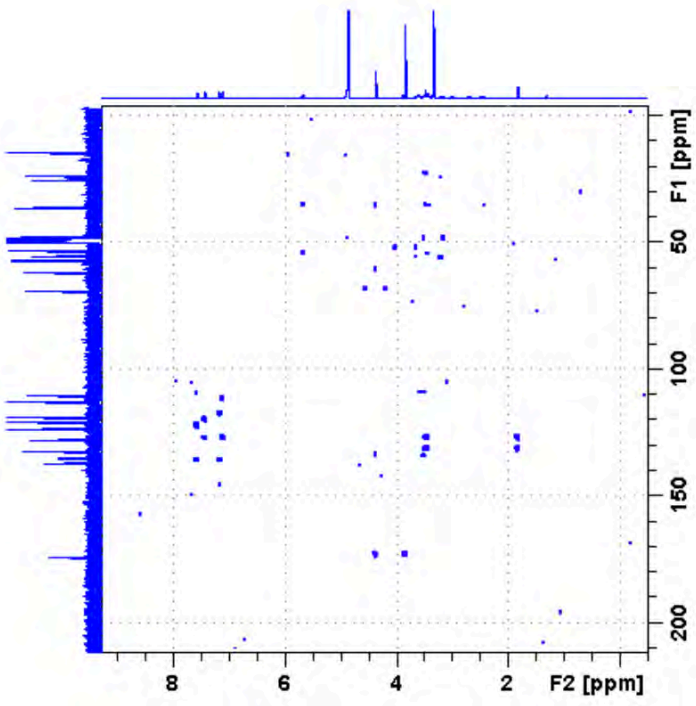

Fig. S5. (Continued)
NMR spectra for stemmadenine **1** (MeOD, 300 K, 400 MHz). Proton: 64 scans; COSY: 32 scans, NOESY: 32 scans; HSQC: 32 scans; HMBC: 32 scans.

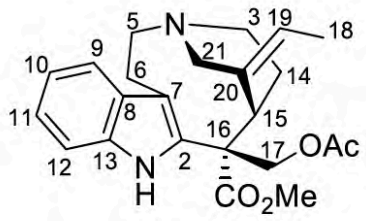

Proton

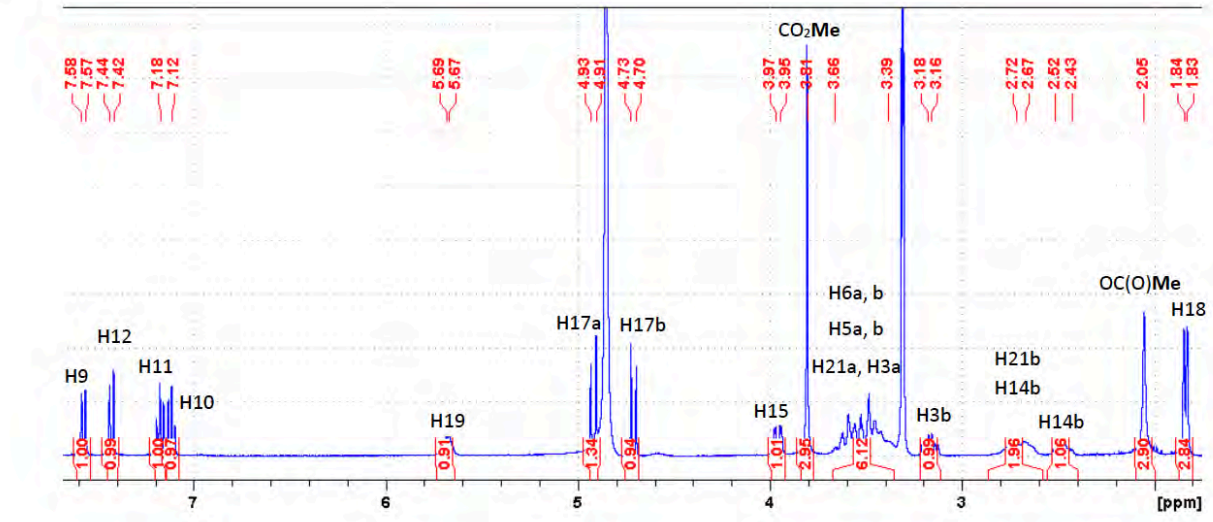

COSY

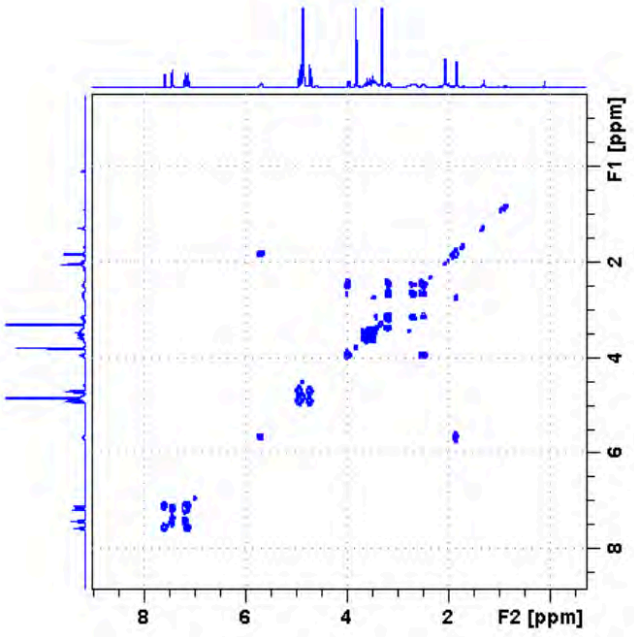

Fig. S6.

TOCSY

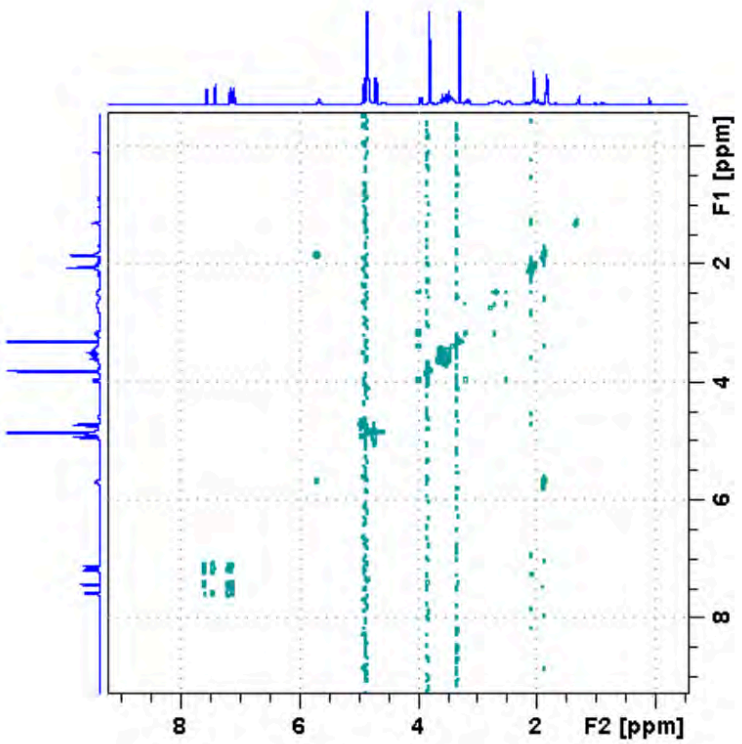

NOESY

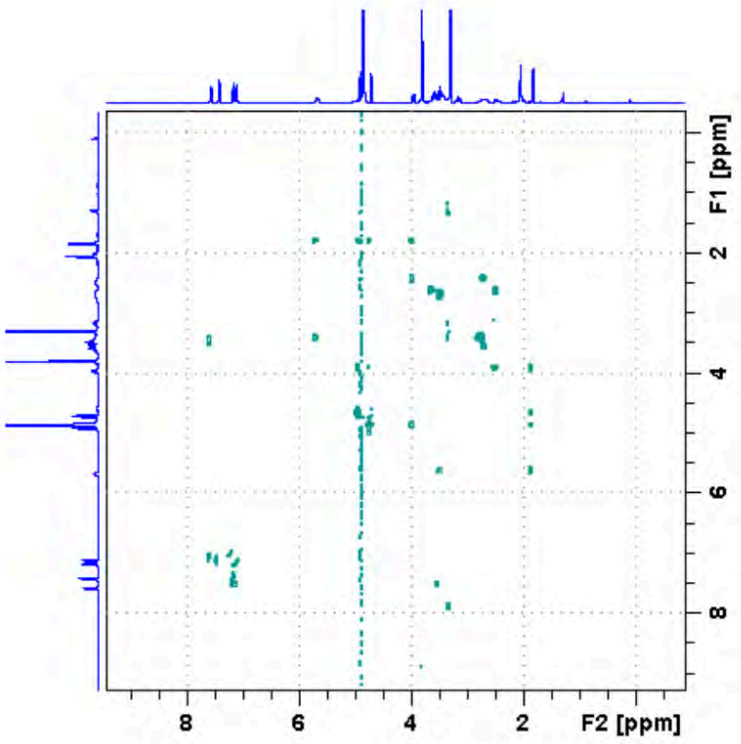

Fig. S6. (continued)

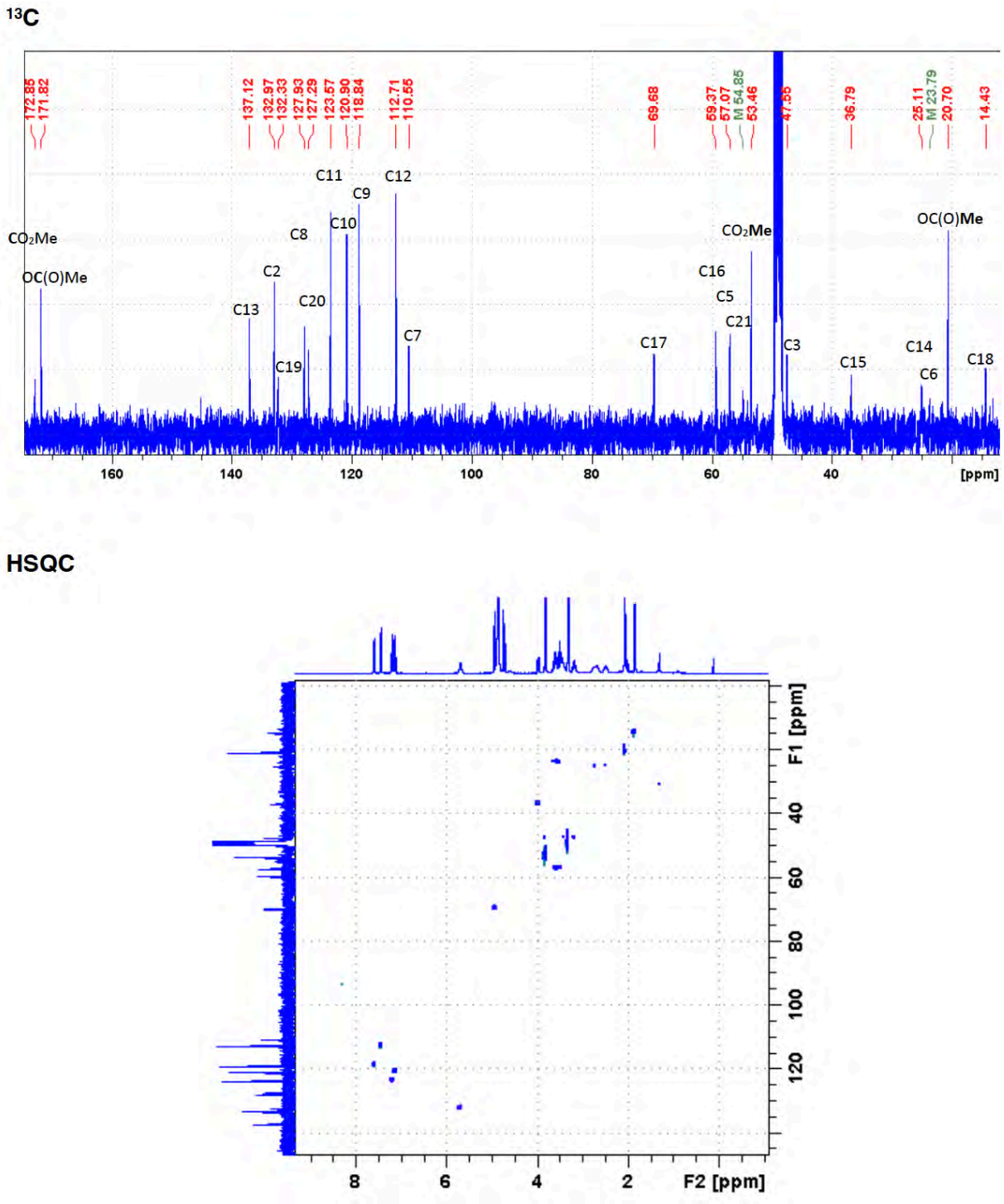

Fig. S6. (continued)

HMBC

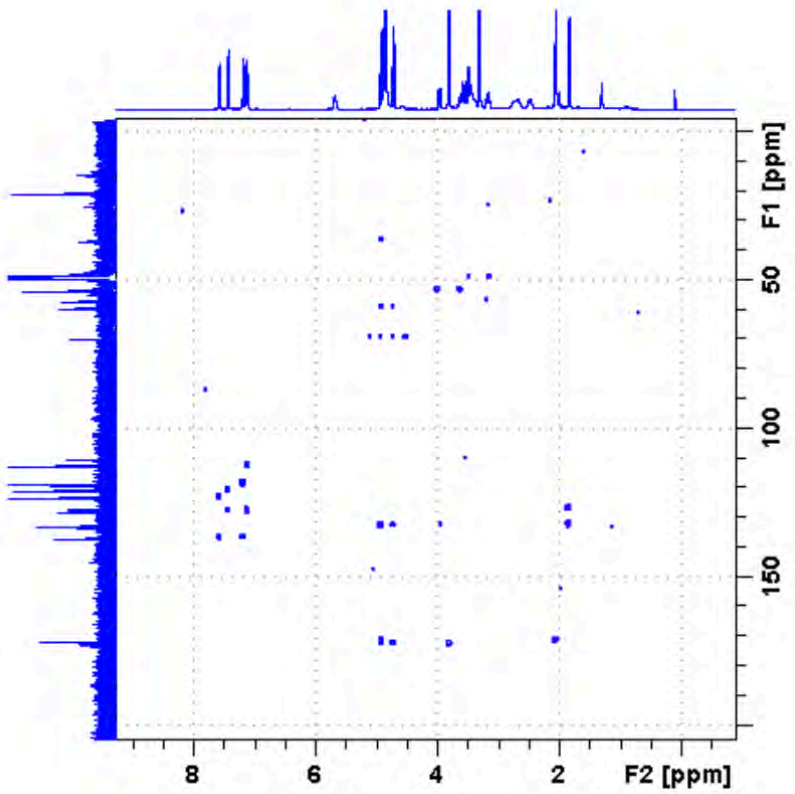

Fig. S6. (continued)
NMR spectra for stemmadenine acetate **7** (MeOD, 300 K, 400 MHz). Proton: 16 scans; COSY: 4 scans; NOESY: 4 scans; TOCSY: 4 scans; Carbon: 4096 scans; HSQC: 4 scans; HMBC: 8 scans.

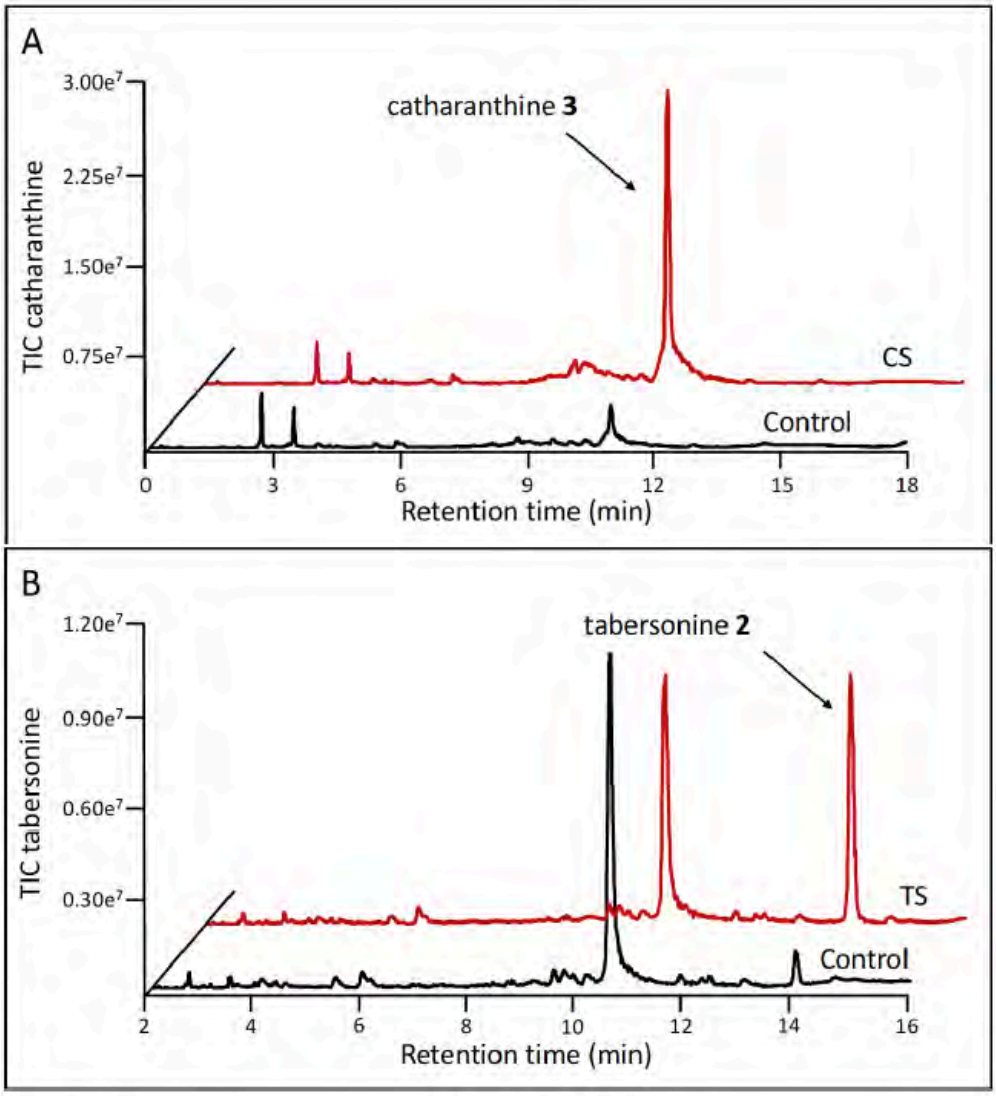

Fig. S7.
Activity guided fractionation of CS/TS substrate from *Tabernaemontana divaricata* leaves. Fractions collected during preparative HPLC were assayed for the presence of the substrate using CS and TS. **A.** A fraction reacted with CS showed formation of catharanthine **3** after UPLC/QqQ-MS analysis. Catharanthine **3** was not formed in the control samples (no enzyme). **B.** The same fraction reacted with TS showed formation of tabersonine **2** after UPLC/QqQ-MS analysis. Tabersonine **2** was not formed in the control samples (no enzyme). Very small peaks of endogenous catharanthine and tabersonine co-purifying with the CS/TS substrate were present in the control samples.

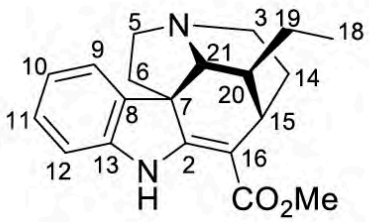

Proton

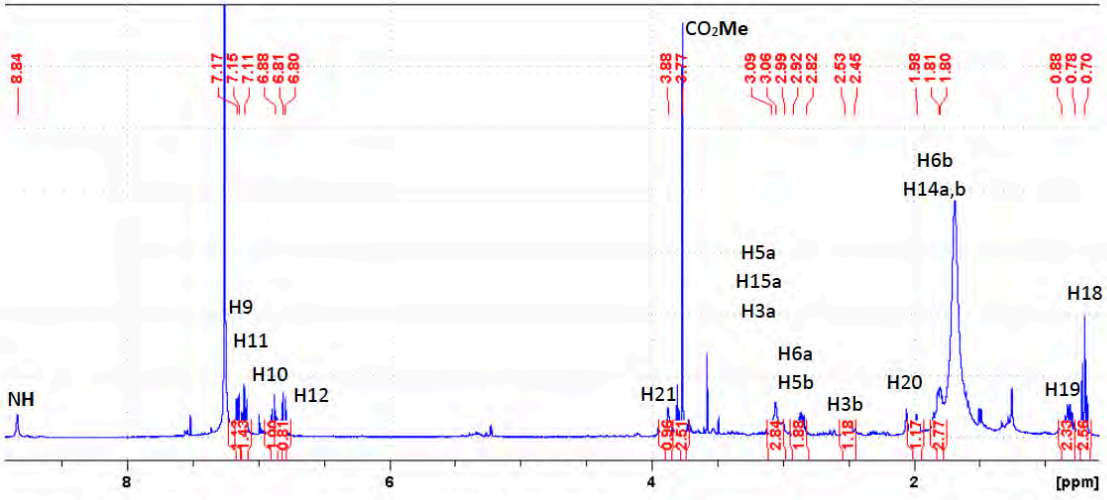

COSY

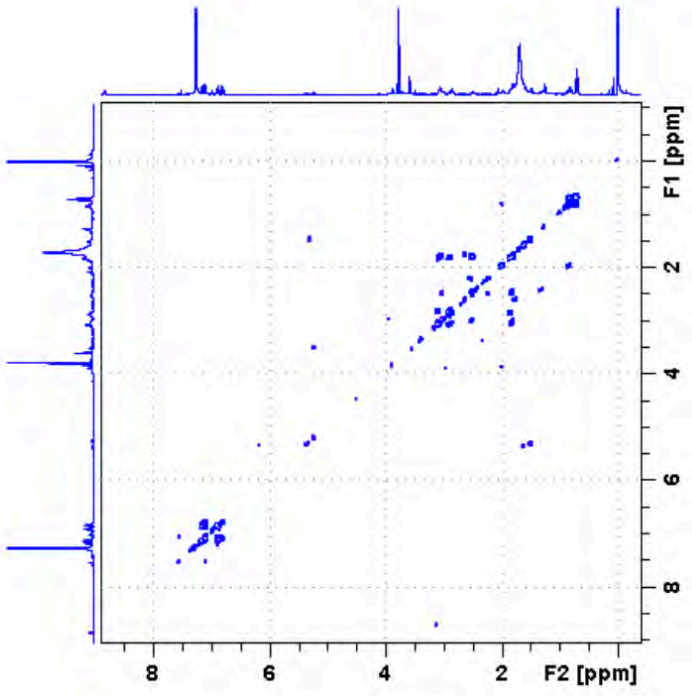

Fig. S8.

NOESY

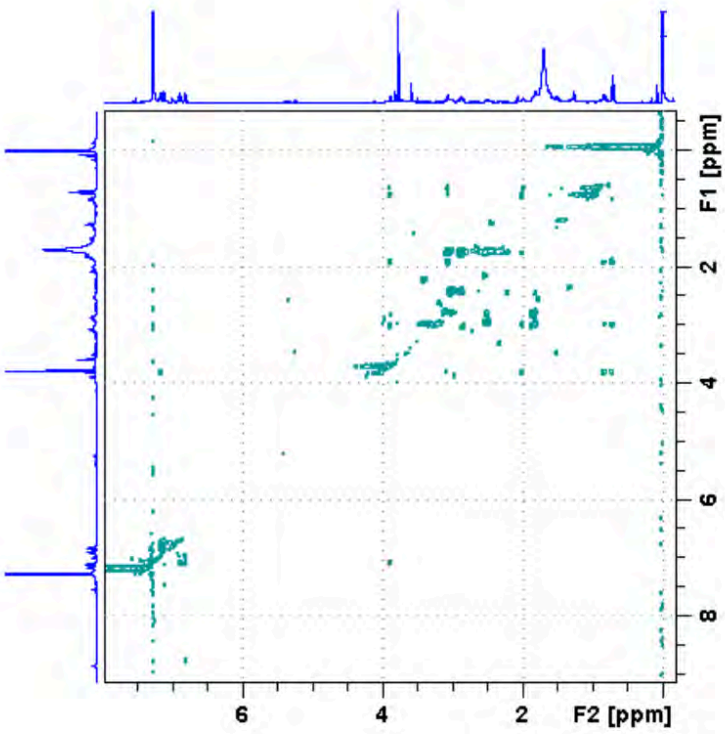

HSQC

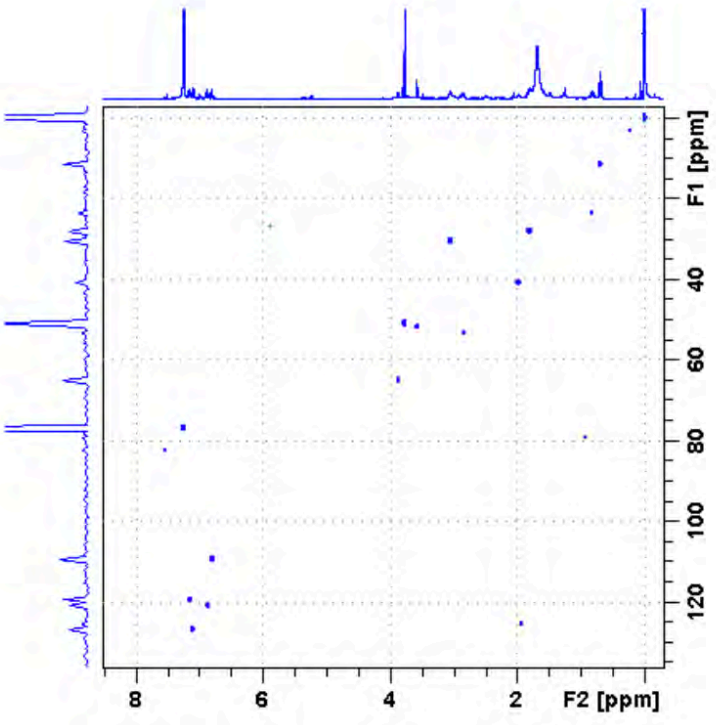

Fig S8. (continued)

HMBC

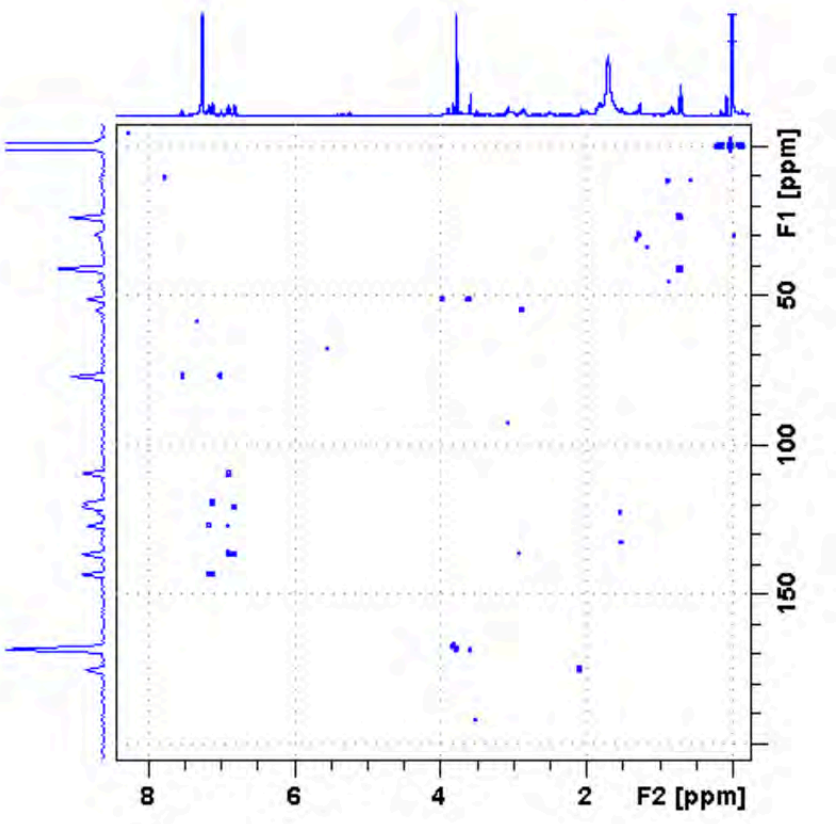

Fig S8. (continued)
NMR data of decomposed CS/TS substrate isolated from plants, tubotaiwine **12** ($CDCl_3$, 300 K, 400 MHz). Proton: 512 scans; COSY: 16 scans; NOESY: 24 scans; HSQC: 32 scans; HMBC: 500 scans.

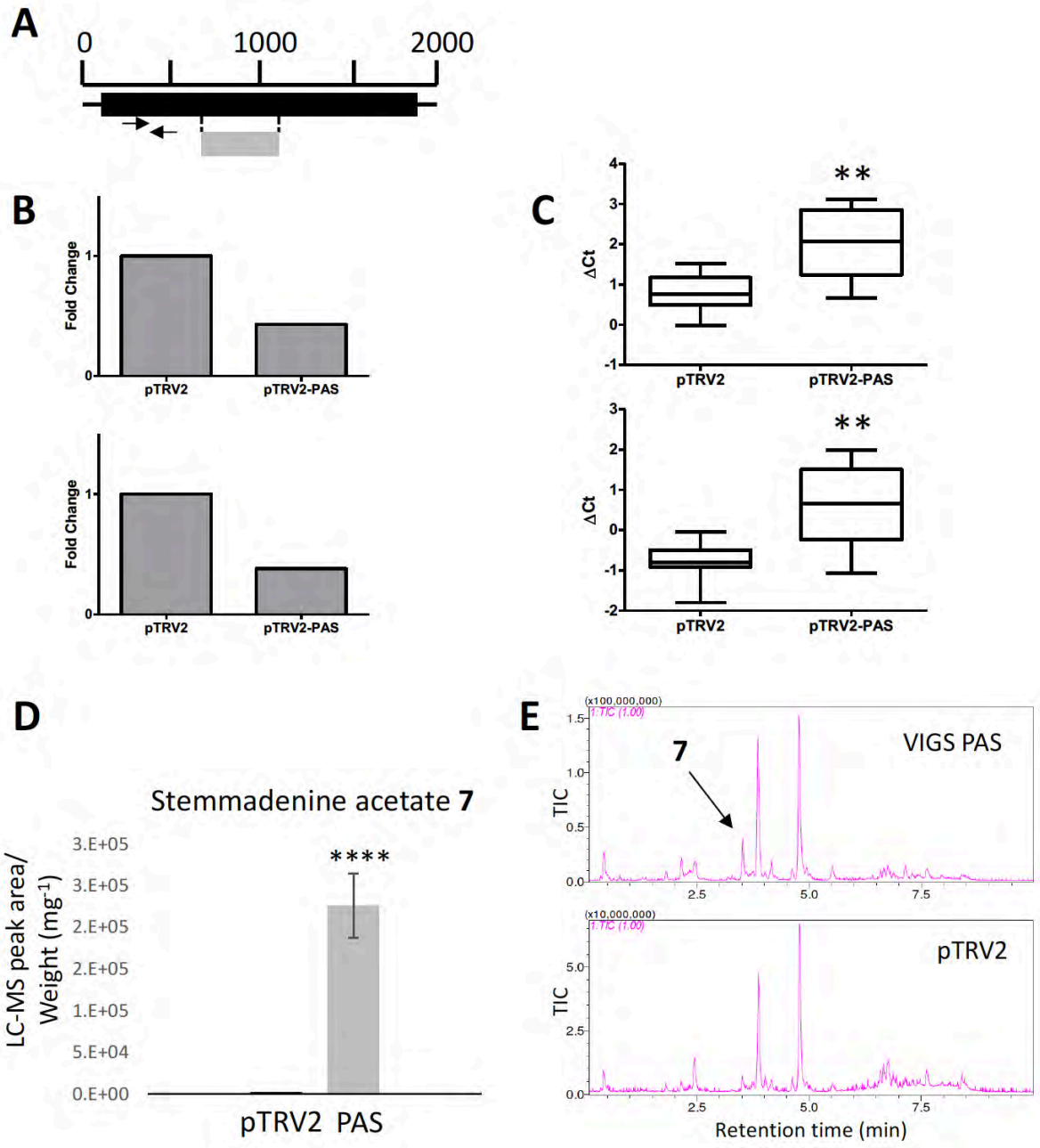
A
0
1000
2000
B
Fold Change
pTRV2
pTRV2-PAS
C
ΔCt
**
D
Stemmadenine acetate 7
LC-MS peak area/ Weight (mg-1)
****
pTRV2 PAS
E
VIGS PAS
7
TIC
pTRV2
Retention time (min)

Fig. S9.

Fig. S9. (continued)
Virus-induced gene silencing of PAS in *C. roseus* using a unique region of the gene. **A.** Fragment (grey box) of PAS cDNA used to assemble the pTRV2 construct. The black box represents the coding region, whereas the black lines are the flanking untranslated regions. Arrows show the annealing sites of the primers used for qRT-PCR analysis (Table S1). **B.** Fold transcript change in PAS silenced (pTRV2-PAS) plants compared to PAS control (pTRV2) plants. Values were calculated using $2^{-\Delta\Delta Ct}$. Upper panel calculated using the EXP reference gene. Lower panel calculated using the N2227 reference gene. **C.** Box plots of ΔCt values of 8 biological replicates for control (pTRV2) and PAS silenced (pTRV2-PAS) plants with median, min and max values indicated. Asterisks represent significant differences determined using an unpaired, two-tailed t-test (** = $p<0.01$). Upper panel calculated using the EXP reference gene. Lower panel calculated using the N2227 reference gene. **D.** UPLC-MS analysis of PAS silenced leaves showed accumulation of stemmadenine acetate **7** (for identification see Fig. S10 and S11). Data shown corresponds to average measurements of 12 plants. Error bars indicate standard error of the mean. Statistical significance calculated with Student's t test (pTRV2 in comparison to pTRV2-PAS) is indicated as **** = $p<0.0001$. **E.** UPLC/MS analysis of VIGS extracts showed the appearance of a new peak assigned as stemmadenine acetate **7** (see Fig. S10 and S11) in the pTRV2-PAS silenced plants that was not present in the pTRV2 empty vector controls.

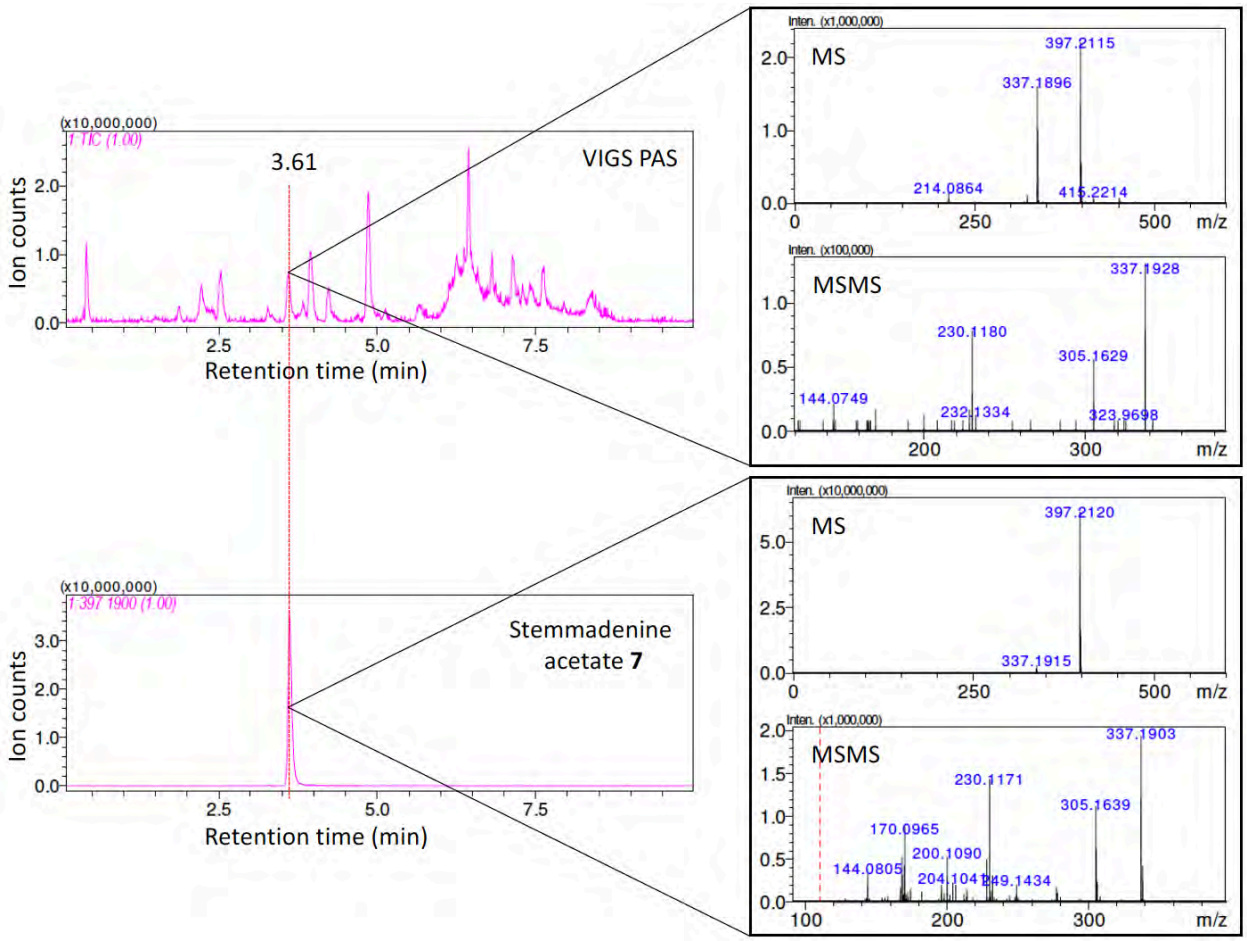

Fig. S10.
UPLC/MS analysis of PAS silenced leaves. The analysis showed that the new peak at *m/z* 397.19 and RT 3.61 in the pTRV2-PAS silenced plants co-eluted with a semi-synthetic standard of stemmadenine acetate **7**. The insets show a comparison between the MS and MS/MS spectra of the two chemical species.

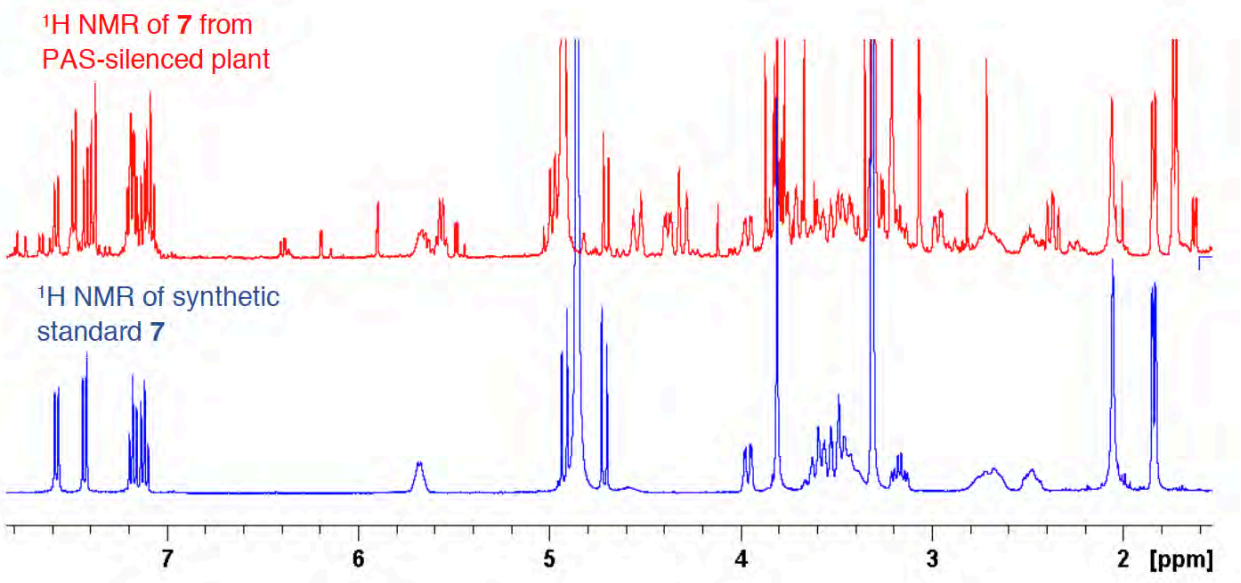

Fig. S11.
^{1}H NMR comparison between synthetic **7** and that obtained by partial purification from PAS-silenced plants.

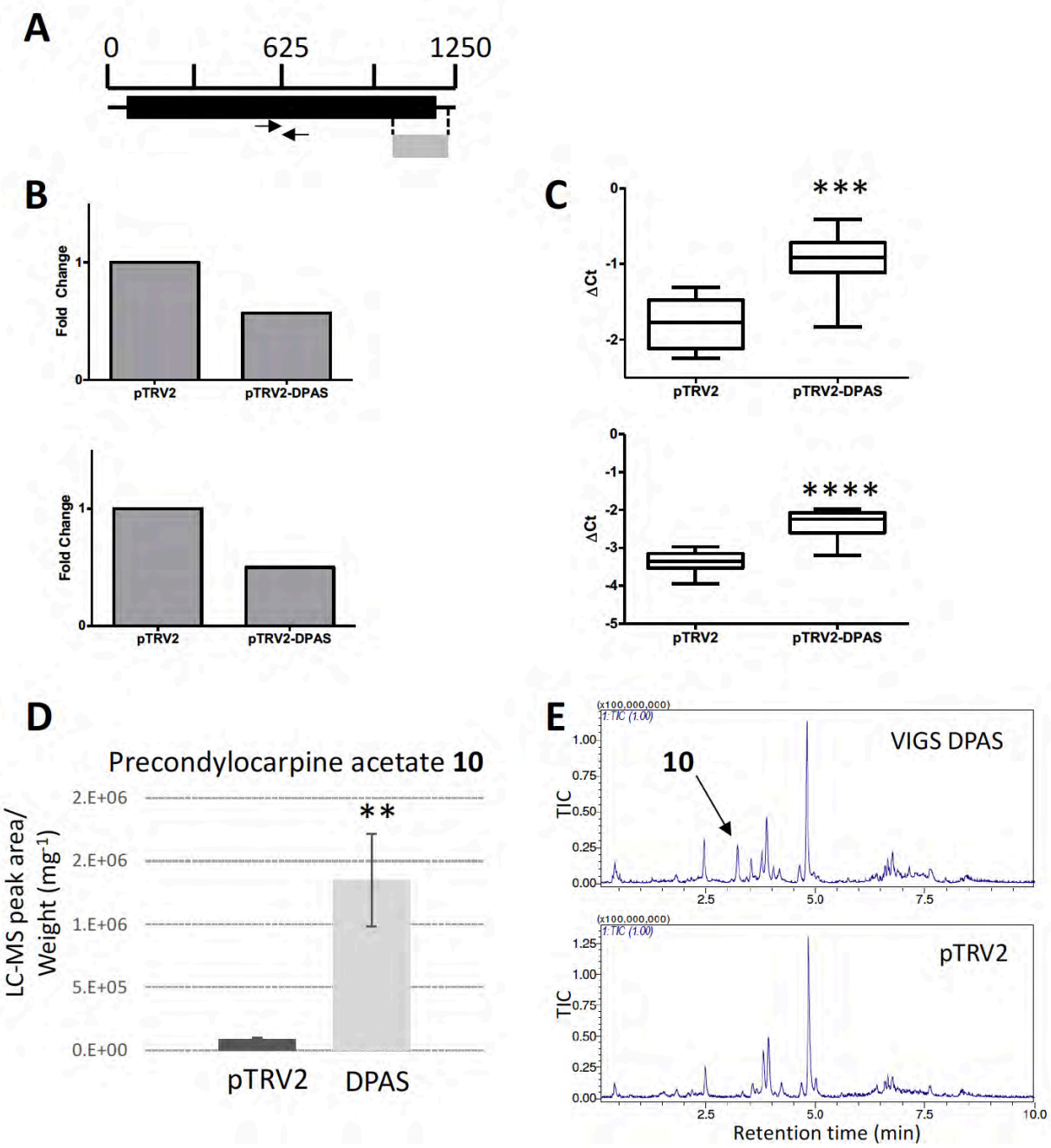
A
0
625
1250
B
Fold Change
1
0
pTRV2
pTRV2-DPAS
Fold Change
1
0
pTRV2
pTRV2-DPAS
C
***
ΔCt
0
-1
-2
pTRV2
pTRV2-DPAS
****
ΔCt
0
-1
-2
-3
-4
-5
pTRV2
pTRV2-DPAS
D
Precondylocarpine acetate 10
LC-MS peak area/ Weight (mg-1)
2.E+06
2.E+06
1.E+06
5.E+05
0.E+00
**
pTRV2
DPAS
E
(x100,000,000)
1: TIC (1.00)
VIGS DPAS
10
TIC
1.00
0.75
0.50
0.25
0.00
2.5
5.0
7.5
(x100,000,000)
1: TIC (1.00)
pTRV2
TIC
1.25
1.00
0.75
0.50
0.25
0.00
2.5
5.0
7.5
10.0
Retention time (min)

Fig. S12.

Fig. S12. (continued)
Virus-induced gene silencing of DPAS in *C. roseus* using a unique region of the gene. **A**. Fragment (grey box) of DPAS cDNA used to assemble the pTRV2 construct. The black box represents the coding region, whereas the black lines are the flanking untranslated regions. Arrows show the annealing sites of the primers used for qRT-PCR analysis (Table S1). **B.** Fold transcript change DPAS silenced (pTRV2-DPAS) plants compared to DPAS control (pTRV2) plants. Values were calculated using $2^{-\Delta\Delta Ct}$. Upper panel calculated using the EXP reference gene. Lower panel calculated using the N2227 reference gene. **C.** Box plots of ΔCt values of 8 biological replicates for control (pTRV2) and DPAS silenced (pTRV2-DPAS) plants with median, min and max values indicated. Asterisks represent significant differences determined using an unpaired, two-tailed t-test (*** = $p<0.001$, **** = $p<0.0001$). Upper panel calculated using the EXP reference gene. Lower panel calculated using the N2227 reference gene. **D.** UPLC-MS analysis of DPAS silenced leaves showed accumulation of precondylocarpine acetate **10** (identification see Fig. S13 and S14). Data shown corresponds to average measurements of 12 plants. Error bars indicate standard error of the mean. Statistical significance calculated with Student's t test (pTRV2 in comparison to pTRV2-DPAS) is indicated as ** = $p<0.01$. **E.** UPLC/MS analysis of VIGS extracts showed a marked increase in a peak with *m/z* 395.19 in pTRV2-DPAS silenced plants that was not very abundant in the pTRV2 empty vector controls (see Fig. S13 and S14).

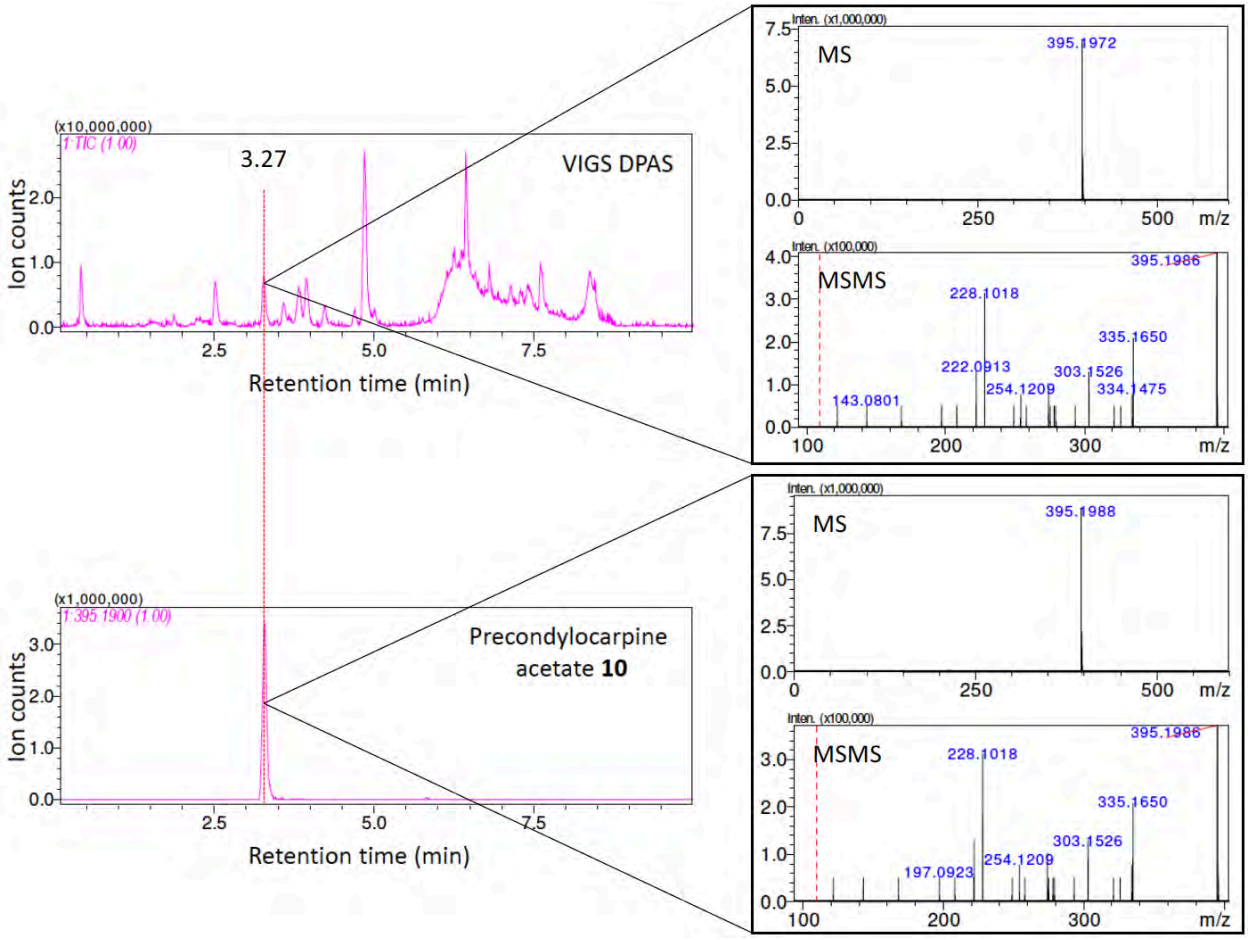

Fig. S13.
UPLC/MS analysis of DPAS silenced leaves. The analysis showed that the new peak at *m/z* 395.19 and RT 3.27 in the pTRV2-DPAS silenced plants co-eluted with a semi-synthetic standard of precondylocarpine acetate **10**. The insets show a comparison between the MS and MS/MS spectra of the two chemical species.

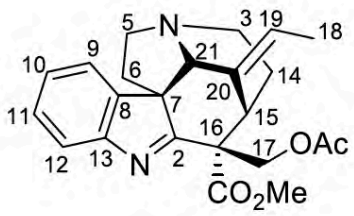

Proton

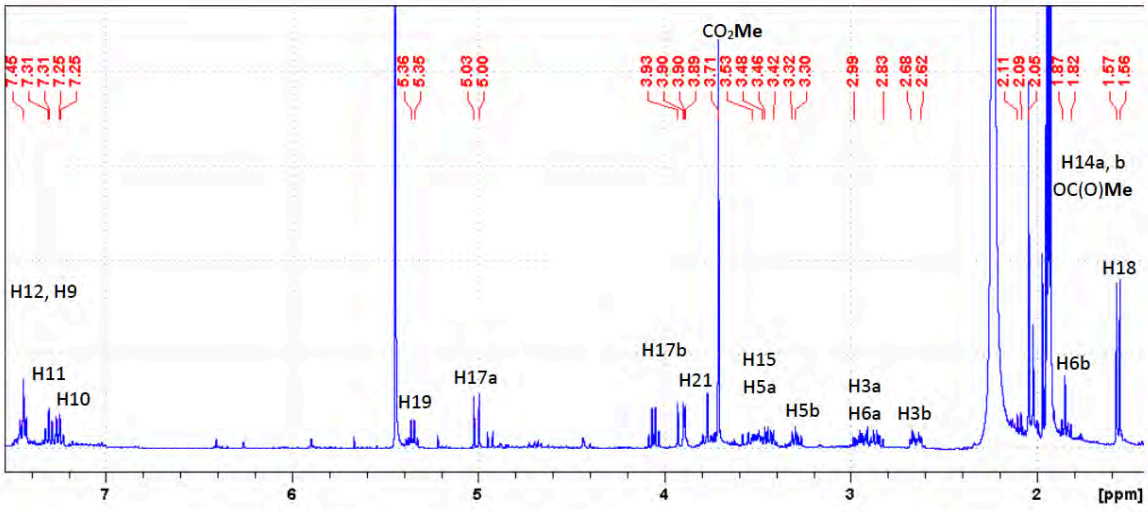

COSY

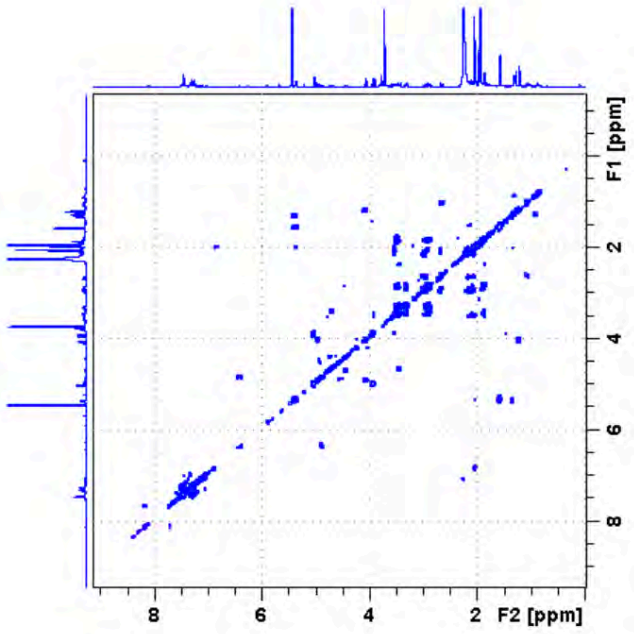

Fig. S14.

NOESY

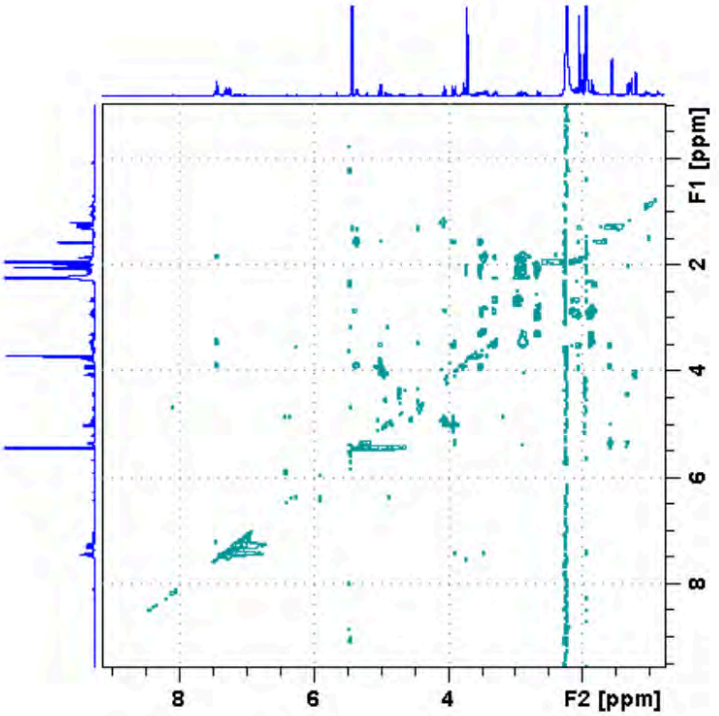

TOCSY

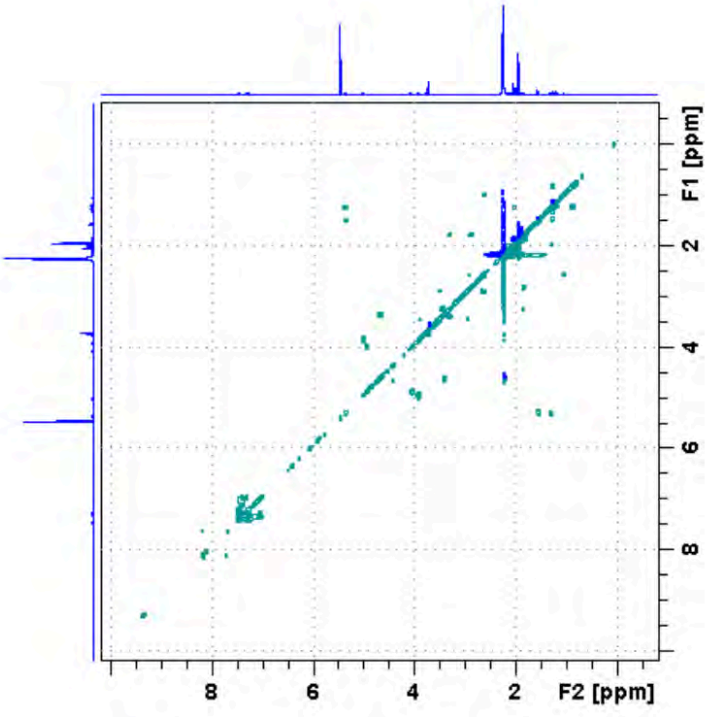

Fig. S14. (continued)

HSQC

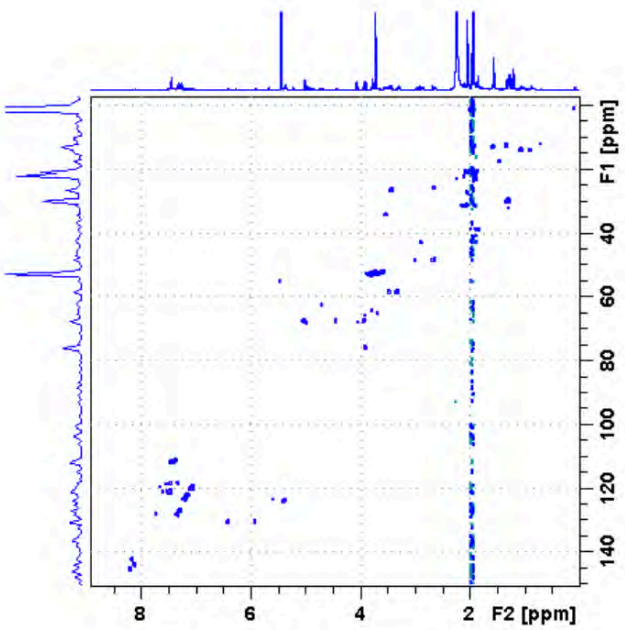

HMBC* (during HMBC acquisition degradation occurred, so not all cross peaks in HMBC match ^{1}H NMR sprectrum)

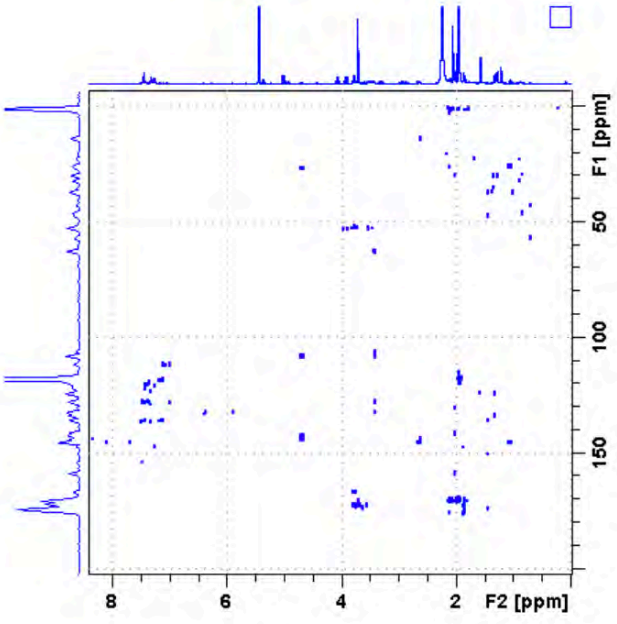

Fig. S14. (continued)
NMR data of synthetic precondylocarpine acetate **10** (CD_3CN, 300 K, 400 MHz). Proton: 256 scans; COSY: 32 scans; NOESY: 16 scans; TOCSY: 24 scans; HSQC: 72 scans, HMBC: 425 scans.

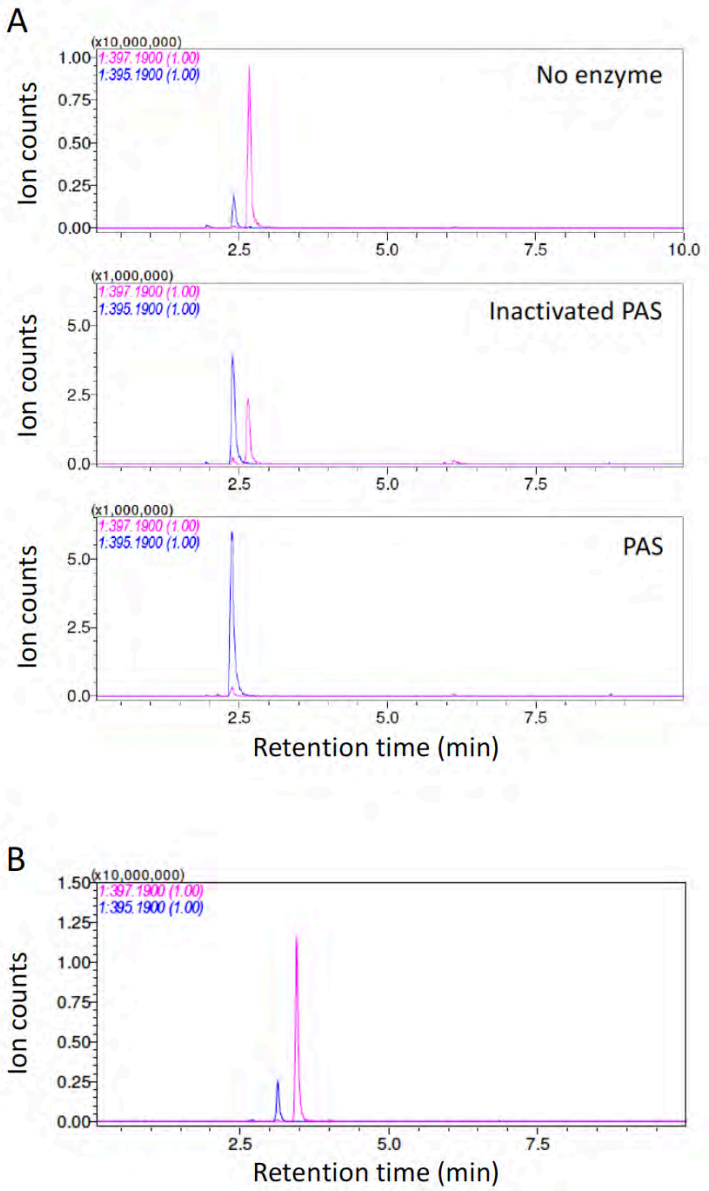

Fig. S15.
In vitro activity of PAS purified from *P. pastoris* culture medium. **A.** Extracted ion chromatograms for ions *m/z* 397.19 (stemmadenine acetate **7**) and *m/z* 395.19 (precondylocarpine acetate **10**). Addition of PAS to the reaction mixture resulted in complete conversion of stemmadenine acetate **7** to precondylocarpine acetate **10**. However, heat inactivated enzyme (20 min in boiling water) was still able to consume some of the substrate, suggesting that this enzyme is quite resilient to heat inactivation. **B.** Non-transformed *P. pastoris* control. Medium from a culture of WT *P. pastoris* was subjected to the same purification process as the PAS producing strain and used for enzyme assays to exclude the possibility that *P. pastoris* could produce enzymes that could oxidize stemmadenine acetate **7**. This negative control did not consume precondylocarpine acetate **10**. This sample was analysed on a slightly different chromatographic system compared to panel A, hence the shift in retention time.

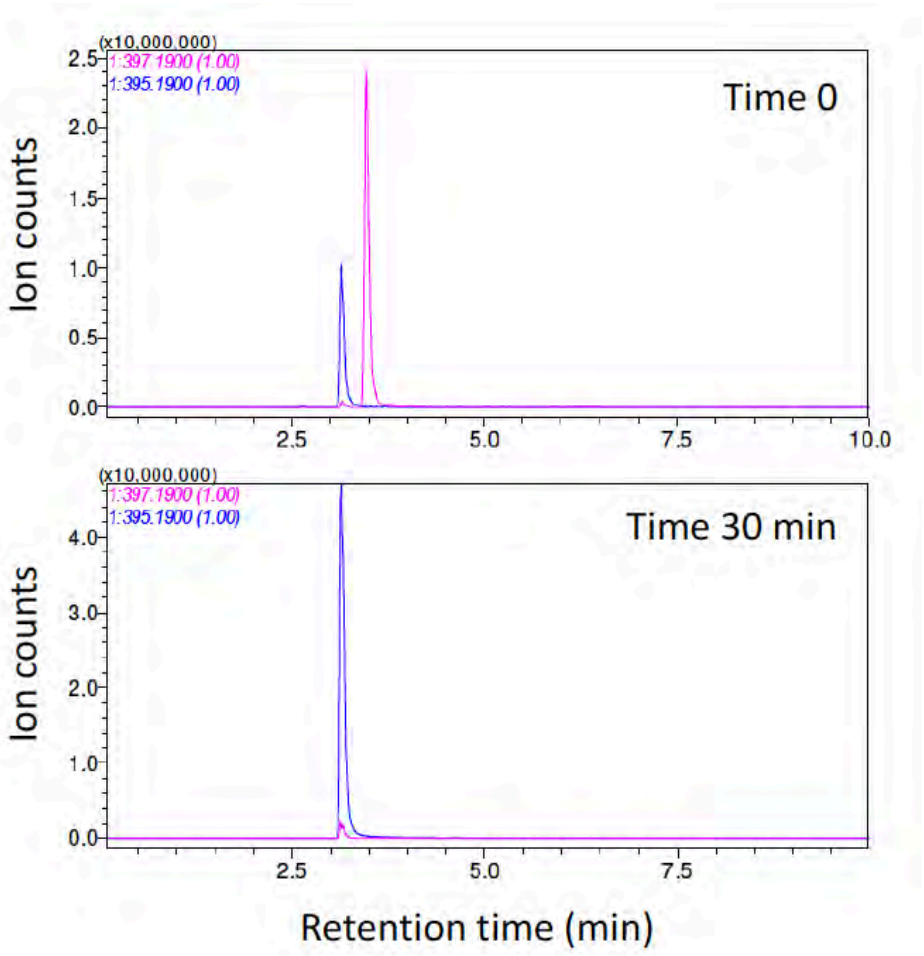

Fig. S16.
In vitro activity of PAS purified from insect cells. Extracted ion chromatograms for ions *m/z* 397.19 (stemmadenine acetate **7**) and *m/z* 395.19 (precondylocarpine acetate **10**). Samples for LC/MS analysis were collected straight after the addition of the enzyme (time 0) and after incubation for 30 min (time 30 min). The analysis showed that after incubation with PAS expressed and purified from insect cells for 30 minutes complete conversion of stemmadenine acetate **7** to precondylocarpine acetate **10** was achieved.

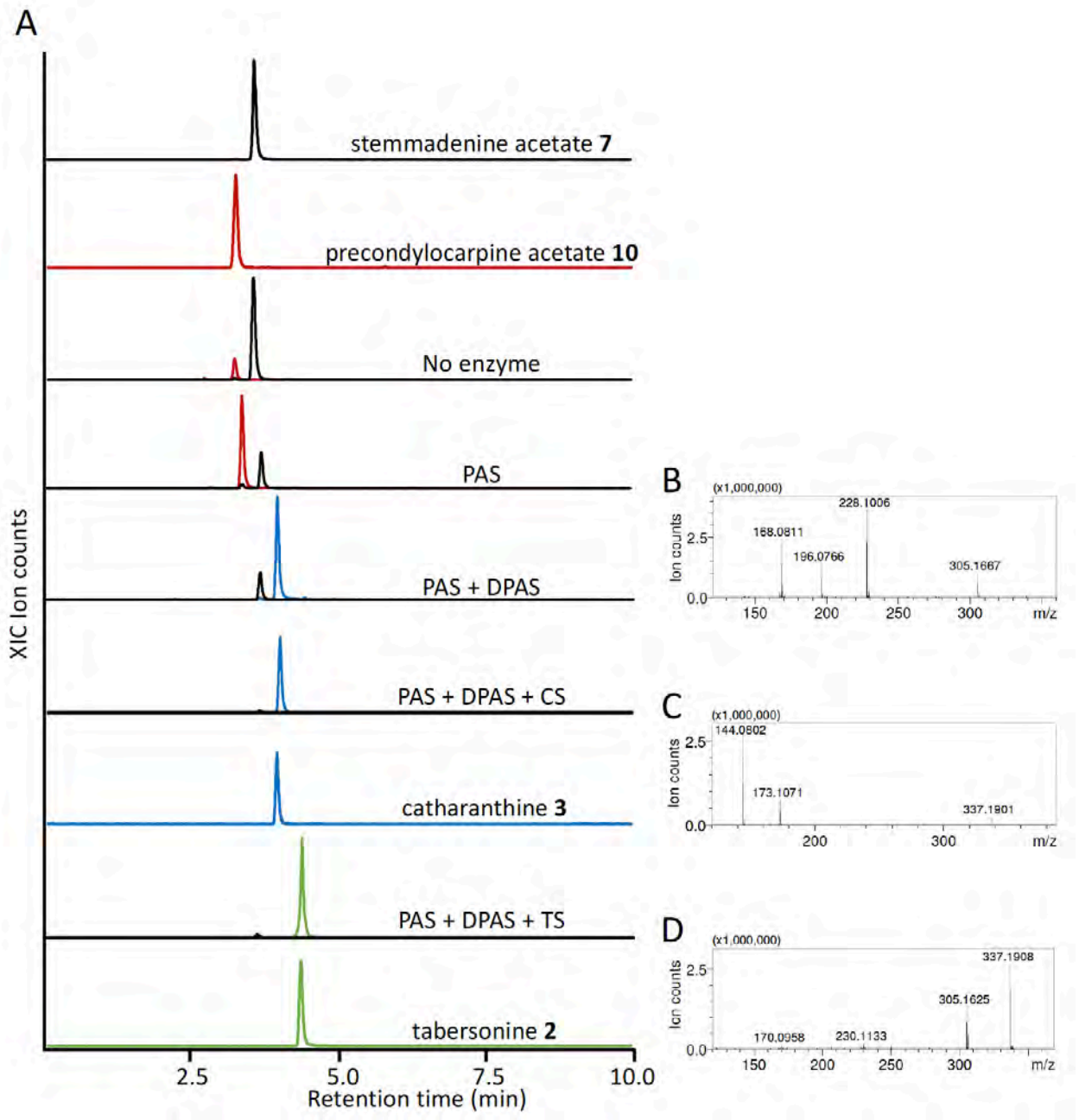
A
stemmadenine acetate 7
precondylocarpine acetate 10
No enzyme
PAS
PAS + DPAS
PAS + DPAS + CS
catharanthine 3
PAS + DPAS + TS
tabersonine 2
XIC Ion counts
2.5
5.0
7.5
10.0
Retention time (min)
B
(x1,000,000)
Ion counts
228.1006
168.0811
196.0766
305.1667
m/z
C
(x1,000,000)
144.0802
173.1071
337.1901
m/z
D
(x1,000,000)
337.1908
305.1625
170.0958
230.1133
m/z

Fig. S17.

Fig. S17. (continued)
Pathway reconstitution *in vitro* using PAS expressed in *N. benthamiana* leaves. **A.** Extracted ion chromatograms for ions *m/z* 397.19 (stemmadenine acetate, the starting material; in black), *m/z* 395.19 (precondylocarpine acetate; in red) and *m/z* 337.19 (catharanthine at RT 4.0, in blue; and tabersonine at RT 4.4, in green). Heterologously expressed and purified proteins were used to reconstitute the biosynthetic pathway from stemmadenine acetate **7** to catharanthine **3** and tabersonine **2**. Extracted ion chromatograms for each compound are shown. When no enzymes were present, very small amounts of precondylocarpine acetate **10** were observed in the reaction, likely due to spontaneous oxidation. After addition of PAS, most of the substrate was converted to precondylocarpine acetate **10**. Addition of DPAS resulted in complete consumption of precondylocarpine acetate **10** and a compound with the same mass and retention time as catharanthine started to appear in the samples. However, a comparison of its MSMS spectrum with that of catharanthine showed that the compound forming spontaneously is a different chemical species. When CS was present, all the initial substrate (stemmadenine acetate **7**) was converted to catharanthine **3**. When PAS, DPAS and TS were combined together in the reaction, all initial substrate was converted to tabersonine **2**. Formation of catharanthine **3** and tabersonine **2** was validated by co-elution with commercial standards. Formation of precondylocarpine acetate **10** was validated by co-elution with the semi-synthetic compound. **B.** MSMS spectrum of the compound forming in solution when PAS and DPAS are present. **C.** MSMS spectrum of a commercial standard of catharanthine **3**. **D.** MSMS spectrum of a commercial standard of tabersonine **2**.

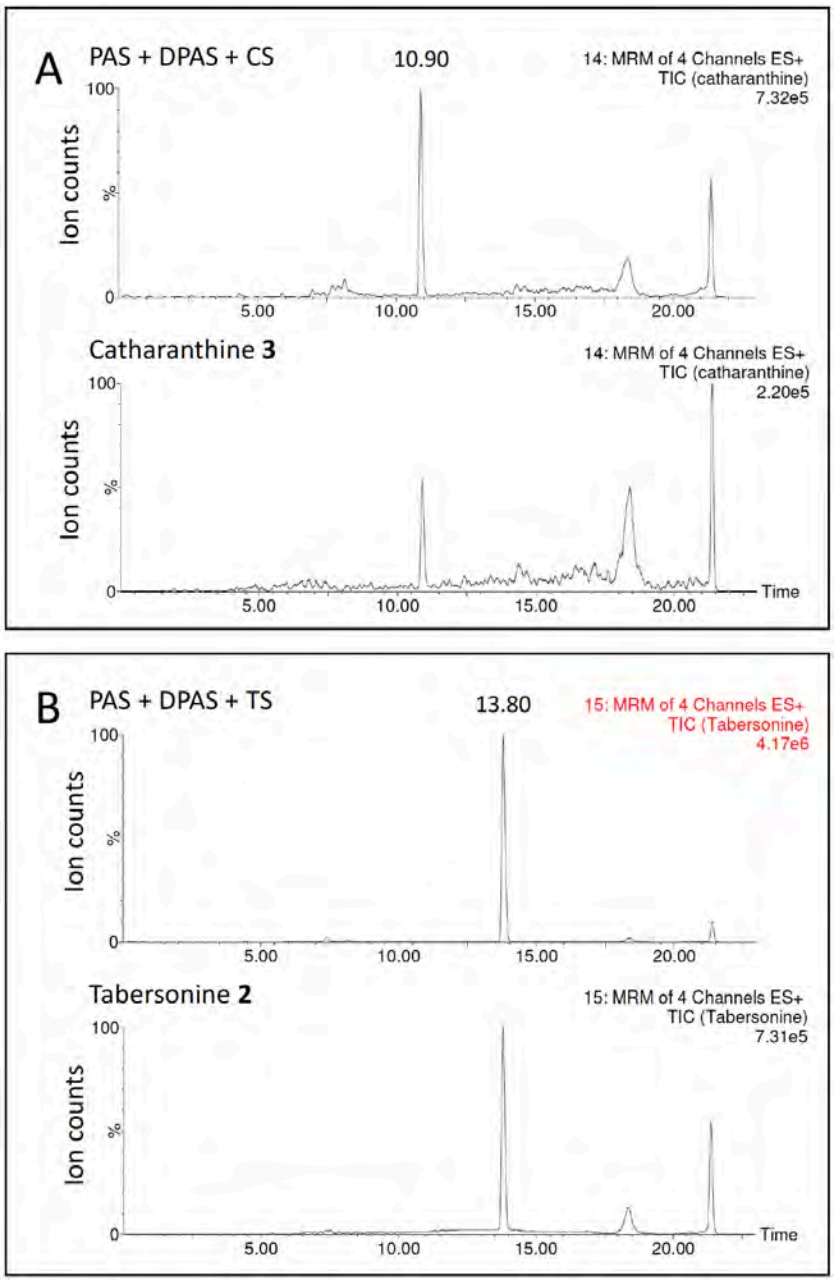

Fig. S18.
Pathway reconstitution *in vitro* using PAS expressed in *P. pastoris*. **A.** Total ion chromatograms for MRMs of catharanthine **3** (RT=10.90) for the reaction of PAS, DPAS and CS with stemmadenine acetate **7**, compared to a commercial standard of catharanthine **3**. **B.** Total ion chromatograms for MRMs of tabersonine **2** (RT=13.80) for the reaction of PAS, DPAS and TS with stemmadenine acetate **7**, compared to a commercial standard of tabersonine **2**.

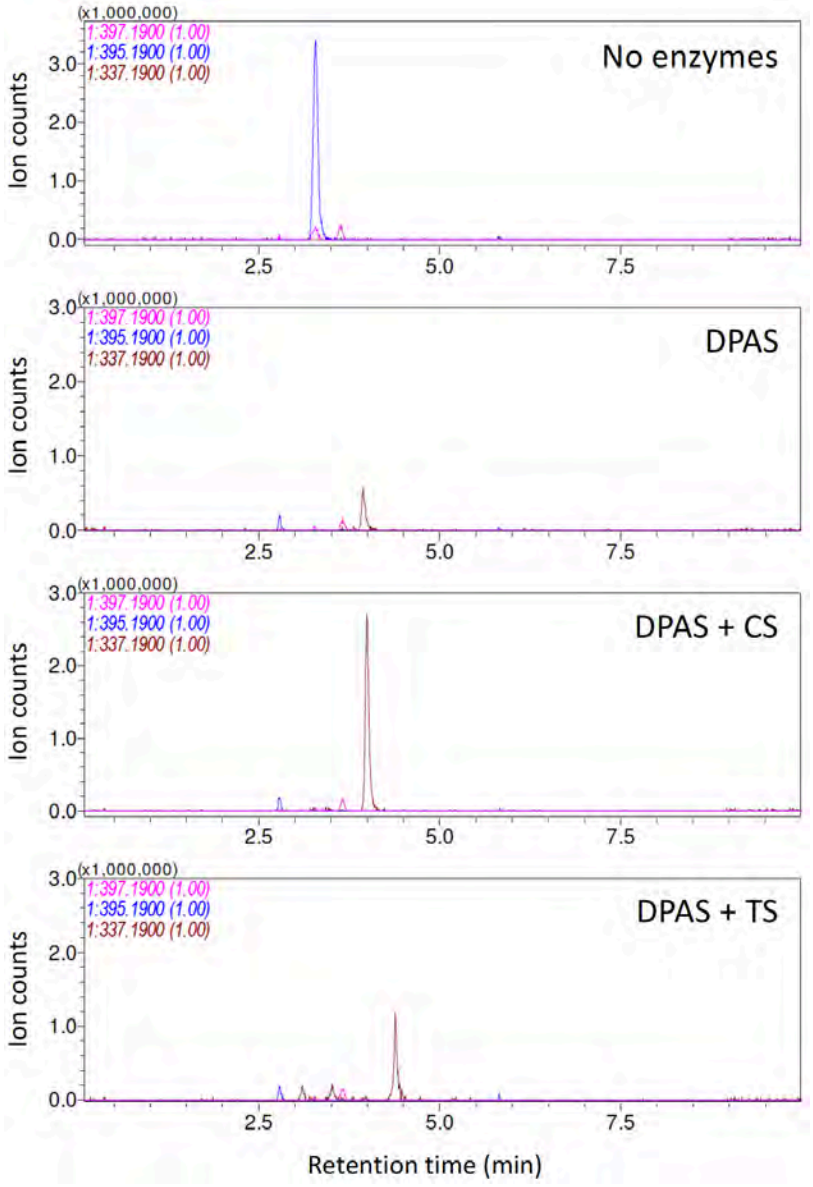

Fig. S19.
In vitro pathway reconstitution from synthetic precondylocarpine acetate **10**. The figure shows the extracted ion chromatograms for ions *m/z* 397.19 (stemmadenine acetate), *m/z* 395.19 (precondylocarpine acetate **10**) and *m/z* 337.19 (catharanthine **3** at RT 4.0 and tabersonine **2** at RT 4.4). Addition of DPAS to the reaction mixture resulted in complete consumption of precondylocarpine acetate and appearance of a small amount of catharanthine **3** but no reduced product (dihydroprecondylocarpine acetate **11**) at *m/z* 397.19 was observed. When DPAS and CS were present, all substrate was converted into catharanthine **3**. When DPAS and TS were incubated with precondylocarpine acetate **10**, tabersonine **2** was formed.

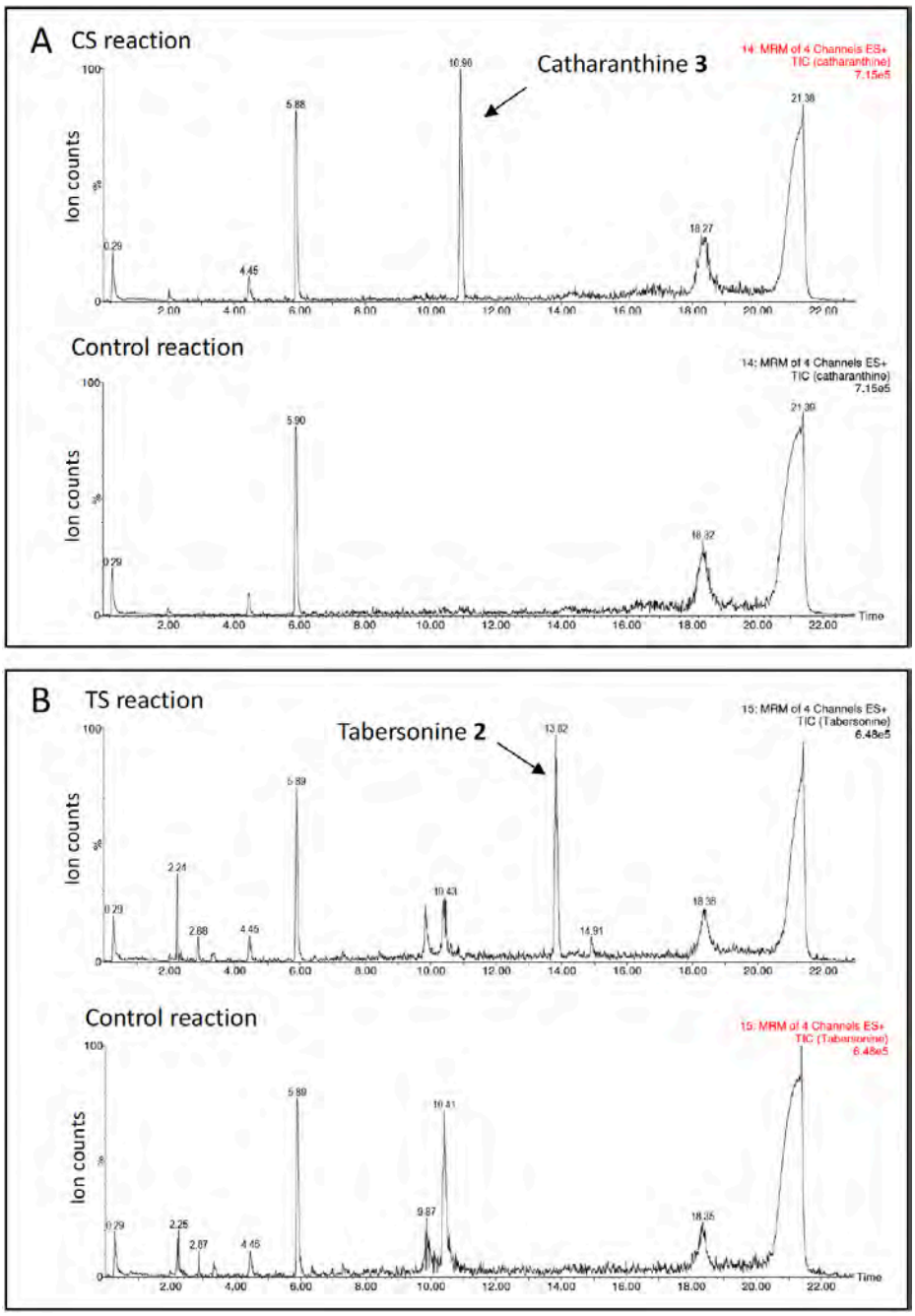

Fig. S20.
In vitro reaction of crude dihydroprecondylocarpine acetate **11** with CS and TS. **A.** Total ion chromatograms for MRMs of catharanthine **3** (RT=10.90) for the reaction of CS with dihydroprecondylocarpine acetate **11**, compared to a control reaction without CS. **B.** Total ion chromatograms for MRMs of tabersonine **2** (RT=13.82) for the reaction of TS with dihydroprecondylocarpine acetate **11**, compared to a control reaction without TS.

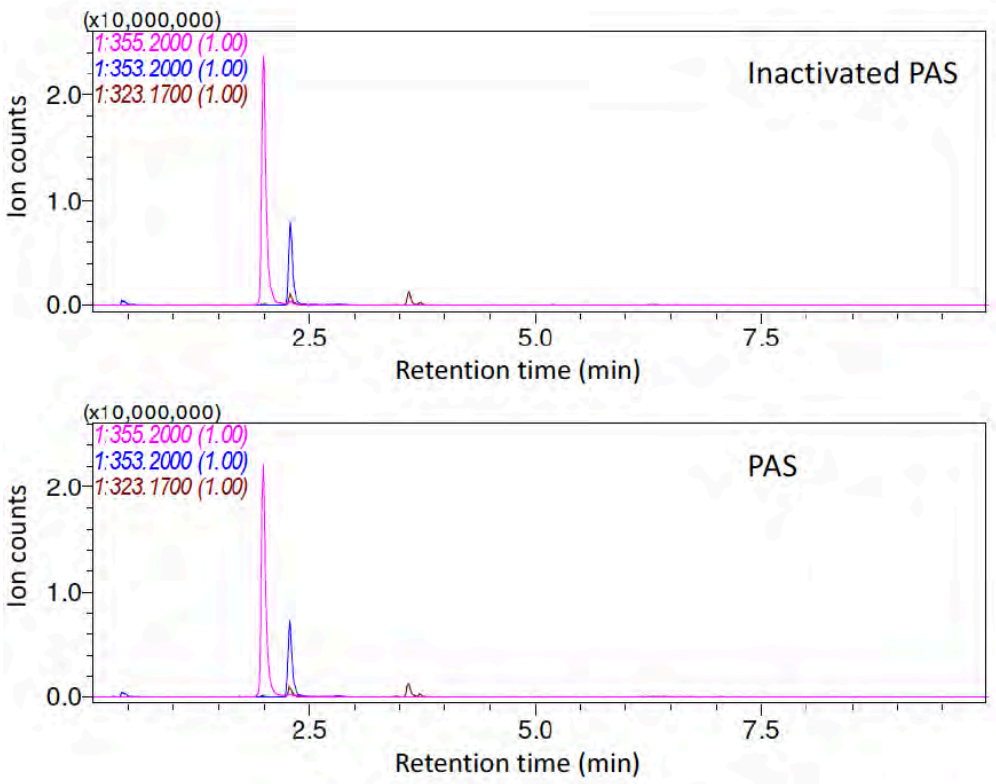

Fig. S21.
Assay of PAS with stemmadenine **1**. UPLC/MS analysis of reactions in which stemmadenine **1** was used as substrate for PAS showed neither consumption of substrate or formation of new products. Extracted ion chromatograms for *m/z* 355.2 (stemmadenine) and *m/z* 353.2 (mass of the expected oxidation product) are shown. The peak at *m/z* 353.2 present in both samples was not a product of PAS activity. Extracted ion chromatogram for *m/z* 323.17 showed that no condylocarpine **13** was formed during the reaction.

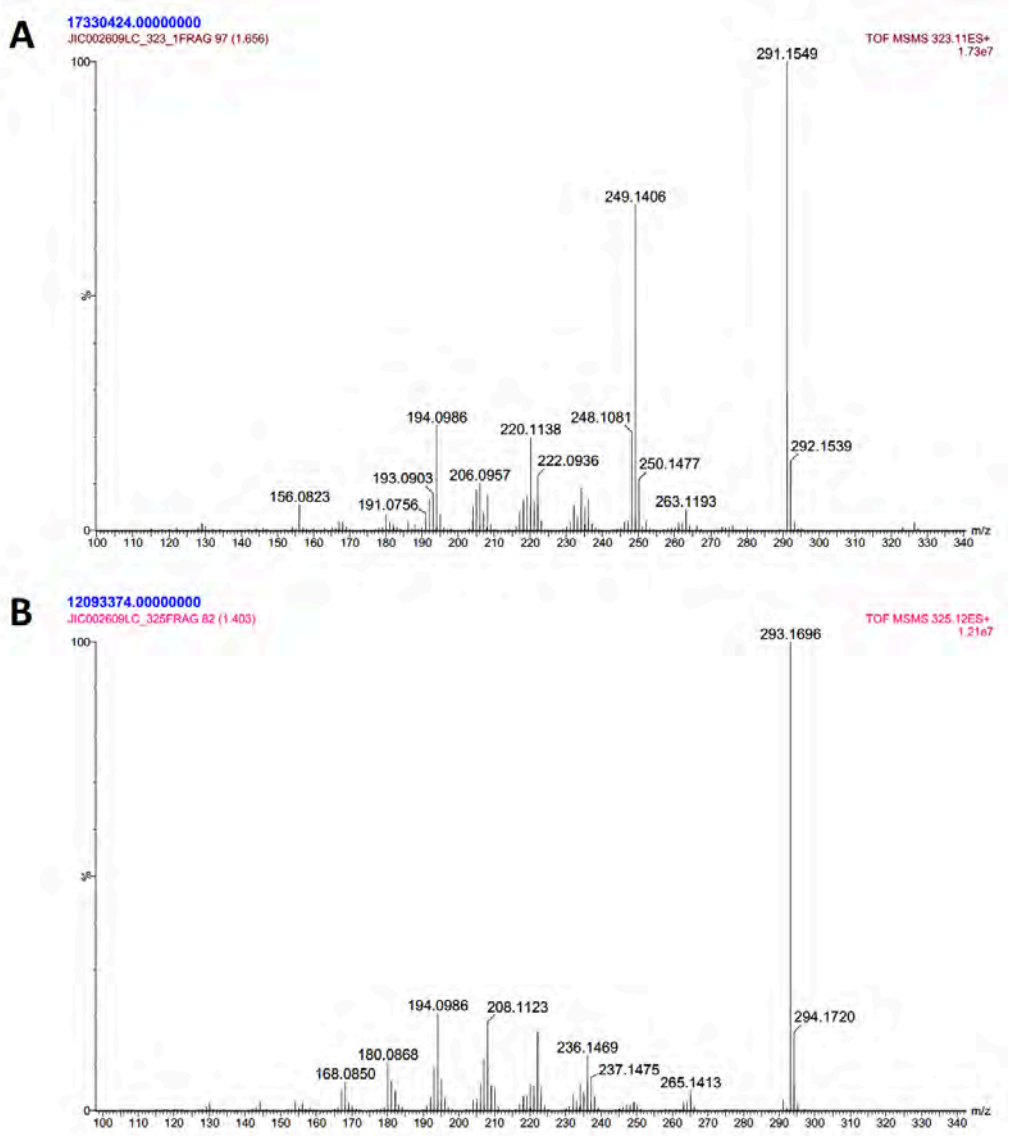

Fig. S22.
MSMS spectra of condylocarpine **13** and tubotaiwine **12**. **A.** MSMS spectrum of condylocarpine **13** (precursor ion *m/z* 323.17) at high energy. **B.** MSMS spectrum of tubotaiwine **12** (precursor ion *m/z* 325.19) at high energy.

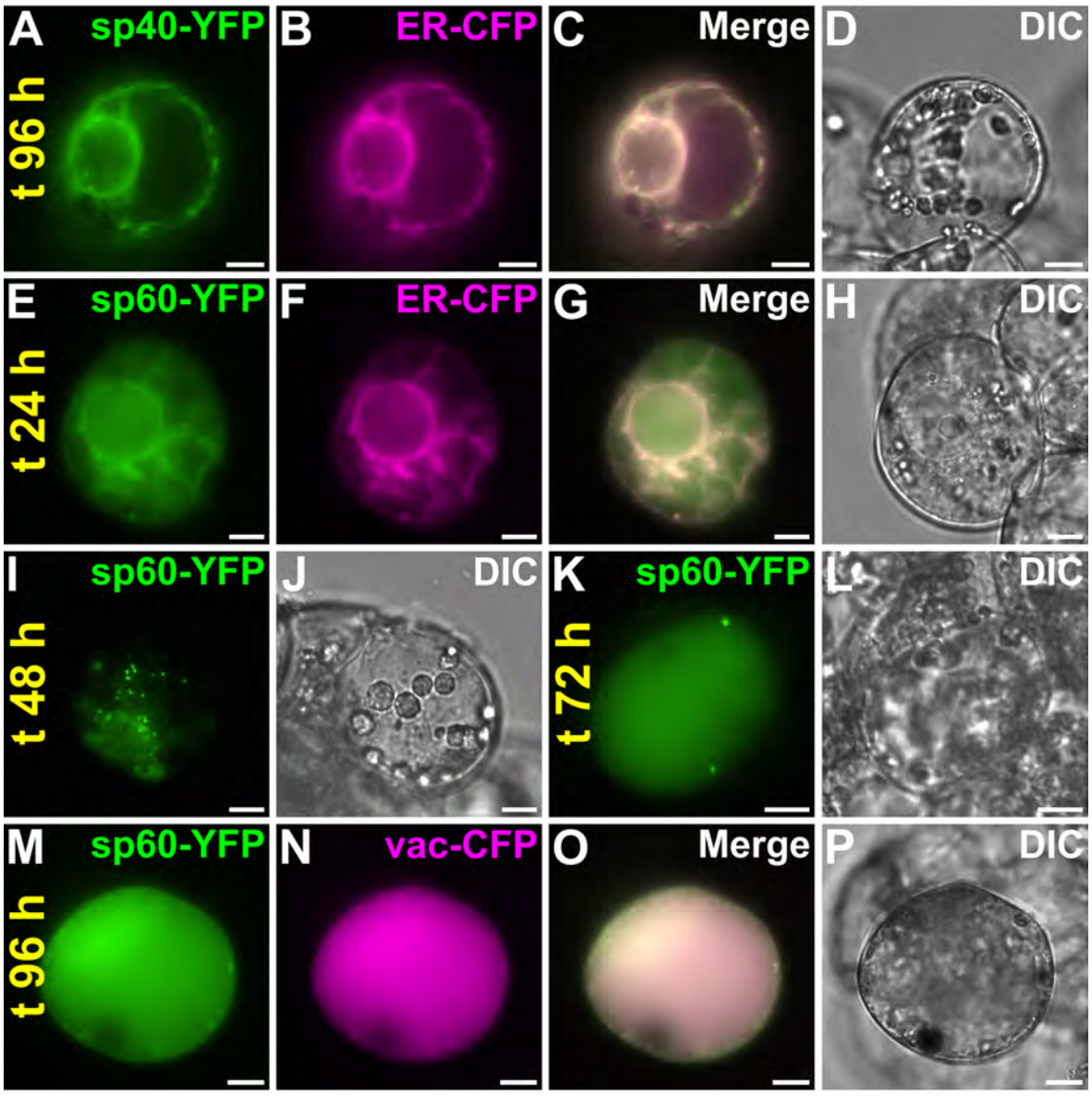

Fig. S23.
PAS is targeted to endoplasmic reticulum and progressively secreted to vacuole by ER-derived vesicles. *C. roseus* cells were transiently co-transformed with plasmids expressing the 40-first (sp40; A) or 60-first (sp60; E, I, K, M) PAS residues fused to YFP and the endoplasmic (ER)-CFP marker (B, F) or vacuole (vac-) CFP marker (N). Localization was investigated during 96 h and representative photos were taken at 24, 48, 72 and 96 h post-transformation to highlight permanent ER localization of sp40-YFP during 96 h (A) and the progressive translocation of sp60-YFP from ER at 24 h(E), vesicles at 48 h (I), to vacuole at 72 h and 96 h (K, M). Co-localization of the fluorescence signals appears in yellow when merging the two individual (green/magenta) false colour images (C, G, O). Cell morphology is observed with differential interference contrast (DIC) (D, H, J, L, P). Scale bars, 10 µm.

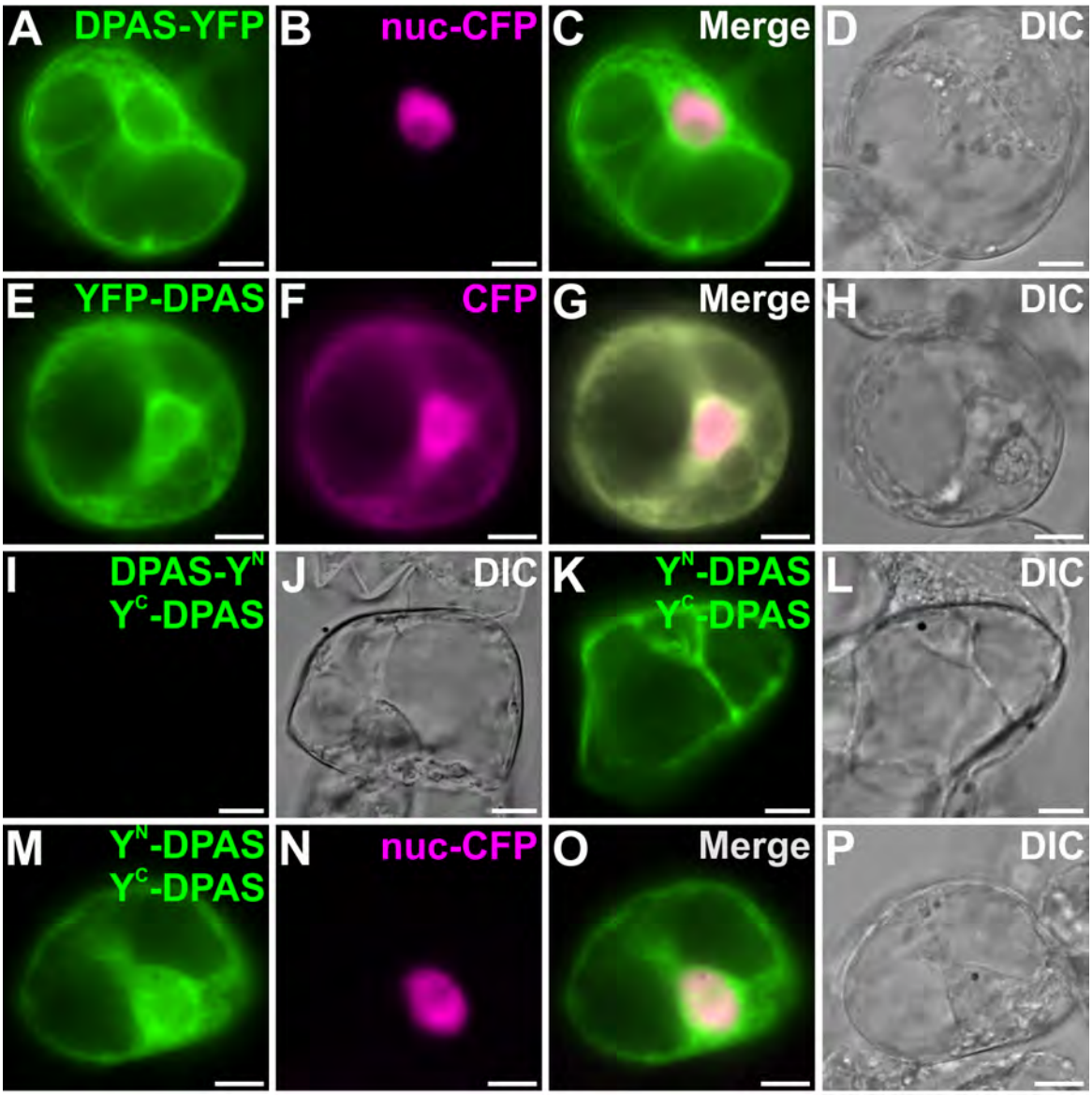

Fig. S24.
DPAS displays a cytosolic localization and homodimerizes. *C. roseus* cells were transiently co-transformed with plasmids expressing DPAS-YFP (A) or YFP-DPAS (E) and the plasmid encoding the nuclear (nuc)-CFP marker (B) or the nucleocytosolic marker CFP (F). DPAS dimerization was analyzed by bimolecular fluorescence complementation (BiFC) assays through transient co-expression of DPAS-YFPN and YFPC-DPAS (I) or YFPN-DPAS and YFPC-DPAS (K, M) with the nuc-CFP marker (N). Co-localization of the fluorescence signals appears in yellow when merging the two individual (green/magenta) false colour images (C, G, O). Cell morphology is observed with differential interference contrast (DIC) (D, H, J, L, P). Scale bars, 10 µm.

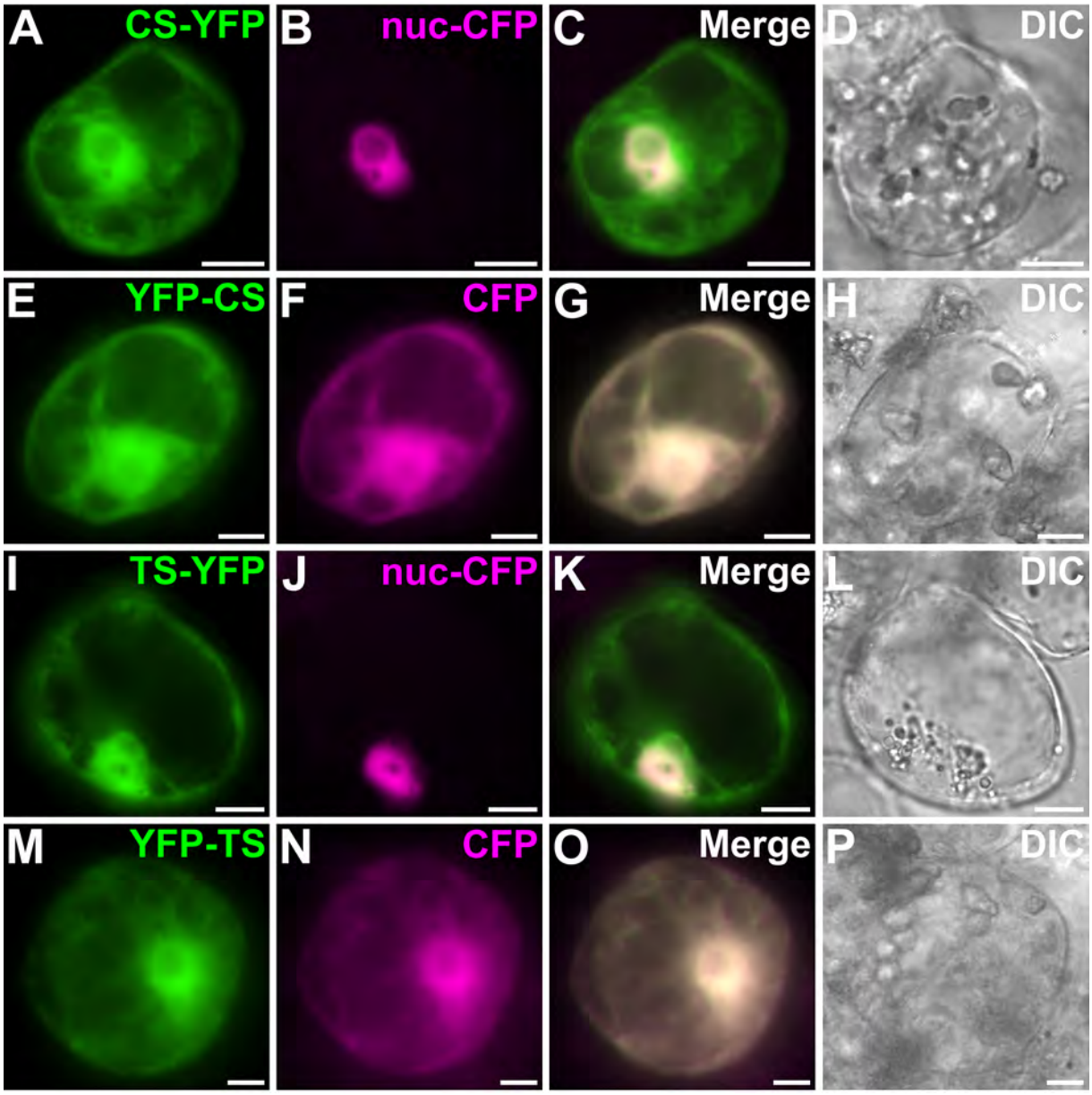

Fig. S25.
CS and TS display nucleocytosolic localization. *C. roseus* cells were transiently co-transformed with plasmids expressing either CS-YFP (A), YFP-CS (E), TS-YFP (I) or YFP-TS (M) and the nuclear (nuc)-CFP marker (B, J) or the cytosolic CFP marker (F, N). Co-localization of the fluorescence signals appears in yellow when merging the two individual (green/magenta) false colour images (C, G, K, O). Cell morphology is observed with differential interference contrast (DIC) (D, H, L, P). Scale bars, 10 µm.

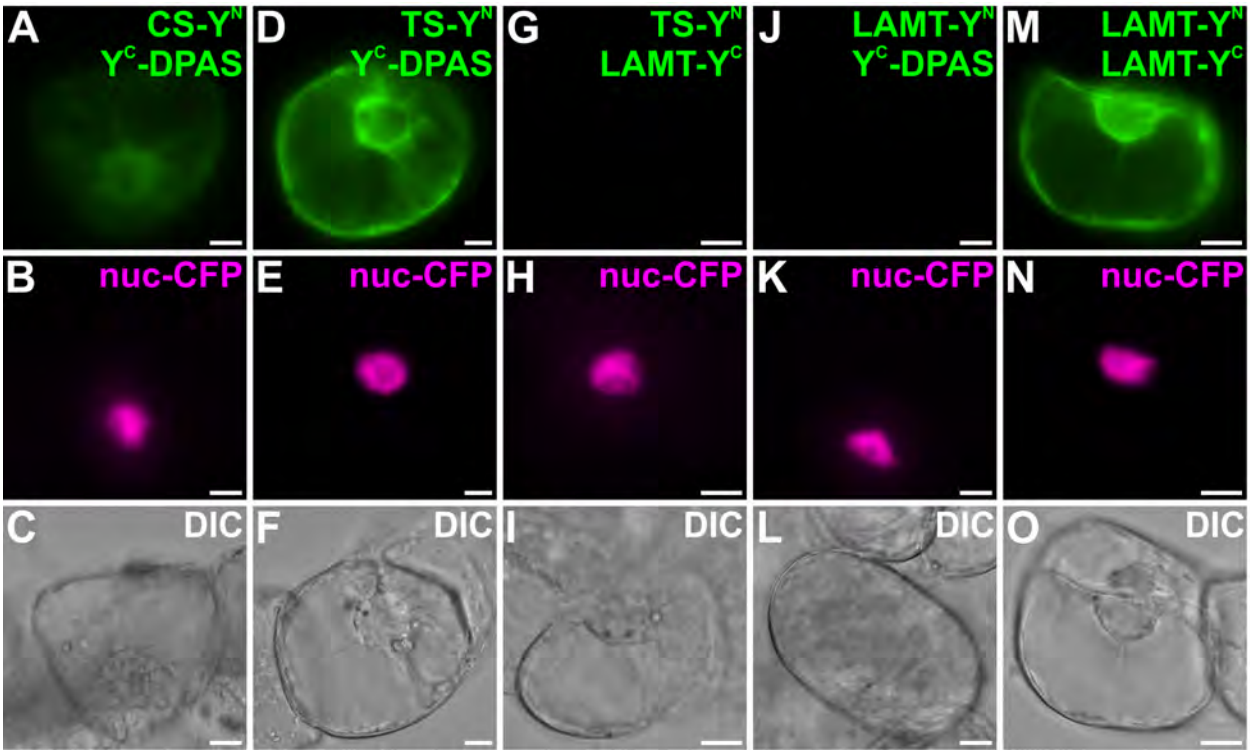

Fig. S26.
Interaction of DPAS with TS and CS. DPAS/CS and DPAS/TS interactions were analyzed by BiFC in *C. roseus* cells transiently transformed by distinct combinations of plasmids encoding fusions with the two split YFP fragments, YFPN (YN) and YFPC (YC) as indicated on each pictures of the first row (A, D, G, J, M). Identification of transiently transformed cells was achieved by co-transformation with the nucleus (nuc)-CFP marker(B, E, H, K, N). Efficient (TS-YN/YC-DPAS) and weak (CS-YN/YC-DPAS) reconstitutions of BiFC complexes revealed by fluorescence intensity reflect corresponding interaction levels. Interactions of DPAS and TS with loganic acid methyltransferase (LAMT)-YN and LAMT-YC were also studied to evaluate the specificity of DPAS/TS interactions. Cell morphology is observed with differential interference contrast (DIC) (C, F, I, L, O). Scale bars, 10 μm.

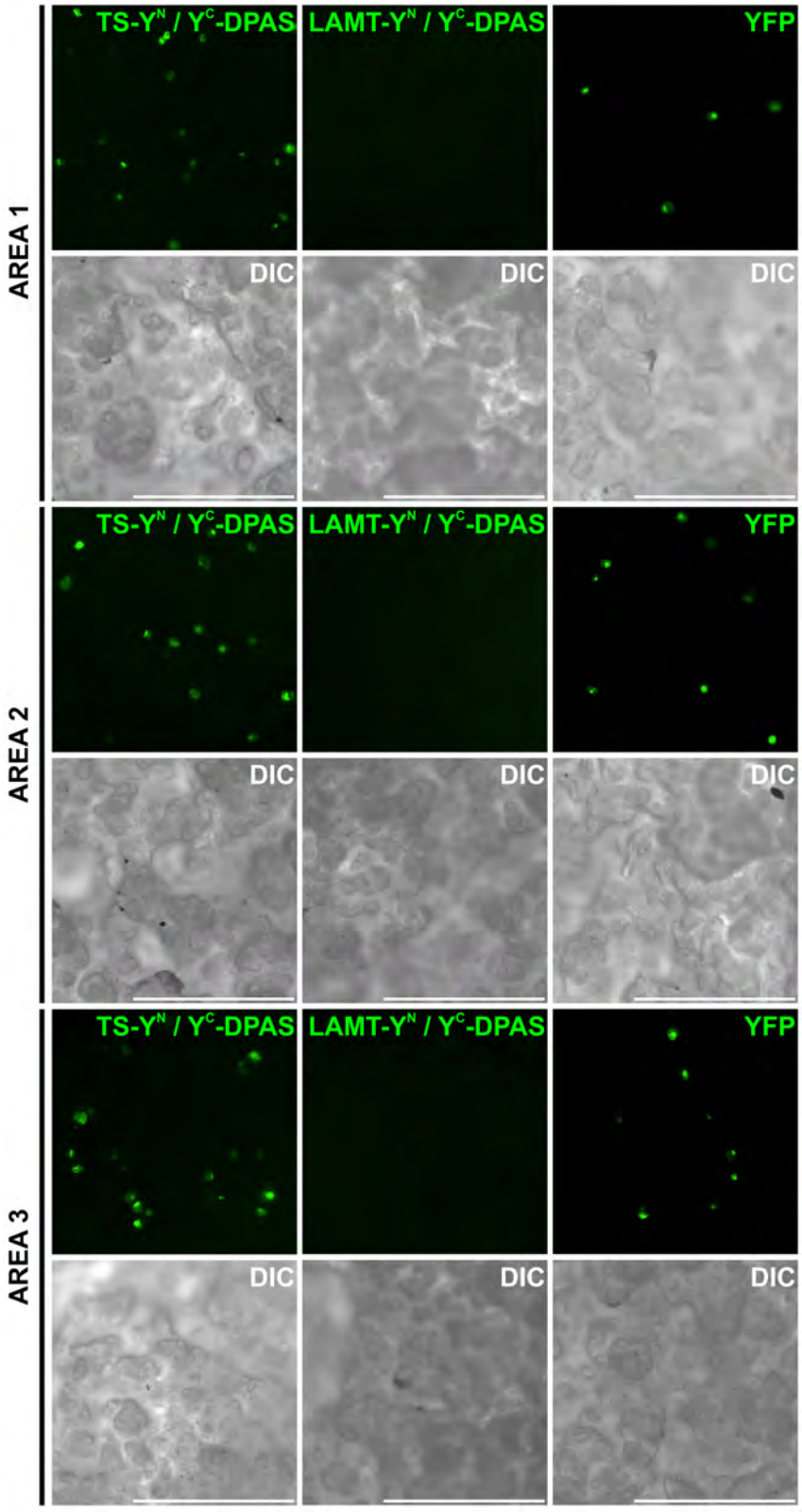

Fig. S27.

Fig. S27. (continued)
Specificity of interaction of DPAS with TS. To study their specificity, DPAS/TS (first column) and DPAS/loganic acid methyltransferase (LAMT – second column) interactions were analyzed by BiFC in *C. roseus* cells transiently transformed by distinct combinations of plasmids encoding fusions with the two split YFP fragments, YFP^N (Y^N) and YFP^C (Y^C) as indicated on each pictures. Additional transformations with an empty pSCA-YFP vector expressing unfused YFP were conducted to evaluate transformation efficiency (third column). Transformed cells were directly observed on the Petri dishes at low magnification (X4) to evaluate the number of transformed cells in each condition reflecting protein interaction through BiFC complex reformation and emission of YFP fluorescence (first two columns) or cell transformation efficiency (last column). Three distinct arears of the Petri dishes were illustrated for each transformation. Small green dots represent transiently transformed cells that were not observed for DPAS/LAMT interaction confirming specificity of interaction of DPAS/TS. Cell morphology is observed with differential interference contrast (DIC) (C, F, I, L, O). Scale bars, 1 mm.

Fig. S28.
Amino acid sequence alignment of PAS with other functionally characterised berberine bridge enzymes and PAS-like proteins identified from other aspidosperma and iboga alkaloids producing plants. Red boxes highlight the residues (His and Cys) involved in bicovalent attachment of the FAD in berberine bridge enzymes involved in benzylisoquinoline alkaloids that are mutated in PAS and other PAS-like enzymes identified in aspidosperma and iboga alkaloids producing plants. Alignment was performed using MUSCLE algorithm (*55*).

For VIGS plasmid construction	
CS_Fwd	CGAGGATCCTAATATTCATCTTTGTTTTACGTTCTTACTTTC
CS_Rev	CGACTCGAGCGCATTATTCAAATTTTTTACTTATCTTCTC
TS_Fwd	CGAGGATCCAAAAAGGCAAAATTTCCTTGC
TS_Rev	CGACTCGAGTAAGCATTTAACATTATTATTATTATCATATTTTATCAAAATCA
DPAS_Fwd	CGAGGATCCGAGTTGCCACCTATTCCTTTATTATCAG
DPAS_Fwd	CGACTCGAGCAGAGTACACACTTATGACTTTTATGTGC
RO_Fwd	GGCGCGAUTCTCTTCCTCTGTTGGAATTGGC
RO_Rev	GGTTGCGAUTCCAATTCATTTCTAAGCAATCTTCCTTTTTCA
For full-length amplification	
CS_pOPINF_Fwd	AAGTTCTGTTTCAGGGCCCGGCTTCCCAAACTCCAACCTCAGATGA
CS_pOPINF_Rev	ATGGTCTAGAAAGCTTTACTCATGTTTGATGAAAGATGCTAAACG
HID2_pOPINF_Fwd	AAGTTCTGTTTCAGGGCCCGGCTTCCCAAACTCCAACCTCAGATGA
HID2_pOPINF_Rev	ATGGTCTAGAAAGCTTTATTTGATGAAAGACGTTAAGCGTCTAATC
TS_pOPINF_Fwd	AAGTTCTGTTTCAGGGCCCGGGTTCCTCAGATGAGACTATTTTTG
TS_pOPINF_Rev	ATGGTCTAGAAAGCTTTACTTGATGAAAGAAGCTAAACGTCTG
PAS_pDONR207_Fwd	GGGGACAAGTTTGTACAAAAAAGCAGGCTTAATGATAAAAAAAGTCCCA
PAS_pDONR207_Rev	GGGGACCACTTTGTACAAGAAAGCTGGGTAAAGTTCGACTTGTAAATGG
For cloning of PAS into pPink-HC	
PAS_Pichia_Fwd	TCTCTCGAGAAAAGGTCAATTCCTGAAGCTTTTCTCAATTGTATTTCC
PAS_Pichia_Rev	TTAAATGGCCGGCCGAAGTTCGACTTGTAAATGGAGAGGGG
For colony PCR	
T7_Fwd	TAATACGACTCACTATAGGG
pOPIN_Rev	TAGCCAGAAGTCAGATGCT
pDONR207_Fwd	TCGCGTTAACGCTAGCATGGATCTC
pDONR207_Rev	GTAACATCAGAGATTTTGAGACAC
pEAQ_Fwd	GGAGAAAGATTGTTAAGCTTCTGT
pEAQ_Rev	AACATAGAAATGCACACCGAATAA
pPINK_AOX1	GACTGGTTCCAATTGACAAGC
pPINK_CYC1	GCGTGAATGTAAGCGTGAC

For qPCR	
CrEX_Fwd	ACAATACCATCGCCATCAC
CrEX_Rev	AAGAGGACTGCTGGAAGG
CrN2227_Fwd	TCCTTACGCCGCATTATCAG
CrN2227_Rev	AGATGAGACAGTAACGCCTTG
PAS_Fwd	CTTCACTCCCATGTCCAATCT
PAS_Rev	CGATAGGATAAGCCCTCGTAATC
DPAS_Fwd	GAAATAGCGGCATCGACAAAC
DPAS_Rev	GCTGGGAGTGGTGCTAATAA
CS_Fwd	CTCCTGGCGGGATGAATAAC
CS_Rev	GGAAACCAGGGTAACCAACA
TS_Fwd	AGATGCTCCTGGTGGAAATG
TS_Rev	CAACCATGGAAATCAGCAACC
For localization	
PAS-YFPfor	CTGAGAACTAGTATGATAAAAAAAGTCCCAATAGTTCTTTCAA
PAS40-YFPrev	CTGAGAACTAGTATCTAATGAAAATTTATTGGAAATACAATTG
PAS60-YFPrev	CTGAGAACTAGTTTTGAGAACAGAATCATAGGAAGAATTGC
DPAS-YFPfor	CTGAGAACTAGTATGGCCGGAAAATCAGCAGAAG
DPAS-YFPrev	CTGAGAACTAGTTTATAACTCTGACGGAGGAGTCAAGGTATTT
TSfor	CTGAGAACTAGTATGGGTTCCTCAGATGAGACTATTTTT
TSrevstop	CTGAGAACTAGTTTACTTGATGAAAGAAGCTAAACGTCT
TSrev	CTGAGAACTAGTCTTGATGAAAGAAGCTAAACGTCTGAG
CSfor	CTGAGAACTAGTATGAATTCCTCAACTAATCCAACTTCAGAT
CSrevstop	CTGAGAACTAGTTTACTCATGTTTGATGAAAGATGCTAAACG
CSrev	CTGAGAACTAGTCTCATGTTTGATGAAAGATGCTAAACG

Table S1.

Primer sequences used in this study. Cloning/restriction sites are underlined.

>PAS (GenBank: MH213134)
ATGATAAAAAAAGTCCCAATAGTTCTTTCAATTTTCTGCTTTCTTCTTCTACTCTCA
TCATCCCATGGCTCAATTCCTGAAGCTTTTCTCAATTGTATTTCCAATAAATTTTCA
TTAGATGTATCCATTTTAAACATTCTTCATGTTCCCAGCAATTCTTCCTATGATTCT
GTTCTCAAATCTACTATCCAAAATCCAAGATTCCTCAAATCACCCAAGCCCTTAGC
TATAATCACCCCAGTACTTCACTCCCATGTCCAATCTGCTGTTATCTGTACCAAAC
AAGCCGGTTTACAAATTAGAATCCGAAGCGGAGGAGCTGATTACGAGGGCTTATC
CTATCGTTCTGAGGTTCCCTTTATTCTGCTAGATCTCCAGAATCTTCGATCAATTTC
CGTTGATATTGAAGACAACAGCGCTTGGGTCGAATCAGGAGCAACAATTGGTGAA
TTCTATCATGAGATAGCTCAGAACAGCCCTGTTCATGCGTTTCCAGCTGGGGTCTC
TTCCTCTGTTGGAATTGGCGGCCATTTGAGTAGCGGCGGTTTTGGTACATTGCTTC
GGAAATATGGATTAGCAGCCGATAATATAATCGATGCAAAAATTGTTGATGCCAG
AGGCAGAATTCTTGATAGGGAATCAATGGGAGAAGATCTATTTTGGGCTATTAGA
GGAGGAGGAGGAGCTAGTTTTGGTGTTATAGTTTCTTGGAAGGTTAAACTTGTAA
AAGTCCCTCCGATGGTAACTGTTTTCATCTTGTCCAAGACTTATGAAGAAGGAGGT
TTAGATCTTCTACACAAATGGCAATATATAGAACACAAACTCCCTGAAGATTTATT
CCTTGCTGTAAGCATCATGGATGATTCATCTAGTGGAAATAAAACACTTATGGCA
GGTTTTATGTCTCTGTTTCTTGGAAAAACAGAGGACCTTCTGAAAGTAATGGCGGA
AAATTTCCCACAACTTGGATTGAAAAAGGAAGATTGCTTAGAAATGAATTGGATT
GATGCAGCAATGTATTTTTCAGGACACCCAATTGGAGAATCCCGATCTGTGCTTAA
AAACCGAGAATCTCATCTTCCAAAGACATGCGTTTCGATCAAATCAGACTTTATTC
AAGAACCACAATCCATGGATGCATTGGAAAAGTTATGGAAGTTTTGTAGGGAAGA
AGAAAATAGTCCCATAATACTGATGCTTCCACTGGGGGGAATGATGAGTAAAATA
TCAGAATCAGAAATCCCATTTCCTTACAGAAAAGATGTGATTTACAGTATGATATA
CGAAATAGTTTGGAATTGTGAAGACGATGAATCATCGGAAGAATATATCGATGGA
TTGGGAAGGCTTGAGGAATTAATGACTCCATATGTGAAACAACCAAGAGGTTCTT
GGTTCAGCACCAGAAACCTTTATACCGGTAAAAATAAAGGTCCAGGAACAACTTA
TTCCAAAGCTAAAGAATGGGGATTTCGGTATTTTAATAATAATTTCAAAAAGTTGG
CCCTTATCAAAGGACAAGTTGATCCAGAAAACTTCTTCTACTATGAACAAAGCATT
CCCCCTCTCCATTTACAAGTCGAACTTTGA

>DPAS (GenBank: KU865331)
ATGGCCGGAAAATCAGCAGAAGAAGAACATCCCATTAAGGCTTACGGATGGGCT
GTTAAAGATAGAACAACTGGGATTCTTTCTCCCTTCAAATTTTCCAGAAGGGCAAC
AGGTGATGATGATGTCCGAATTAAGATACTCTACTGTGGAATTTGTCACACTGATC
TTGCCTCAATCAAGAACGAATACGAGTTTCTTTCTTATCCTCTTGTGCCCGGGATG
GAGATCGTTGGAATAGCAACGGAGGTTGGAAAAGATGTCACAAAAGTGAAAGTT
GGCGAAAAAGTAGCATTATCAGCCTATTTAGGATGTTGTGGCAAATGCTATAGTT
GTGTAAATGAACTCGAGAATTATTGTCCGGAAGTAATCATAGGTTATGGCACCCC
ATACCATGACGGAACAATTTGCTATGGGGGCCTTTCAAACGAAACTGTCGCAAAT
CAAAGTTTTGTTCTTCGTTTTCCTGAAAGACTTTCTCCAGCTGGCGGAGCTCCTTTG
CTTAGCGCCGGAATTACTTCGTTTAGTGCAATGAGAAATAGCGGCATCGACAAAC
CTGGATTACACGTGGGAGTCGTCGGTCTCGGCGGATTAGGTCATCTTGCTGTAAAA
TTTGCTAAGGCTTTTGGTCTTAAAGTAACTGTTATTAGCACCACTCCCAGCAAGAA
GGATGATGCTATAAATGGTCTTGGTGCTGATGGATTCTTACTCAGCCGCGATGATG
AACAAATGAAGGCTGCTATTGGAACCTTGGATGCAATTATTGATACACTGGCGGT
TGTTCATCCCATAGCACCATTGCTTGATCTCCTGAGAAGTCAAGGGAAATTTTTGT

TACTTGGGGCGCCATCTCAATCACTTGAGTTGCCACCTATTCCTTTATTATCAGGT GGGAAATCTATCATTGGAAGTGCGGCCGGAAATGTGAAGCAAACTCAAGAAATG CTTGATTTTGCAGCGGAGCATGATATAACTGCAAATGTTGAGATTATTCCAATAGA GTACATAAATACTGCAATGGAACGTTTAGACAAGGGCGATGTTAGATACCGATTT GTAGTTGACATCGAAAATACCTTGACTCCTCCGTCAGAGTTATAA
>CS (GenBank: MF770512) ATGGCTTCCCAAACTCCAACCTCAGATGAGACTATTTGGGATCTTTCTCCATATAT TAAAATTTTCAAAGATGGAAGAGTAGAAAGACTCCATAATAGTCCTTATGTTCCC CCATCACTTAATGATCCAGAAACTGGCGTTTCTTGGAAAGATGTCCCGATTTCATC ACAAGTTTCCGCTAGGGTATACATTCCAAAAATCAGCGACCATGAAAAACTCCCT ATTTTTGTGTATGTGCATGGGGCTGGCTTTTGTCTAGAATCTGCCTTCAGATCATTT TTCCACACTTTTGTCAAACACTTCGTAGCCGAAACCAAAGTTATTGGGGTTTCGAT TGAATATAGACTTGCCCCAGAGCACCTTTTACCCGCAGCTTATGAAGATTGTTGGG AAGCCCTTCAATGGGTTGCTTCTCATGTGGGTCTCGACAATTCCGGCCTAAAGACA GCTATTGATAAAGATCCATGGATAATAAACTATGGTGATTTCGATAGACTGTATTT GGCGGGTGACAGTCCTGGTGCTAATATTGTTCACAACACACTTATCAGAGCTGGA AAAGAGAAACTGAAGGGCGGAGTGAAAATTTTGGGGGCAATTCTTTACTACCCAT ATTTCATTATCCCAACCAGCACGAAACTTAGTGATGATTTTGAGTATAACTACACA TGTTACTGGAAATTGGCTTATCCAAATGCTCCTGGCGGGATGAATAACCCAATGAT AAACCCCATAGCTGAAAATGCTCCAGACTTGGCTGGATACGGTTGCTCGAGGTTG TTGGTTACCCTGGTTTCCATGATTTCAACGACTCCAGATGAGACTAAAGACATAAA TGCGGTTTATATTGAGGCATTAGAAAAGAGTGGATGGAAAGGGGAATTGGAAGTG GCTGATTTTGACGCAGATTATTTTGAACTCTTCACCTTGGAAACGGAGATGGGCAA GAATATGTTCAGACGTTTAGCATCTTTCATCAAACATGAGTAA
>TS (GenBank: MF770513) ATGGGTTCCTCAGATGAGACTATTTTTGATCTTCCTCCATACATCAAAGTCTTCAA AGATGGAAGAGTAGAAAGACTCCATTCTTCCCCATATGTTCCCCCATCTCTTAATG ATCCAGAAACCGGTGGAGTCTCTTGGAAAGACGTCCCAATTTCTTCAGTAGTTTCA GCTAGAATTTACCTTCCTAAAATCAACAACCATGATGAAAAACTCCCCATTATAGT CTATTTCCATGGAGCTGGTTTTTGTCTTGAATCGGCCTTCAAATCATTTTTCCACAC TTATGTGAAACACTTTGTAGCAGAAGCCAAAGCTATTGCGGTTTCTGTTGAGTTCA GGCTCGCCCCTGAAAACCATTTACCCGCAGCTTATGAAGATTGCTGGGAAGCCCTT CAATGGGTTGCTTCTCATGTGGGTCTCGACATTTCCAGCTTGAAGACATGTATTGA TAAAGATCCATGGATAATCAACTATGCCGATTTCGATAGACTCTATTTGTGGGGTG ATAGCACCGGTGCCAATATTGTTCACAACACACTTATCAGATCTGGTAAAGAGAA ATTGAACGGCGGCAAAGTGAAGATTTTGGGGGCAATTCTTTACTACCCATATTTCT TAATCAGGACGAGTTCAAAACAGAGTGATTATATGGAGAATGAGTATAGATCTTA CTGGAAATTGGCTTACCCAGATGCTCCTGGTGGAAATGATAACCCAATGATAAAC CCTACAGCTGAGAATGCTCCTGATCTGGCTGGATATGGTTGCTCGAGGTTGCTGAT TTCCATGGTTGCCGATGAAGCTAGAGATATAACTCTTCTTTATATTGATGCATTGG AAAAGAGTGGATGGAAAGGTGAATTAGATGTGGCTGATTTTGATAAACAGTATTT TGAACTGTTTGAAATGGAAACAGAGGNTGCCAAGAACATGCTCAGACGTTTAGCT TCTTTCATCAAGTAA

Table S2.
Sequences of the genes used in this investigation.

Compound	Parent ion	Daughter ion	Collision Energy (V)
Catharanthine	337.2	173.1	16
		165.1	20
		144.1	20
Tabersonine	337.2	305.2	22
		228.2	22
		168.1	36
Stemmadenine acetate	397.2	337.1	18
		228.1	24
		168.0	40
Precondylocarpine acetate	395.2	234.0	38
		228.1	22
		196.1	32

Table S3.
MRM transitions used for metabolites detection with UPLC/QqQ-MS method.

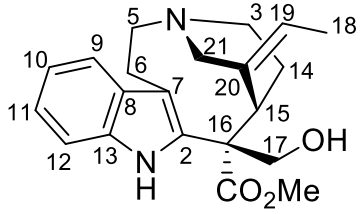

	^{13}C (DMSO)			^{1}H (DMSO)		
No	**This report** [a]	**Grover et al. (*56*)** [b]	**Feng et al. (*57*)** [c,d]	**This report** [a]	**Grover et al. (*56*)** [b]	**Feng et al. (*57*)** [c,d]
1 (N**H**)	n/a	n/a	n/a	10.45 (s)	10.47 (s)	10.36 (s)
2	133.9	133.8	133.8	n/a	n/a	n/a
3	45.5	45.2	45.6	3.30 (1H, m)	3.30 (1H, m)	3.3 (1H, m) [d]
				2.87 (1H, ddd, 13.3, 13.3, 6.8)	2.83 (1H, m)	2.8 (1H, m) [d]
5	54.9	54.7	55.2	3.45 (1H, m)	3.43 (1H, m)	unclear [d]
				3.17 (1H, m)	3.14 (1H, m)	unclear [d]
6	22.4	22.1	24.0	3.36 (2H, m)	3.33 (2H, m)	unclear [d]
7	109.0	108.8	110.2	n/a	n/a	n/a
8	126.5	126.4	unclear [d]	n/a	n/a	n/a
9	117.9	117.4	117.9	7.59 (1H, d, 7.9)	7.60 (1H, d, 7.8)	7.54 (1H, d) [d]
10	118.9	118.8	118.8	7.03 (1H, ddd, 8.0, 7.9, 1.0)	7.02 (1H, d, 7.2)	7.02 (1H, m) [d]
11	121.4	121.3	121.2	7.10 (1H, ddd, 8.0, 7.9, 1.1)	7.10 (1H, d, 7.0)	7.05 (1H, m) [d]
12	111.8	111.7	111.7	7.44 (1H, d, 8.0)	7.45 (1H, d, 7.8)	7.42 (1H, d) [d]
13	135.1	135.0	135.1	n/a	n/a	n/a
14	23.9	23.8	25.8	2.48 (1H, m)	2.50 (1H, m?)	unclear [d]
				2.32 (1H, m)	2.32 (1H, m?)	unclear [d]
15	34.4	34.3	35.3	3.69 (1H, m)	3.70 (1H, dd, 12.2, 3.1)	3.65 (1H, m) [d]
16	60.0	59.9	60.3	n/a	n/a	n/a
17	67.0	66.9	67.4	4.22 (1H, dd, 10.4, 4.8)	4.25 (1H, dd, 10.5, 4.5)	4.21 (1H, m) [d]
				4.13 (1H, dd, 10.4, 5.2)	4.22 (1H, dd, 10.5, 4.5)	4.13 (1H, m) [d]
18	13.9	13.8	14.0	1.70 (3H, dd, 6.9, 2.0)	1.69 (3H, d, 6.0)	1.68 (3H, d) [d]
19	129.4	129.5	unclear [d]	5.56 (1H, q, 6.9)	5.55 (1H, q, 6.0)	5.45 (1H, m) [d]
20	127.0	126.8	126.8	n/a	n/a	n/a
21	52.8	52.4	53.5	3.36 (1H, m)	3.35 (1H, m)	unclear [d]

				2.51 (1H, m)	2.50 (1H, m)	2.5 (1H, m) [d]
COOMe	172.1	172.0	172.4	n/a	n/a	n/a
COO**Me**	52.4	52.0	52.3	3.70 (3H, s)	3.70 (3H, s)	3.69 (3H, s) [d]
O**H**	n/a	n/a	n/a	5.76 (1H, t, 4.2)	5.79 (1H, t, 5.0)	5.73 (1H, br s)

[a] recorded at 300 K, 400 MHz (100 MHz for ^{13}C)
[b] recorded at 298 K, 300 MHz (75 MHz for ^{13}C)
[c] temperature and frequency not reported
[d] No assignments or numerical data reported, just images of spectra. Assignments here are based on comparison with Grover et al. and our data.

Table S4.
NMR data for stemmadenine **1**. HRMS, ESI positive: *m/z* calculated for $C_{21}H_{27}N_2O_3^+$ $[M+H]^+$: 355.2016, observed: 355.2021, Δppm= 1.4.

	Stemmadenine 1 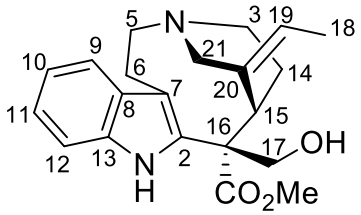		**Stemmadenine acetate 7** 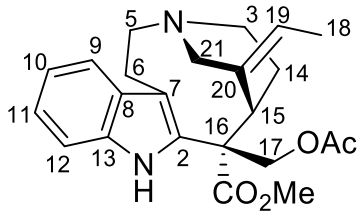	
No	**^{13}C MeOD** [a]	**^{1}H MeOD** [a]	**^{13}C MeOD** [a]	**^{1}H MeOD** [a]
1 (NH)	n/a	not detected	n/a	not detected
2	135.0	n/a	133.0	n/a
3	47.5	3.17 (1H, ddd, 13.8, 13.8, 6.6) 3.41 (1H, m)	47.5	3.17 (1H, ddd, 13.6, 13.6, 7.0) 3.41 (1H, m)
5	57.0	3.59 (1H, m) 3.47 (1H, m)	57.1	3.59 (1H, m) 3.48 (1H, m)
6	23.7	3.63 (1H, m) 3.47 (1H, m)	23.8	3.61 (1H, m) 3.51 (1H, m)
7	110.3	n/a	110.6	n/a
8	128.1	n/a	128.0	n/a
9	118.7	7.56 (1H, ddd, 8.0, 1.0, 1.0)	118.9	7.58 (1H, ddd, 7.8, 0.9, 0.9)
10	120.7	7.10 (1H, ddd, 8.0, 8.0, 1.2)	120.9	7.12 (1H, ddd, 8.0, 7.1, 1.1)
11	123.4	7.16 (1H, ddd, 8.3, 8.3, 1.2)	123.6	7.18 (1H, ddd, 8.0, 7.1, 1.2)
12	112.7	7.42 (1H, ddd, 8.0, 1.0, 1.0)	112.7	7.43 (1H, ddd, 8.0, 0.9, 0.9)
13	137.0	n/a	137.1	n/a
14	25.3	2.44 (1H, ddd, 16.6, 12.9, 6.5) 2.68 (1H, dddd, 16.6, 16.6, 6.6, 3.4)	25.2	2.47 (1H, m) 2.70 (1H, m)
15	36.1	3.86 (1H, dd, 12.9, 3.5)	36.8	3.96 (1H, dd, 12.5, 3.3)
16	61.6	n/a	59.4	n/a
17	69.2	4.35 (2H, s)	69.7	4.71 (1H, d, 11.1) 4.92 (1H, d, 11.1)
18	14.5	1.80 (3H, dd, 7.0, 2.2)	14.5	1.84 (3H, dd, 7.0, 2.1)
19	132.4	5.65 (1H, qd, 7.0, 1.7)	132.4	5.68 (1H, q, 6.0)
20	127.7	n/a	127.3	n/a
21	55.2	2.99 (1H, br d, 15.0) 3.44 (1H, br d, 15.0)	54.8	2.74 (1H, m) 3.45 (1H, m)
COOMe	174.1	n/a	172.9	n/a
COOMe	53.2	3.81 (3H, s)	53.5	3.81 (3H, s)
OC(O)Me	n/a	n/a	171.9	n/a

OC(O)Me	n/a	n/a	20.7	2.05 (3H, s)

[a] recorded at 300 K, 400 MHz (100 MHz for ^{13}C)

Table S5.
NMR data for stemmadenine acetate **7** in comparison to the starting material stemmadenine **1**. HRMS, ESI positive: *m/z* calculated for $C_{23}H_{29}N_2O_4^+$ $[M+H]^+$: 397.2122, observed: 397.2122, Δppm= 0.0.

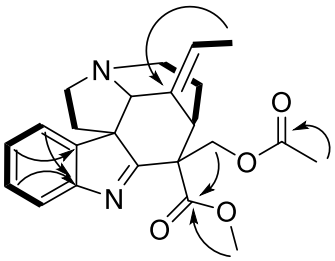

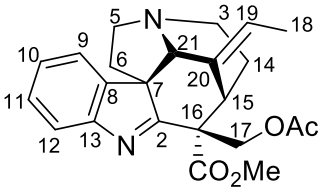

precondylocarpine acetate

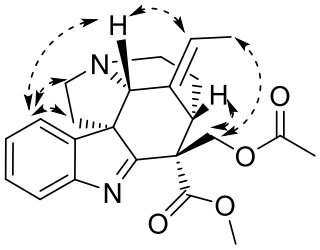

COSY

HMBC

NOESY

No	^{13}C CD_3CN [a]	^{1}H CD_3CN [a]
2	n.d.[b]	n/a
3	48.7	2.98 (1H, m)
		2.65 (1H, m)
5	58.7	3.46 (1H, m)
		3.31 (1H, m)
6	39.1	2.90 (1H, m)
		1.84 (1H, m)
7	n.d.[b]	n/a
8	147.5	n/a
9	112.2	7.44 (1H, m)
10	127.3	7.25 (1H, ddd, 7.3, 7.3, 1.3)
11	128.4	7.31 (1H, ddd, 7.5, 7.5, 1.4)
12	121.3	7.45 (1H, m)
13	154.4	n/a
14	31.5	2.13 (1H, m)
		2.05 (1H, m)
15	34.6	3.52 (1H, m)
16	n.d.[b]	n/a
17	67.8	5.01 (1H, d, 11.2)
		3.92 (1H, d, 11.2)
18	13.3	1.57 (3H, d, 6.9)
19	124.2	5.35 (1H, q, 6.9)
20	134.8	n/a
21	76.1	3.89 (1H, d, 2.3)
COOMe	172.5	n/a
COO**Me**	52.9	3.71 (3H, s)
O**C**(O)Me	171.4	n/a
OC(O)**Me**	21.0	2.05 (3H, s)

[a] recorded at 300 K, 400 MHz (100 MHz for ^{13}C)

[b] Not identified by HMBC due to instability and low scale

Table S6.
NMR data and key correlations for precondylocarpine acetate **10**. HRMS, ESI positive: *m/z* calculated for $C_{23}H_{27}N_2O_4$ $[M+H]^+$: 395.1965, observed: 395.1967, Δppm= 0.5.

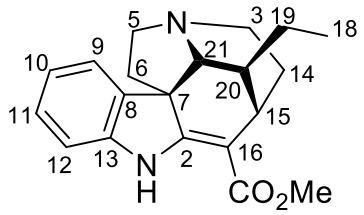

	^{13}C			^{1}H		
No	**This report $CDCl_3$ [a]**	**Yamauchi et al. (*58*) $CDCl_3$ [b]**	**Martin et al. (*59*) $CDCl_3$ [c, d]**	**This report $CDCl_3$ [a]**	**Yamauchi et al. (58) $CDCl_3$ [b]**	**Martin et al. (59) $CDCl_3$ [c,d]**
1 (NH)	n/a	n/a	n/a	8.84 (1H, s)	8.85 [g]	8.86 (1H, s)
2	170.5 [e]	168.8	170.9	n/a	n/a	n/a
3	45.0	45.2	45.5	2.49 (1H, m) 3.01 (1H, m)	2.46 (1H, m) 3.02-2.80 (1H) [g]	2.46 (1H, ddd, 11.7, 9.6, 8.6) 3.06–2.99 (1H, m)
5	53.6	53.9	54.2	2.85 (2H, m)	3.02-2.80 (2H) [g]	2.96 (1H, dt, 11.8, 4.0) 2.84 (1H, dd, 10.8, 7.1)
6	43.8	44.0	44.3	1.80 (1H, m) 2.90 (1H, m)	1.81-1.75 (1H) [g] 3.02-2.80 (1H) [g]	1.82– 1.76 (1H, m) 2.94–2.87 (1H, m)
7	55.1	55.1	55.4	n/a	n/a	n/a
8	137.0	137.2	137.5	n/a	n/a	n/a
9	119.6	119.5	119.9	7.16 (1H, d, 7.4)	7.13 (1H, br d, 7)	7.14 (1H, d, 7.3)
10	121.2	121.0	121.2	6.88 (1H, ddd, 7.5, 7.5, 0.8)	6.86 (1H, td, 7, 1)	6.88 (1H, t, 7.5)
11	127.3	127.1	127.3	7.11 (1H, ddd, 7.7, 7.7, 1.2)	7.09 (1H, td, 7, 1)	7.11 (1H, t, 7.7)
12	109.7	109.6	109.8	6.80 (1H, d, 7.7)	6.79 (1H, br d, 7)	6.81 (1H, d, 7.7)
13	143.7	143.7	143.9	n/a	n/a	n/a
14	28.3	28.5	28.7	1.80 (2H, m)	1.81-1.75 (2H) [g]	1.82–1.76 (2H, m)
15	30.7	30.9	31.2	3.06 (1H, m)	3.04 (1H, br s)	3.06–2.99 (1H, m)
16	n.d. [f]	95.7	95.8	n/a	n/a	n/a
18	11.5	11.5	11.8	0.70 (3H, t, 7.0)	0.70 (3H, t, 7)	0.70 (3H, t, 7.3)

19	23.7	23.9	24.1	0.88-0.78 (2H, m)	0.87-0.79 (2H) [g]	0.86–0.78 (2H, m)
20	41.0	41.2	41.5	1.98 (1H, m)	1.97 (1H, m)	2.00–1.95 (1H, m)
21	65.3	65.5	65.8	3.88 (1H, br s)	3.81 (1H, br s)	3.81 (1H, s)
COOMe	168.9 [e]	170.5	169.1	n/a	n/a	n/a
COOMe	51.1	51.0	51.3	3.77 (3H, s)	3.76 (3H) [g]	3.77 (3H, s)

[a] recorded at 300 K, 400 MHz (100 MHz for ^{13}C)
[b] recorded at 400 MHz (100 MHz for ^{13}C); temperature not reported
[c] recorded at 298 K, 500 MHz (125 MHz for ^{13}C)
[d] No assignments reported; signals assigned here based on similarity to Yamauchi et al. and our data
[e] Assignment supported by HMBC correlations (COOMe to COOMe, H-6 to C-2)
[f] Not detected by HMBC
[g] No multiplicity reported

Table S7.
NMR data for tubotaiwine **12** obtained as the degradation product of dihydroprecondylocarpine acetate **11** (580 µg crude mass, 1.79 µmol).

Data S1. (separate file)
Communities of closely co-expressed genes were identified with a fast greedy algorithm.

Data S2. (separate file)
Proteomic analysis of PAS, DPAS, CS and TS expressed in *N. benthamiana*.

Data S3. (separate file)
Proteomic analysis of PAS expressed in *P. pastoris*.

References and Notes

1. S. E. O'Connor, J. J. Maresh, Chemistry and biology of monoterpene indole alkaloid biosynthesis. *Nat. Prod. Rep.* **23**, 532–547 (2006). doi:10.1039/b512615k Medline

2. T. Dugé de Bernonville, M. Clastre, S. Besseau, A. Oudin, V. Burlat, G. Glévarec, A. Lanoue, N. Papon, N. Giglioli-Guivarc'h, B. St-Pierre, V. Courdavault, Phytochemical genomics of the Madagascar periwinkle: Unravelling the last twists of the alkaloid engine. *Phytochemistry* **113**, 9–23 (2015). doi:10.1016/j.phytochem.2014.07.023 Medline

3. S. Vonny, V. De Luca, "Towards complete elucidation of monoterpene indole alkaloid biosynthesis pathway: Catharanthus roseus as a pioneer system" in "*Advances in Botanical Research*" (Elsevier, 2013), pp. 1–37.

4. S. C. Benson, L. Lee, W. Wei, F. Ni, J. D. J. Olmos, K. R. Strom, A. B. Beeler, K. C.-C. Cheng, J. Inglese, S. Kota, V. Takahashi, A. D. Strosberg, J. H. Connor, G. G. Bushkin, J. K. Snyder, Truncated aspidosperma alkaloid-like scaffolds: Unique structures for the discovery of new, bioactive compounds. *Heterocycles* **84**, 135–155 (2012). doi:10.3987/REV-11-SR(P)4

5. G. K. Jana, S. Paul, S. Sinha, Progress in the synthesis of iboga-alkaloids and their congeners. *Org. Prep. Proced. Int.* **43**, 541–573 (2011). doi:10.1080/00304948.2011.629563

6. E. Wenkert, Biosynthesis of indole alkaloids. The aspidosperma and iboga bases. *J. Am. Chem. Soc.* **84**, 98–102 (1962). doi:10.1021/ja00860a023

7. J. P. Kutney, Y. Karton, N. Kawamura, B. R. Worth, Dihydropyridines in synthesis and biosynthesis. IV. Dehydrosecodine, in vitro precursor of indole alkaloids. *Can. J. Chem.* **60**, 1269–1278 (1982). doi:10.1139/v82-187

8. A. I. Scott, C. C. Wei, Regio- and stereospecific models for the biosynthesis of the indole alkaloids—II: Biogenetic type synthesis of *Aspidosperma* and *Iboga* alkaloids from a corynanthe precursor. *Tetrahedron* **30**, 3003–3011 (1974). doi:10.1016/S0040-4020(01)97545-3

9. H. Mizoguchi, H. Oikawa, H. Oguri, Biogenetically inspired synthesis and skeletal diversification of indole alkaloids. *Nat. Chem.* **6**, 57–64 (2014). doi:10.1038/nchem.1798 Medline

10. F. Kellner, J. Kim, B. J. Clavijo, J. P. Hamilton, K. L. Childs, B. Vaillancourt, J. Cepela, M. Habermann, B. Steuernagel, L. Clissold, K. McLay, C. R. Buell, S. E. O'Connor, Genome-guided investigation of plant natural product biosynthesis. *Plant J.* **82**, 680–692 (2015). doi:10.1111/tpj.12827 Medline

11. Y. Qu, M. E. A. M. Easson, R. Simionescu, J. Hajicek, A. M. K. Thamm, V. Salim, V. De Luca, Solution of the multistep pathway for assembly of corynanthean, strychnos, iboga, and aspidosperma monoterpenoid indole alkaloids from 19*E*-geissoschizine. *Proc. Natl. Acad. Sci. U.S.A.* **115**, 3180–3185 (2018). doi:10.1073/pnas.1719979115 Medline

12. N. Petitfrere, A. M. Morfaux, M. M. Debray, L. Le Men-Olivier, J. Le Men, Alcaloides des feuilles du *Pandaca minutiflora*. *Phytochemistry* **14**, 1648–1649 (1975). doi:10.1016/0031-9422(75)85373-8

13. B. A. Dadson, J. Harley-Mason, Total synthesis of (±)-tubotaiwine (dihydrocondylocarpine). *J. Chem. Soc. D* **1969**, 665b (1969). doi:10.1039/C2969000665B

14. E. C. Tatsis, I. Carqueijeiro, T. Dugé de Bernonville, J. Franke, T.-T. T. Dang, A. Oudin, A. Lanoue, F. Lafontaine, A. K. Stavrinides, M. Clastre, V. Courdavault, S. E. O'Connor, A three enzyme system to generate the Strychnos alkaloid scaffold from a central biosynthetic intermediate. *Nat. Commun.* **8**, 316 (2017). doi:10.1038/s41467-017-00154-x Medline

15. A. I. Scott, C. C. Wei, Regio- and stereospecific models for the biosynthesis of the indole alkaloids. The Corynanthe-Aspidosperma relationship. *J. Am. Chem. Soc.* **94**, 8264–8265 (1972). doi:10.1021/ja00778a074 Medline

16. A. I. Scott, Biosynthesis of the indole alkaloids. *Acc. Chem. Res.* **3**, 151–157 (1970). doi:10.1021/ar50029a002

17. N. G. H. Leferink, D. P. H. M. Heuts, M. W. Fraaije, W. J. H. van Berkel, The growing VAO flavoprotein family. *Arch. Biochem. Biophys.* **474**, 292–301 (2008). doi:10.1016/j.abb.2008.01.027 Medline

18. A. Stavrinides, E. C. Tatsis, E. Foureau, L. Caputi, F. Kellner, V. Courdavault, S. E. O'Connor, Unlocking the diversity of alkaloids in *Catharanthus roseus*: Nuclear localization suggests metabolic channeling in secondary metabolism. *Chem. Biol.* **22**, 336–341 (2015). doi:10.1016/j.chembiol.2015.02.006 Medline

19. A. Stavrinides, E. C. Tatsis, L. Caputi, E. Foureau, C. E. M. Stevenson, D. M. Lawson, V. Courdavault, S. E. O'Connor, Structural investigation of heteroyohimbine alkaloid synthesis reveals active site elements that control stereoselectivity. *Nat. Commun.* **7**, 12116 (2016). doi:10.1038/ncomms12116 Medline

20. A. I. Scott, "Laboratory models for the biogenesis of indole alkaloids" in *Recent Advances in Phytochemistry*, V. C. Runeckles, Ed. (Plenum Press, 1975), chap. 9, pp. 189–241.

21. M. El-Sayed, Y. H. Choi, M. Frédérich, S. Roytrakul, R. Verpoorte, Alkaloid accumulation in *Catharanthus roseus* cell suspension cultures fed with stemmadenine. *Biotechnol. Lett.* **26**, 793–798 (2004). doi:10.1023/B:BILE.0000025879.53632.f2 Medline

22. T. T. Dang, X. Chen, P. J. Facchini, Acetylation serves as a protective group in noscapine biosynthesis in opium poppy. *Nat. Chem. Biol.* **11**, 104–106 (2015). doi:10.1038/nchembio.1717 Medline

23. A. Bock, G. Wanner, M. H. Zenk, Immunocytological localization of two enzymes involved in berberine biosynthesis. *Planta* **216**, 57–63 (2002). doi:10.1007/s00425-002-0867-5 Medline

24. Y. Qu, M. L. A. E. Easson, J. Froese, R. Simionescu, T. Hudlicky, V. De Luca, Completion of the seven-step pathway from tabersonine to the anticancer drug precursor vindoline and its assembly in yeast. *Proc. Natl. Acad. Sci. U.S.A.* **112**, 6224–6229 (2015). doi:10.1073/pnas.1501821112 Medline

25. N. Lenfant, T. Hotelier, E. Velluet, Y. Bourne, P. Marchot, A. Chatonnet, ESTHER, the database of the α/β-hydrolase fold superfamily of proteins: Tools to explore diversity of functions. *Nucleic Acids Res.* **41**, D423–D429 (2013). doi:10.1093/nar/gks1154 Medline

26. E. M. Stocking, R. M. Williams, Chemistry and biology of biosynthetic Diels-Alder reactions. *Angew. Chem. Int. Ed.* **42**, 3078–3115 (2003). doi:10.1002/anie.200200534 Medline

27. A. Casini, F.-Y. Chang, R. Eluere, A. M. King, E. M. Young, Q. M. Dudley, A. Karim, K. Pratt, C. Bristol, A. Forget, A. Ghodasara, R. Warden-Rothman, R. Gan, A. Cristofaro, A. E. Borujeni, M.-H. Ryu, J. Li, Y.-C. Kwon, H. Wang, E. Tatsis, C. Rodriguez-Lopez, S. O'Connor, M. H. Medema, M. A. Fischbach, M. C. Jewett, C. Voigt, D. B. Gordon, A pressure test to make 10 molecules in 90 days: External evaluation of methods to engineer biology. *J. Am. Chem. Soc.* **140**, 4302–4316 (2018). doi:10.1021/jacs.7b13292 Medline

28. M. Sottomayor, A. Ros Barceló, Peroxidase from *Catharanthus roseus* (L.) G. Don and the biosynthesis of α-3′,4′-anhydrovinblastine: A specific role for a multifunctional enzyme. *Protoplasma* **222**, 97–105 (2003). doi:10.1007/s00709-003-0003-9 Medline

29. H. Ishikawa, D. A. Colby, S. Seto, P. Va, A. Tam, H. Kakei, T. J. Rayl, I. Hwang, D. L. Boger, Total synthesis of vinblastine, vincristine, related natural products, and key structural analogues. *J. Am. Chem. Soc.* **131**, 4904–4916 (2009). doi:10.1021/ja809842b Medline

30. H. M. do Carmo, R. Braz-Filho, I. J. C. Vieira, A novel alkaloid from aspidosperma pyricollum (Apocynaceae) and complete ^{1}H and ^{13}C chemical shift assignments. *Helv. Chim. Acta* **98**, 1381–1386 (2015). doi:10.1002/hlca.201500176

31. E. Góngora-Castillo, K. L. Childs, G. Fedewa, J. P. Hamilton, D. K. Liscombe, M. Magallanes-Lundback, K. K. Mandadi, E. Nims, W. Runguphan, B. Vaillancourt, M. Varbanova-Herde, D. Dellapenna, T. D. McKnight, S. O'Connor, C. R. Buell, Development of transcriptomic resources for interrogating the biosynthesis of monoterpene indole alkaloids in medicinal plant species. *PLOS ONE* **7**, e52506 (2012). doi:10.1371/journal.pone.0052506 Medline

32. R. M. Payne, D. Xu, E. Foureau, M. I. S. Teto Carqueijeiro, A. Oudin, T. D. Bernonville, V. Novak, M. Burow, C.-E. Olsen, D. M. Jones, E. C. Tatsis, A. Pendle, B. Ann Halkier, F. Geu-Flores, V. Courdavault, H. H. Nour-Eldin, S. E. O'Connor, An NPF transporter exports a central monoterpene indole alkaloid intermediate from the vacuole. *Nat. Plants* **3**, 16208 (2017). doi:10.1038/nplants.2016.208 Medline

33. T. Dugé de Bernonville, I. Carqueijeiro, A. Lanoue, F. Lafontaine, P. Sánchez Bel, F. Liesecke, K. Musset, A. Oudin, G. Glévarec, O. Pichon, S. Besseau, M. Clastre, B. St-Pierre, V. Flors, S. Maury, E. Huguet, S. E. O'Connor, V. Courdavault, Folivory elicits a strong defense reaction in *Catharanthus roseus*: Metabolomic and transcriptomic analyses reveal distinct local and systemic responses. *Sci. Rep.* **7**, 40453 (2017). doi:10.1038/srep40453 Medline

34. I. Carqueijeiro, T. Dugé de Bernonville, A. Lanoue, T. T. Dang, C. N. Teijaro, C. Paetz, K. Billet, A. Mosquera, A. Oudin, S. Besseau, N. Papon, G. Glévarec, L. Atehortùa, M. Clastre, N. Giglioli-Guivarc'h, B. Schneider, B. St-Pierre, R. B. Andrade, S. E. O'Connor, V. Courdavault, A BAHD acyltransferase catalyzing 19-O-acetylation of tabersonine derivatives in roots of *Catharanthus roseus* enables combinatorial synthesis of monoterpene indole alkaloids. *Plant J.* **94**, 469–484 (2018). Medline

35. T. Dugé de Bernonville, E. Foureau, C. Parage, A. Lanoue, M. Clastre, M. A. Londono, A. Oudin, B. Houillé, N. Papon, S. Besseau, G. Glévarec, L. Atehortùa, N. Giglioli-Guivarc'h, B. St-Pierre, V. De Luca, S. E. O'Connor, V. Courdavault, Characterization of a second secologanin synthase isoform producing both secologanin and secoxyloganin allows enhanced *de novo* assembly of a *Catharanthus roseus* transcriptome. *BMC Genomics* **16**, 619 (2015). doi:10.1186/s12864-015-1678-y Medline

36. R. Patro, G. Duggal, M. I. Love, R. A. Irizarry, C. Kingsford, Salmon provides fast and bias-aware quantification of transcript expression. *Nat. Methods* **14**, 417–419 (2017). doi:10.1038/nmeth.4197 Medline

37. F. Liesecke *et al*., Ranking genome-wide correlation measurements improves microarray and RNA-seq based global and targeted co-expression networks. bioRxiv 299909 [Preprint]. 12 April 2018. https://doi.org/10.1101/299909

38. R Core Team, R: A Language and Environment for Statistical Computing (2017); www.R-project.org/.

39. G. Csardi, T. Nepusz, The igraph software package for complex network research. *InterJ. Complex Syst.* **1695**, 1–9 (2006).

40. A. Clauset, M. E. Newman, C. Moore, Finding community structure in very large networks. *Phys. Rev. E* **70**, 066111 (2004). doi:10.1103/PhysRevE.70.066111 Medline

41. F. Geu-Flores, N. H. Sherden, V. Courdavault, V. Burlat, W. S. Glenn, C. Wu, E. Nims, Y. Cui, S. E. O'Connor, An alternative route to cyclic terpenes by reductive cyclization in iridoid biosynthesis. *Nature* **492**, 138–142 (2012). doi:10.1038/nature11692 Medline

42. D. K. Liscombe, S. E. O'Connor, A virus-induced gene silencing approach to understanding alkaloid metabolism in *Catharanthus roseus*. *Phytochemistry* **72**, 1969–1977 (2011). doi:10.1016/j.phytochem.2011.07.001 Medline

43. J. Pollier, R. Vanden Bossche, H. Rischer, A. Goossens, Selection and validation of reference genes for transcript normalization in gene expression studies in *Catharanthus roseus*. *Plant Physiol. Biochem.* **83**, 20–25 (2014). doi:10.1016/j.plaphy.2014.07.004 Medline

44. N. S. Berrow, D. Alderton, S. Sainsbury, J. Nettleship, R. Assenberg, N. Rahman, D. I. Stuart, R. J. Owens, A versatile ligation-independent cloning method suitable for high-throughput expression screening applications. *Nucleic Acids Res.* **35**, e45 (2007). doi:10.1093/nar/gkm047 Medline

45. J. A. Lindbo, TRBO: A high-efficiency tobacco mosaic virus RNA-based overexpression vector. *Plant Physiol.* **145**, 1232–1240 (2007). doi:10.1104/pp.107.106377 Medline

46. F. Sainsbury, P. Saxena, K. Geisler, A. Osbourn, G. P. Lomonossoff, Using a virus-derived system to manipulate plant natural product biosynthetic pathways. *Methods Enzymol.* **517**, 185–202 (2012). doi:10.1016/B978-0-12-404634-4.00009-7 Medline

47. D. Wessel, U. I. Flügge, A method for the quantitative recovery of protein in dilute solution in the presence of detergents and lipids. *Anal. Biochem.* **138**, 141–143 (1984). doi:10.1016/0003-2697(84)90782-6 Medline

48. S. Tyanova, T. Temu, J. Cox, The MaxQuant computational platform for mass spectrometry-based shotgun proteomics. *Nat. Protoc.* **11**, 2301–2319 (2016). doi:10.1038/nprot.2016.136 Medline

49. G. Guirimand, V. Burlat, A. Oudin, A. Lanoue, B. St-Pierre, V. Courdavault, Optimization of the transient transformation of *Catharanthus roseus* cells by particle bombardment and its application to the subcellular localization of hydroxymethylbutenyl 4-diphosphate synthase and geraniol 10-hydroxylase. *Plant Cell Rep.* **28**, 1215–1234 (2009). doi:10.1007/s00299-009-0722-2 Medline

50. G. Guirimand, V. Courdavault, A. Lanoue, S. Mahroug, A. Guihur, N. Blanc, N. Giglioli-Guivarc'h, B. St-Pierre, V. Burlat, Strictosidine activation in Apocynaceae: Towards a "nuclear time bomb"? *BMC Plant Biol.* **10**, 182 (2010). Medline

51. R. Waadt, L. K. Schmidt, M. Lohse, K. Hashimoto, R. Bock, J. Kudla, Multicolor bimolecular fluorescence complementation reveals simultaneous formation of alternative CBL/CIPK complexes in planta. *Plant J.* **56**, 505–516 (2008). doi:10.1111/j.1365-313X.2008.03612.x Medline

52. G. Guirimand, A. Guihur, O. Ginis, P. Poutrain, F. Héricourt, A. Oudin, A. Lanoue, B. St-Pierre, V. Burlat, V. Courdavault, The subcellular organization of strictosidine biosynthesis in *Catharanthus roseus* epidermis highlights several trans-tonoplast translocations of intermediate metabolites. *FEBS J.* **278**, 749–763 (2011). doi:10.1111/j.1742-4658.2010.07994.x Medline

53. J. M. Mérillon, P. Doireau, A. Guillot, J. C. Chénieux, M. Rideau, Indole alkaloid accumulation and tryptophan decarboxylase activity in *Catharanthus roseus* cells cultured in three different media. *Plant Cell Rep.* **5**, 23–26 (1986). doi:10.1007/BF00269710 Medline

54. E. Foureau, I. Carqueijeiro, T. Dugé de Bernonville, C. Melin, F. Lafontaine, S. Besseau, A. Lanoue, N. Papon, A. Oudin, G. Glévarec, M. Clastre, B. St-Pierre, N. Giglioli-Guivarc'h, V. Courdavault, Prequels to synthetic biology: From candidate gene identification and validation to enzyme subcellular localization in plant and yeast cells. *Methods Enzymol.* **576**, 167–206 (2016). doi:10.1016/bs.mie.2016.02.013 Medline

55. R. C. Edgar, MUSCLE: Multiple sequence alignment with high accuracy and high throughput. *Nucleic Acids Res.* **32**, 1792–1797 (2004). doi:10.1093/nar/gkh340 Medline

56. R. K. Grover, S. Srivastava, D. K. Kulshreshtha, R. Roy, A new stereoisomer of stemmadenine alkaloid from *Tabernaemontana heyneana*. *Magn. Reson. Chem.* **40**, 474–476 (2002). doi:10.1002/mrc.1039

57. T. Feng, X.-H. Cai, Y.-P. Liu, Y. Li, Y.-Y. Wang, X.-D. Luo, Melodinines A–G, monoterpenoid indole alkaloids from *Melodinus henryi*. *J. Nat. Prod.* **73**, 22–26 (2010). doi:10.1021/np900595v Medline

58. T. Yamauchi, F. Abe, W. G. Padolina, F. M. Dayrit, Alkaloids from leaves and bark of Alstonia scholaris in the Philippines. *Phytochemistry* **29**, 3321–3325 (1990). doi:10.1016/0031-9422(90)80208-X

59. C. L. Martin, S. Nakamura, R. Otte, L. E. Overman, Total synthesis of (+)-condylocarpine, (+)-isocondylocarpine, and (+)-tubotaiwine. *Org. Lett.* **13**, 138–141 (2011). doi:10.1021/ol102709s Medline